Summer 2015

Particulate and gas-phase PCBs and OH-PCBs in Chicago air

Andrew Magdi Awad
University of Iowa

PARTICULATE AND GAS-PHASE PCBS AND OH-PCBS IN CHICAGO AIR

by

Andrew Magdi Awad

A thesis submitted in partial fulfillment
of the requirements for the Master of Science degree in
Civil and Environmental Engineering (Environmental Science)
in the Graduate College of The University of Iowa

August 2015

Thesis Supervisors: Professor Keri C. Hornbuckle
Adjunct Assistant Professor Andres Martinez

Graduate College
The University of Iowa
Iowa City, Iowa

CERTIFICATE OF APPROVAL

_____

MASTER'S THESIS

_____

This is to certify that the Master's thesis of

Andrew Magdi Awad

has been approved by the Examining Committee for
the thesis requirement for the Master of Science degree in
Civil and Environmental Engineering (Environmental Science)
at the August 2015 graduation.

Thesis Committee: _____
Keri C. Hornbuckle, Thesis Supervisor

_____
Andres Martinez, Thesis Supervisor

_____
Scott N. Spak

_____
Craig L. Just

To my parents; for all they have done and continue to do for me.

ACKNOWLEDGEMENTS

First and foremost I'd like to thank Keri Hornbuckle for the opportunity she gave me and the insight she provided me with; not only about this research, but about my future and finding my way in the world. I'd also like to thank Andres Martinez, for working so closely with me and guiding and mentoring me during this journey.

It goes without say that I could not have completed this process without the support of my family and the many, many wonderful people I met during my time at Iowa. To all of you, thank you.

ABSTRACT

This study extends the work we have previously done by reporting on both gas-phase and particulate phase PCB concentrations in Chicago air as well as giving a first report on airborne OH-PCBs in Chicago. Gas phase PCB concentrations ranged from 43.1 pg/m^3 to 2250 pg/m^3, with an average concentration of 594 pg/m^3 ± 445 pg/m^3, and exhibited strong temporal trends. Particulate phase PCBs accounted on average for 4.3% of total PCBs in a sample. OH-PCBs were detected in both the gas and particulate phase and exhibit characteristics of either emission sources or atmospheric reactions depending on the congener.

PUBLIC ABSTRACT

PCBs are chemicals that have long been known to pollute the environment. They were produced heavily throughout much of the twentieth century for various industrial purposes. However, their production was banned in 1979 when the government realized that although very useful, these chemicals were toxic to humans as well as other living organisms. PCBs are extremely well distributed in the environment, and have been detected in the air, water, and soil in virtually all parts of the world.

OH-PCBs are chemicals that are very closely related to PCBs in their chemical structure, and also exhibit many of the same toxic effects as PCBs. Although OH-PCBs have been known about for a long time, their presence in the environment has only recently been reported.

This study reports on levels of PCBs and OH-PCBs in air samples collected from Chicago. This is the first time anyone has reported on OH-PCBs in air samples.

TABLE OF CONTENTS

LIST OF TABLES

LIST OF FIGURES

CHAPTER 1 INTRODUCTION AND BACKGROUND TO THIS STUDY

1.1 A Brief Overview of Polychlorinated Biphenyls and Hydroxylated Polychlorinated Biphenyls.

Polychlorinated biphenyls (PCBs) are a group of anthropogenic semi-volatile organic compounds (SVOCs) that fall under the category of persistent organic pollutants (POPs). They were produced heavily in the United States from 1929 up until their ban from commercial production by the federal government in 1979. By definition, a polychlorinated biphenyl is any molecule that consists of a two ringed biphenyl molecule in which one or more of the constituent hydrogen ions is replaced with a chlorine atom. In total, there are 209 and distinct PCBs known as congeners containing anywhere from one to ten chlorine atoms. Each PCB congener has distinct physical and chemical properties dependent on the number and location of chlorine molecules attached to the biphenyl rings. The chemical structure of PCB molecules causes them to be largely electrically and thermally resistant as well as extremely chemically stable[1, 2]. These properties made PCBs desirable chemicals for a wide variety of industrial applications. PCBs were used as electrical insulating fluids in capacitors and transformers, and also as flame retardant hydraulic heat transfer and lubricating fluids. Other well-known uses of PCBs included blending with other chemicals to make plasticizers and flame retardants that were used in caulking, adhesives, plastics, and carbonless copy paper[2]. Despite their many and wide spread uses, there is considerable concern regarding PCBs due to their persistence, abundance, and mobility in the environment[2].

Environmental exposure to PCBs is typically from ingestion of contaminated food and/or from inhilation[3]. Primary concerns regarding PCBs in the environment are due to the relative toxicological effects PCBs are known to have on animals and humans. Potential toxic effects to humans and animals are dependent upon PCB congener, and include but are not limited to compromised endocrine, respiratory, renal and hepatic functions[3, 4]. Certain PCBs have been found to exhibit dioxin-like[5], neurotoxic[6], and potentially carcinogenic[7] effects have already been identified in Chicago air samples[5-8].

Hydroxylated polychlorinated biphenyls (OH-PCBs) are closely related to PCBs in their chemical stucture. An OH-PCB is any PCB in which one or more of the constituent hydrogen atoms has been replaced with a hydroxide ion. The differences in structures causes OH-PCBs to have different physical chemical properties as well as toxicological effects from PCBs with the same number and placement of chlorine atoms. OH-PCBs are generally considered to be the hydroxylated metabolites of PCBs in people[9, 10], mammals, and birds[11], although their presence in the atmosphere has been hypothesized[12-14] and they have been identified as environmental contaminants present in precipitation[15], and recently in sediment and original Aroclor samples[16].

1.2 Objectives and Hypotheses

This study was designed to extend work we previously done by the Hornbuckle lab by reporting on both gas-phase and particulate phase PCBs in Chicago as well as providing a first report on airborne OH-PCBs. Previously, Hu et al. reported on gas phase PCB congener concentrations across Chicago[8], as well as the presence the non-Aroclor PCB 3-3'dichlorobiphenyl in Chicago air[17] and it's origin from commercial paint pigments

common throughout the city[18]. In this study, we examine Chicago air samples, this time with the intent to look for OH-PCBs in addition to PCBs. Presence of OH-PCBs in the atmosphere has been hypothesized as the byproducts of reactions between PCBs and the hydroxyl radical[12-14, 19, 20], but they have yet to be directly identified in atmospheric samples. Recent work published by Marek et al.[16] reports the presence of OH-PCBs in sediment and original Aroclor samples, suggesting that these matrices could function as volatilization sources to OH-PCBs.

This study was designed with several objectives in mind:

- Measure airborne PCB concentrations in both the gas and particulate phase in Chicago air and to compare concentrations to literature values for Chicago and other North American cities.
- Compare Chicago PCB congener profile to previously reported profile for Chicago
- Analyze temporal and spatial information and see if there is any correlation to airborne PCB concentrations.
- Determine congener k_d values for congeners present in both the gas and particulate phase and compare to values reported in literature.
- Attempt to measure airborne OH-PCBs for the first time in both the gas and particulate phase in Chicago.
- Given OH-PCBs are detected in Chicago air, investigate temporal and spatial relationships of atmospheric OH-PCBs in Chicago

We formed the following specific hypotheses regarding each of these objectives:

- PCBs in the gas phase will be easily measureable in Chicago air and levels will be comparable to levels previously measured in Chicago and other North American cities.
- Particulate phase PCBs will be difficult to detect do to their low concentrations in the air.
- Congener profile for particulate phase PCBs will have a higher percentage of less volatile higher chlorinated homologue group PCBs than gas phase profile.
- OH-PCBs, if present, will likely favor the particulate phase as the physical chemical properties associated with having a hydroxyl group will make them more likely to adsorb to particulate matter in the air. Additionally, OH-PCBs have been reported in precipitation, and airborne particles seem a likely source to precipitation.

CHAPTER 2 MATERIALS AND METHODS

2.1 Field Study and Sampling Methods

2.1.1 Passive and Active Sampling

There are two methods of air sampling that have been employed in the Hornbuckle lab: High volume air sampling (Hi-Vol) and passive air sampling; each with their inherent advantages and disadvantages. Hi-Vol sampling is a method of active sampling in which vacuum pump draws a more or less constant flow of air through a filtering device over a measured period of time. The air passes through a quartz fiber filter (QFF) which collects particulate phase contaminants and subsequently through a polymeric adsorbent resin (XAD) to adsorb gas phase organics in the air. Passive sampling does not employ the use of a vacuum pump, but rather relies on the natural movement of air to create contact with the polyurethane foam (PUF) sampling media, and does not separate particulate and gas phase contaminants. The PUF sampler generally remains unattended in the sampling location over a period of several weeks to several months. The volume of air that comes into contact with the media is estimated from appropriate models[21]. Despite the advantages of Hi-Vol sampling, it is an energy intensive process to run the pumps, and requires constant monitoring, making it a much less cost effective option that passive sampling.

2.1.2 Field Study and Sampling Methods

The samples used in this study were collected as part of a much larger study that was part of Project 4 of the Iowa Superfund Research Program (ISRP). The aim of this project was to acquire a better understanding about the sources of atmospheric PCBs and their consequences. In total, there were over 750 samples collected from over 30 locations throughout Chicago (sampling sites shown in figure 2-1 below), the majority of which were public schools. The studied employed the use of the Hi-Vol samplers described above that were adapted by Keri Hornbuckle and Andres Martinez to fit on the back of medical clinic vans used to service children with respiratory conditions over the duration of the school day[17]. The vans remained in the school parking lots during school hours (typically 6 – 8 hours), and Dingei Hu coordinated with trained personal from the Mobile C.A.R.E. foundation of Chicago (Comprehensive Care for Chicagoland's Children with Asthma) to operate and maintain the samplers. The configuration of the samplers mounted to the asthma vans is shown below as a schematic in figure 2-2 [17] and in implementation in figure 2-3.

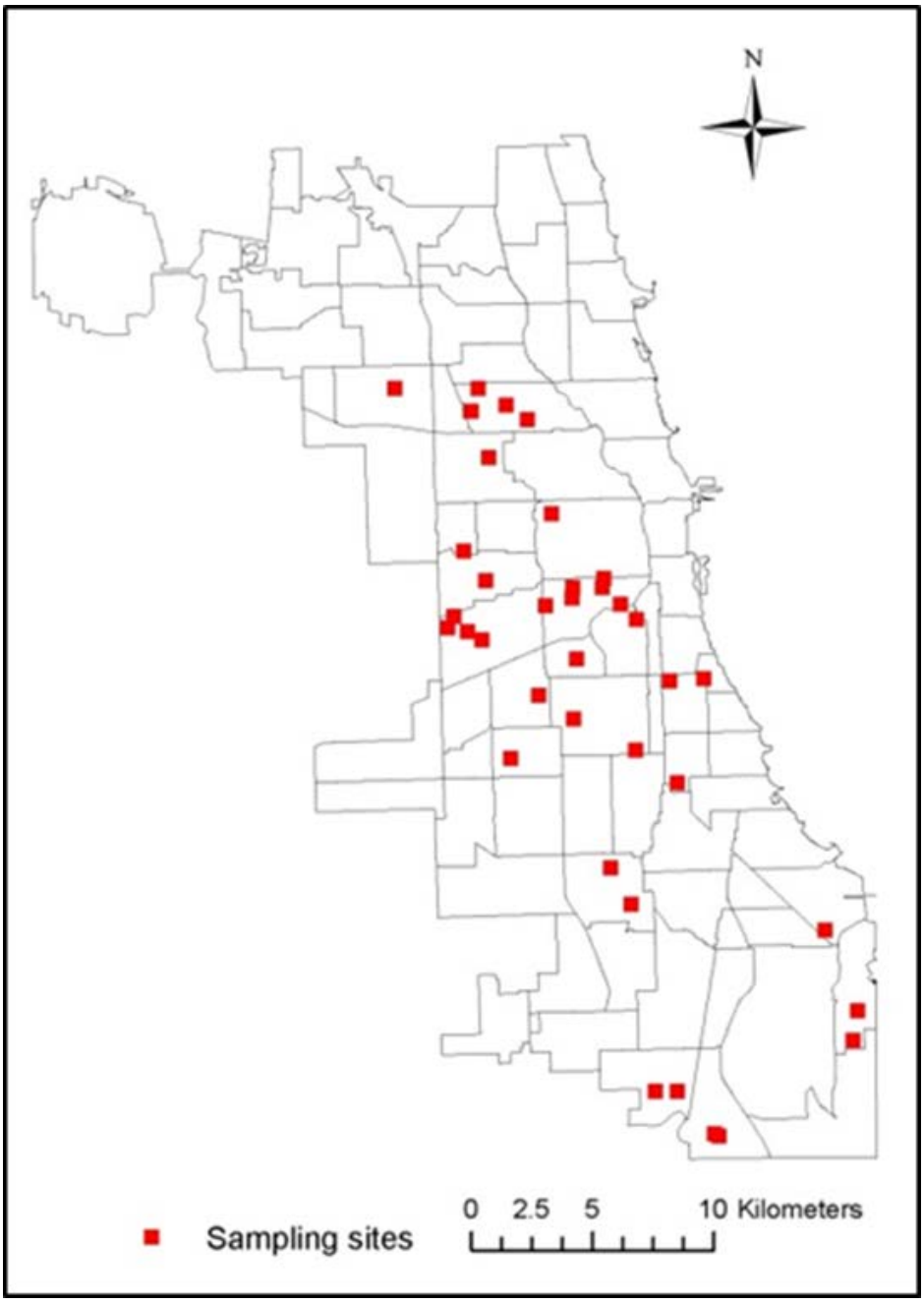

Figure 2-1: The city of Chicago shown with the sampling sites used in Project 4

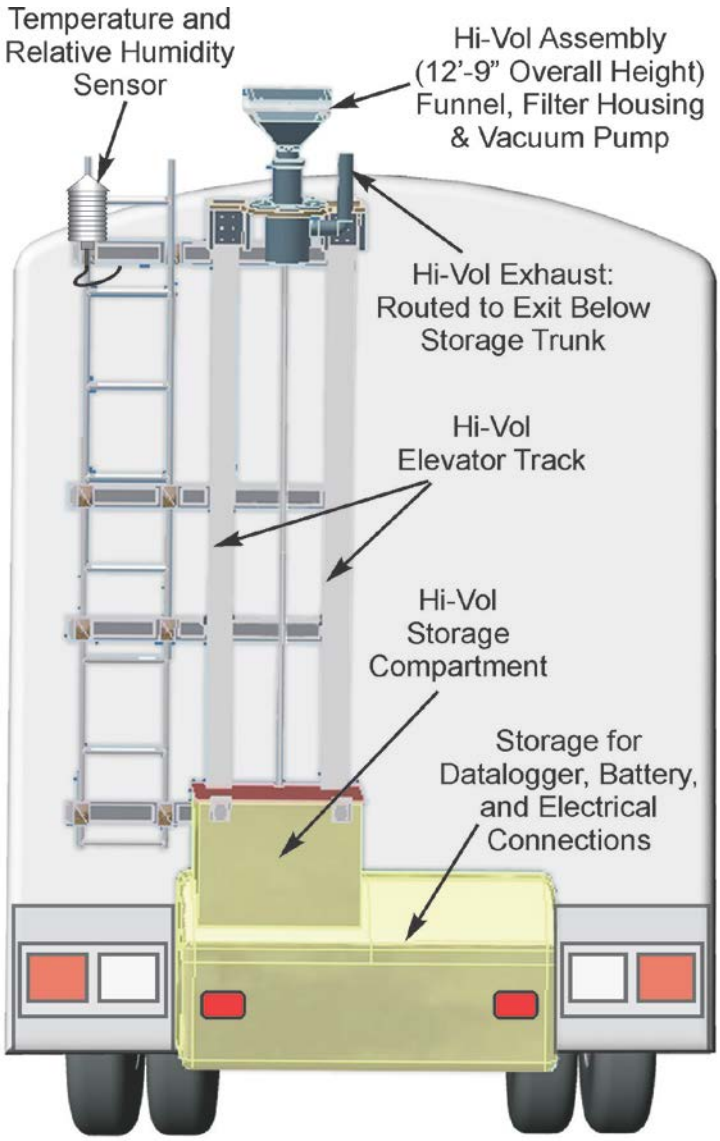

Figure 2-2: Schematic showing the detailed workings of the Hi-Vol samplers mounted to the rear of the mobile clinic vans. (Hu et al. 2008 ES&T)

Figure 2-3: Implementation of the Hi-Vol samplers onto the backs of the asthma vans (photo courtesy of Timothy Schoon, University of Iowa)

2.1.3 Sample Transport and Storage

Following collection, QFF filters were individually wrapped in combusted, labeled aluminum foil and stored in labeled zip lock plastic bags, while the XAD resins were stored in combusted, labeled amber glass jars inside of labeled zip lock bags. The samples were shipped via priority mail and stored in a freezer at -4 °F until extraction and

analysis. It has been verified that this is an effective in preventing cross contamination between samples stored in the same location for extended periods of time[22].

2.2 Sample Extraction and Processing for Analysis

2.2.1 Accelerated Solvent Extraction; the ASE 300

All extractions for this study were carried out using the ASE 300 Accelerated Solvent Extractor (ASE). In this study, PCBs and OH-PCBs were extracted from samples using a 1:1 mixture of hexane and acetone. The ASE was operated at 100 °C and 1500 psi using a method based on EPA method 3545A. The ASE operates under an eight step run, which is summarized below:

1: Cell is placed into the oven and pressurized to seal the cell
2: Solvent is pumped into the cell until it is filled
3: Cell is heated to 100 °C
4: Cell is held at a constant pressure of 1500 psi at 100 °C
5: Cell is flushed with fresh solvent to fill the collection bottle
6: Cell is purged with N_2 gas to ensure remaining solvent is in collection bottle
7: Residual pressure is released from the cell
8: Cell is unloaded from the oven and allowed to cool before sampling media is appropriately discarded

Preparation of 100 mL ASE cells began by first securing one of the lids tight, and placing a glass fiber filter at the closed end. Next the sampling media was added and spiked with PCB surrogate standards 14, D65, and 166, and OH-PCB surrogate standards 13C12, 13'C120, and 13'C 187. Before securing the top of the cell, another glass fiber filter was placed on top of the media (schematic shown in figure 2-4 below, courtesy of Colin O'Sullivan). Collection jars were prepared by securely fitting each jar with a new PTFE silicone septa (item number 288-7222) from Thermo Scientific.

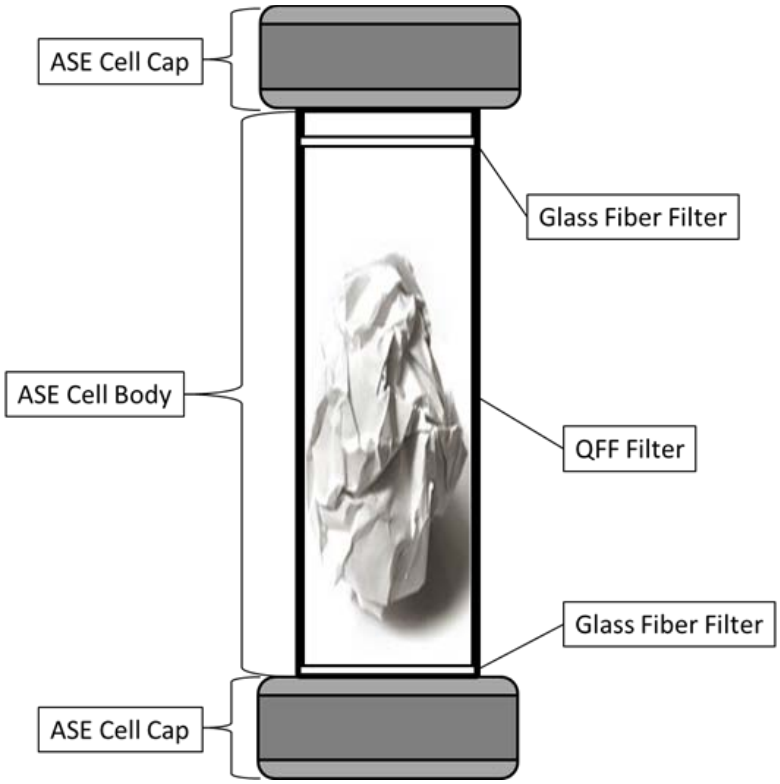

Figure 2-4: Diagram of a QFF sample in an ASE cell prior to extraction; the XAD are stored in the ASE the exact same way, and resemble small white beads in appearance

It was not uncommon during the period that these samples were being run to encounter errors on the ASE. These errors often resulted in the termination of the run sequence for the sample that was being run. When this happened, the sample was rerun and the error was documented in a laboratory notebook. Often times these errors resulted in a loss of sample, which was always accounted for in adjusting for surrogate recoveries.

2.2.2 Reference Standards

At the same time as samples and method blanks were prepared for extraction, the two separate references were created, one each containing PCB surrogate standards and OH-PCB surrogate standards. The PCB reference consisted of spiking the same amount of PCB surrogate standards used in the samples directly into a GC vial containing approximately 0.5 ml of hexane. The OH-PCB reference was created by spiking the OH-PCB surrogate standards directly into a test tube containing 10 drops of methanol. Both references were immediately stored in the freezer in 4248 SC until they were needed for either analysis, or in the case of the OH-PCB reference, until derivatization with diazomethane.

2.2.3 Sample Concentration and Reconstitution with Hexane

Extraction with the ASE 300 yields approximately 50 ml of eluent per each sample. Following extraction, the eluent was transferred from the ASE cells to 200 ml TurboVap II evaporation tube. The ASE collection jars were rinsed two times each with ~ 2 ml of hexane and the rinse was added to the samples in the TurboVap tubes. Subsequently the samples were concentrated to approximately 0.5 ml in a TurboVap II and transferred to a combusted test tube. Each TurboVap evaporation tube was rinsed with ~ 3.5 ml of

hexane which was added to the test tubes resulting in a sample volume of ~ 4 ml. At this point, the samples were ready for the separation step, but if needed they could be stored in test tubes for a period of up to a few weeks in the freezer at -4 °C.

2.2.4 PCB OH-PCB Separation

Due to their physical chemical properties, we are not able to directly analyze OH-PCBs using our GC/MS/MS, and they had to be converted to methoxylated PCBs (MeO-PCBs) by a derivatization process using diazomethane prior to GC/MS/MS analysis. Therefore it is necessary to separate the OH-PCBs from the PCBs. This was accomplished by adding 2 ml of 0.5 M potassium hydroxide in a 50% ethanol solution to the hexane in the test tubes. The aqueous solution and the organic solution do not mix, and two distinct phase layers can be seen. Because they contain a hydroxyl group, the OH-PCBs have a higher affinity toward the alkaline solution than the organic solution. To ensure adequate separation, the test tubes underwent inversion for 3 min followed by 3 min in the centrifuge adjusted to the following settings:

Rotor: 10
Speed: 3000 rpm
Temperature: 20°C.

Afterwards, the top organic layer containing PCBs was pipetted into a different test tube. Any remaining PCBs in the organic phase were re-extracted by twice adding 3 ml of hexane and repeating the inversion, centrifugation, and extraction process. After a total of three extractions, the PCB solution (~10 ml) was stored in a freezer in room 4248 SC at 0°F until cleanup with acidified silica gel (see section 2.2.10 below).

2.2.5 OH-PCB Re-extraction to Organic Phase

The OH-PCBs were in an alkaline solution, and needed to be extracted back into an organic solvent in order to carry out the derivatization. This was accomplished by first acidifying the alkaline solution by adding 1 ml of 2M hydrochloric acid and vortexing. To ensure the solution was acidic enough, a sample (not the blank) from each batch was tested to make sure it had a pH of at least 1. After checking the pH, 4 ml of a 9:1 solution of hexane:methyl tertiary butyl ether (MTBE) were added to each sample. The test tubes were inverted and centrifuged the same way as described in the separation procedure above. The OH-PCB containing solvent layer on top was then pipetted into a 40 ml TurboVap evaporation tube. This process was repeated one time with the addition of 3 ml of the hexane MTBE solution to the acidic solution. The acidic solution remained in the test tubes overnight in a fume hood to enable any remaining solvent layer to evaporate. Afterwards, the acidic solution was disposed of accordingly. The solvent containing the OH-PCBs was concentrated in the TurboVap II to a volume of ~ 0.2 ml. The concentrates were then pipetted into test tubes. The evaporation tubes were rinsed once with 10 drops of hexane and the rinse was pipetted into the transfer test tubes. 5 drops of methanol (MeOH) was added to each sample to increase the efficiency of the derivatization process (see next section). The test tubes were then marked with a permanent marker at the sample level as well as at 4 ml. Samples were then stored in the freezer in 4248 SC at 0°C until derivatization the next morning. Derivatization was always carried out no more than 24 hrs after the separtation process.

2.2.6 Derivatization of OH-PCBs to MeO-PCBs with Diazomethane

Preparation of diazomethane was carried out by Prof. Hans Joachim-Lehmler, and he supplied all of the diazomethane needed in this study.

Following separation, the OH-PCB samples and OH-PCB reference were taken to the Synthesis Core lab at the Oakdale campus at the University of Iowa where the OH-PCBs were derivatized with diazomethane to become MeO-PCBs. It should be noted here that diazomethane is an extremely hazardous compound if not handled appropriately, and only those trained in the essential safety and handling protocl by Prof. Lehmler are authorized to use it. Samples and references were derivatized by adding 0.5 ml of diazomethane solution to each test tube. Test tubes were stored in a freezer in the Synthesis Core lab for at least three hours to ensure a complete reaction with the diazomethane. After at least three hours, the samples were concentrated under a gentle flow of nitrogen gas in a ventilation hood until only one drop of sample remained to ensure all diazomethane had evaporated. Samples were then reconstituted to 4 ml with hexane and subsequently stored in the freezer in 4248 SC until cleanup, or in the case of the reference, until analysis.

Care was taken to not allow the samples to completely evaporate during this process, but occasionally one or more did dry out. However, there were no apparent differences observed in surrogate recoveries in these samples as compared to those that did not dry out.

2.2.7 MeO-PCB Lipid Removal

After reconstitution, 2 ml of concentrated sulfuric acid (12M) were added to each sample. Subsequently the samples then were inverted for two minutes and then centrifuged for five minutes using the same settings as in the separation process detailed above. After centrifugation, the MeO-PCB containing top hexane layer was pipetted into a 40 ml TurboVap tube. 3 ml of hexane was added to the sulfuric acid and this process was repeated, resulting in ~ 7 ml of hexane in the TurboVap tube. The test tubes with sulfuric acid stayed under the ventilation hood overnight to allow any residual hexane to evaporate, and the next day the acid solution was disposed of accordingly. The samples were concentrated to ~ 0.5 ml in the TurboVap II before a final cleaning step in an acidified silica gel column.

Eventually, it was deemed that this step was unnecessary for air samples, and it was eliminated from the procedure. This step was left over from the modification process of a method for extracting OH-PCBs from sediment. Sediment samples contain many more unwanted contaminants that air samples, and the sulfuric acid cleanup is necessary to prepare those samples for GC/MS/MS analysis.

2.2.8 MeO-PCB Sample Cleanup with Acidified Silica Gel

After the lipid removal, various contaminants still remained in solution with the MeO-PCBs that needed to be removed prior to analysis on the GC/MS/MS. Acidified silica gel cleanup columns were made using combusted 9” pasture pipettes, combusted glass wool, combusted silica gel, and a 2:1 mixture of combusted silica gel and 12M concentrated sulfuric acid. Under a ventilation hood, a small amount of combusted glass wool was

placed in the bottom of the funnel of the pipette. Approximately 0.1 g of combusted silica was added followed by approximately 1 g of acidified silica gel. These columns were prepared immediately before use. When one becomes familiar with this process, it can easily be accomplished while the samples are concentrating in the TurboVap. When the acidified silica gel columns were completed, they were placed in a specially designed holding apparatus, and the samples were passed through the columns into a clean 40 ml TurboVap tube (setup shown in figure 2-5 below). The TurboVap tubes containing the original samples were rinsed twice with 10 drops of hexane into the columns to remove any remaining MeO-PCBs. The columns were then rinsed with 10 ml of methylene chloride.

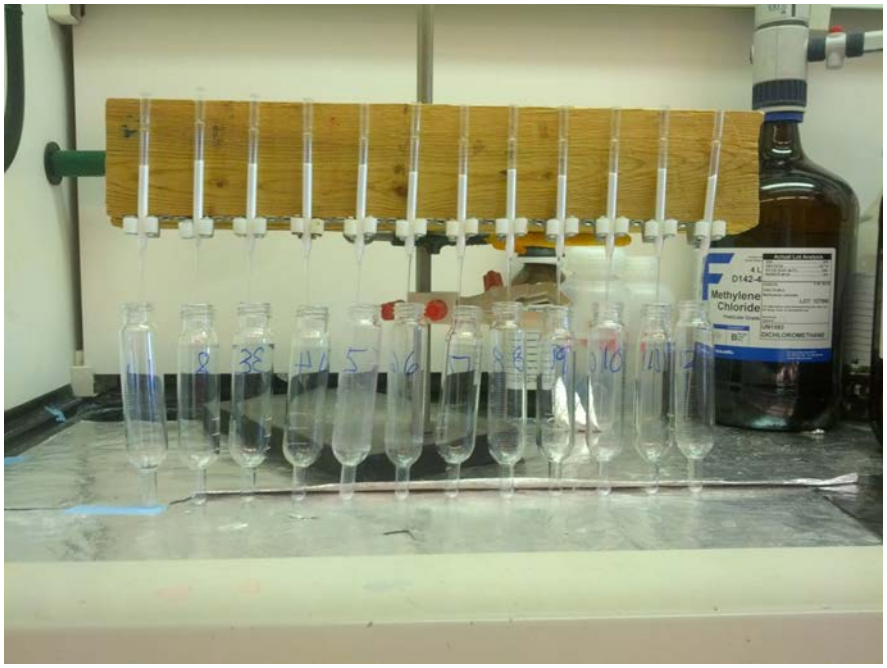

Figure 2-5: Acidified silica gel columns for used in cleaning of PCB and MeO-PCB samples eluted into TurboVap tubes

2.2.9 MeO-PCB Sample Solvent Exchange and Transfer to GC Vials

After the samples were run through the acidified silica gel columns, a solvent exchange was performed to change the solvent from methylene chloride to hexane. The samples were concentrated to 0.5 ml in the TurboVap tubes in the TurboVap II. 2 ml of hexane was added to each sample and they were again concentrated to a volume of 0.5 ml, then 1 ml of hexane was added to the samples and they were concentrated to a volume of ~ 0.1 ml. At this point, the samples were transferred to a 2 ml GC sample vial containing a Wheaton Cat. No. 225350-631 limited volume insert. At this time, the reference was also concentrated to ~ 0.1 ml and transferred to a GC vial. Samples and the reference TurboVap tubes were rinsed twice with 10 drops of hexane which was pipetted into the inserts in the GC vials. The GC vials were left in the fume hood and allowed to evaporate until the samples and the reference reached ~ 0.2 ml, which is approximately when the level of solution in the insert is at the 0.5 ml point on the GC vial. At this point, the samples were spiked with internal standard and capped before running on the GC/MS/MS.

2.2.10 PCB Sample Cleanup with Acidified Silica Gel

The process for PCB cleanup and preparation is quite a bit less involved than for OH-PCBs. After the separation, the PCBs were stored in a solution of ~ 10 ml of hexane in test tubes in the freezer in 4248 SC at 0°F. These samples were transferred to 40 ml TurboVap tubes and the test tubes were rinsed into the TurboVap tubes twice with approximately 2 ml of hexane. The samples were concentrated to 0.5 ml and run through acidified silica gel columns that were set up identically to the method described above for the cleanup of OH-PCBs. The TurboVap tubes containing PCB samples were rinsed with

5 mls of hexane which was run through the columns. An additional 5 mls of hexane was also run through each column resulting in a final volume of 10 ml.

When the PCB samples came from filters, they were concentrated and transferred to GC vial inserts the same way as the OH-PCBs, where they also remained under the fume hood until the final insert volume was approximately at the 0.5 ml mark on the GC vial and they were ready to be spiked with internal standard and analyzed.

If the PCB samples came from XAD resins, the concentrations were high enough that inserts were not needed. The samples were concentrated to 0.5 ml and transferred to GC vials before being spiked with internal standard and analyzed. No rinsing of the TurboVap tubes was necessary. Occasionally, the PCB samples from XADs were too dirty and needed to be run through columns multiple times. Additional cleaning was determined to be necessary if the sample was not completely clear after concentration.

2.3 Sample Analysis Using GC/MS/MS

2.3.1 Instrumental Analysis Methods and Run Parameters

This study used a modified version of EPA method 1668C[23] for PCB analysis. The major differences include the use of Tandem Mass Spectrometry GC/MS/MS in place of high resolution mass spectrometry, and the use of three surrogate standards and two internal standards as opposed to the 20+ radiolabeled PCB congener standards used in the EPA method[22, 23]. An Agilent Technologies 7890A BC in series with an Agilent Technologies 7000 GC/MS Triple Quadrupole were used to separate and identify all of the 209 and PCB congeners as well as the two deuterated compounds. The data output from this process was provided in the form of a chromatogram, in which the size of the

peak corresponding to a compound is directly related to the concentration of the compound in the injected solution. Due to the modifications of the method used in this study, some of the 209 PCB congeners coeluted, and we therefore detected 176 peaks, including 5 peaks for the surrogate and internal standards. Adjusting for standards, we measured for 206 PCB congeners among 171 distinct peaks. The operational details parameters for the GC/MS/MS can be found in detail elsewhere[24].

MeO-PCBs were analyzed using the same Agilent technologies GC/MS/MS set up as described for the PCBs. The operational methods for analyzing MeO-PCBs can be found in detail elsewhere[16]. Briefly, 65 OH-PCBS (as MeO-PCB standards) were identified as 59 individual or coeluting peaks from our calibration standards. Although there are 837 theoretical mono-hydroxylated PCB congeners alone[25],standards are not yet commercially available for all of them. The standards used in this study are the standards that were available at the time.

2.3.2 Congener Mass Determination from GC/MS/MS Chromatograms

Due to the nature of how the PCB and OH-PCB congeners fractionate and are detected by our instruments, each PCB an OH-PCB has a unique peak size to congener concentration response; meaning that peak size alone cannot directly give us the concentration or mass of any one congener in our sample solution. This is accounted for by using the calibration standards to determine a relative response factor (RRF) for each of the 176 peaks in the PCB chromatograms and the 59 peaks in the OH-PCB chromatograms for every calibration standard run with a sample batch. The RRF is a ratio that allows us to calculate the unknown mass of a compound in a solution (any given PCB or OH-PCB congener in a sample) given that we know the mass of at least one compound in solution (internal standards injected right before GC/MS/MS), so long

as we have a reference solution for which we know either the masses or concentrations of both compounds of interest (our calibration standard). The RRF is defined as follows:

$$RRF = \frac{\left(\frac{conc_{Cal,PCBi}}{area_{Cal,PCBi}}\right)}{\left(\frac{conc_{cal\ int\ std,PCBi}}{area_{cal\ int\ std,PCBi}}\right)}$$

Where $conc_{cal,PCBi}$ is concentration of either PCB_i, or OH-PCB_i in the calibration standard solution, and $area_{cal,PCBi}$ is the unit area of either PCB_i, or OH-PCB_i and $conccal_{\ int\ std,PCBi}$ and $area_{cal\ int\ std,\ PCBi}$ pertain to the respective concentrations and areas in the calibration standard solution of the PCB congener used as internal standard in the samples and references. The RRF for the mono to penta chlorinated PCB congeners was calculated using PCB D-30 as the internal standard compound; the hexa through decachlorinated PCB congeners used PCB 204 to calculate their respective RRFs. All of the OH-PCBs used PCB 204 as the only standard to calculate RRF values. The reason for doing this was because the method run for OH-PCBs exhibited unusually high sensitivity to PCB D-30, and the peaks were unusually large, often times exceeding the window of quantification in the MassHunter software. Note that the RRF for the internal standards will always be one.

Once the RRF values are calculated, the mass of an individual compound in solution, including surrogate standards in both the samples and the reference vials, can be calculated by applying the following formula

$$mass_{PCBi} = n \times RRF \times area_{PCBi} \times \left(\frac{mass_{int\ std,PCBi}}{Area_{int\ std,PCBi}}\right)$$

where $mass_{PCBi}$ is the calculated mass of the PCB in the sample, n is the number of PCBs that coelute in one peak, $mass_{int\ std,\ PCBi}$ is the konwn mass of internal standard added before the analysis run, and $area_{PCBi}$ is the unit area under the PCB's peak in the sample chromatogram. Note that calculated mass for an internal standard using the above formula will always equal exactly what was injected into the sample.

Note that the RRF returns the total mass of a congener contained in a sample solution, and not its concentration. This is because in the formula above, we use the mass of the internal standard injected directly into the GC vial. This gives us the inherent advantage of not needing to know the precise volume of sample solution in the GC vial, or even injected into the instrument. After all, it is the ratio of internal standard to sample congener that matters, and this remains the same whether considering concentration or mass.

Since the reference vials remain untouched throughout the sample processing, the mass calculated for the surrogate standards in the reference are taken to be true masses, without any losses. Once the surrogate masses are calculated, they can be used to calculate the percent of surrogates recovered in the samples by applying the following formula

$$\%_{recovery} = \frac{mass_{surrogate\ std,sample}}{mass_{surrogate\ std,ref}} \times 100$$

where $mass_{PCBi}$ is the measured mass of PCB_i or OH-PCB_i in the sample, *n* is the number of PCBs or OH-PCBs that coelute in one peak, and $area_{PCBi}$ is the measured area under the peak for PCB_i or OH-PCB_i in the sample. The percent recovery of the surrogates in a sample is used to approximate initial masses of PCBs by applying the following formula

$$mass_{cor,PCBi} = \frac{mass_{PCBi}}{\%_{recovery}}$$

Where $mass_{cor,PCBi}$ is the mass before losses, and is dependent on which surrogate recovery is used. In our lab, we use recoveries of PCB 14 to correct for the mono – trichlorobyphenyls, PCB D-65 for the tetra – hexachlorobiphenyls, and PCB 166 for the hepta – decachlorobipheynl.

It should be noted that the mass of the surrogates calculated in the references is never exactly what was added (usually about 70 - 80%). This is part of the inherent variability in conducting experiments of this nature. There is always some degree of both human error and instrument error that will introduce inconsistencies from one run to the next, no matter how careful the operator is. Nonetheless, the calculated surrogate masses were taken to be the true masses present at the beginning of the sampling procedure. This is perhaps the only thing that is taken for granted in the entire process from sample extraction to final quantification.

After individual congener masses were calculated, concentrations were found by using the following formula

$$conc_{PCBi} = \frac{mass_{PCBi}}{volume_{air}}$$

Where $conc_{PCBi}$ is the concentration of PCB_i or OH-PCB_i and $volume_{air}$ is the volume of air that passed through the Hi-Vol sampler calculated

$$volume_{air} = r \times t$$

Where r is the sampling rate of $0.4 m^3 s^{-1}$ and t is the sampling time, in seconds.

2.4 Quality Assurance and Quality Control

2.4.1 Laboratory Maintenance

Method integrity is maintained and ensured by diligently maintaining the laboratory and following strict protocol for cleaning lab equipment. All non-disposable laboratory equipment was always thoroughly washed either by hand or in a laboratory glassware dishwasher, and subsequently either combusted overnight at 450 °C or cleaned by an extensive rinsing process with methanol, hexane, and acetone to remove any potential contaminants.

2.4.2 Method Blanks

In addition to the laboratory maintenance mentioned above, method blanks of the same media (either a QFF or ~20 grams of XAD resin) were run identically to the samples with

each batch to monitor potential contamination from glassware, chemicals, and any other unknown sources that could be introduced over the course of sample processing. These method blanks were used in determining the limits of quantification (LOQ) for this study.

2.4.3 Mysterious Peaks

It seems to be the case that, no matter how careful and well intentioned one is in the lab, contamination issues can arise from time to time. There was a contamination issue that arose in our lab that affected not only this study, but everyone who was running air samples and using our same standards at the time. The contamination was discovered when looking at a batch of OH-PCB samples I had run. There were strange peaks that appeared at consistent intervals in some of the same mass transitions and eluted at times very close to some the congeners I was interested in looking at. Not only were these peaks an issue because I couldn't identify the congeners they eluted with, but their presence gave reason to doubt the validity of the other peaks as well – it isn't good for any study, especially one as novel as this, to introduce any doubt into the methods or results.

The study was put on hold for some time while this process was investigated further. Credit goes primarily to Andres Martinez, Nick Herckert, and Sean Nichols for their diligent efforts in getting to the bottom of this. They tested literally every variable that could possibly be introduced to our laboratory methods from purity of the chemicals we use to the quality of our combustion and glass cleaning methods. Everything that was tested kept coming back as a non-potential contamination source, until finally it was discovered that the contamination was coming from a new method of storing our standards. In an effort to streamline the process of injecting samples with standards, I

had changed the lids that sealed our surrogate and internal standards while they were stored. I had replaced the VICI Precision Sampling, Inc. Mininert Valves for Septum Bottles that we were using with Thermo Fischer Scientific PTFE Silicone Septa.

The Mininert Valves have a rubber stopper that the injections syringe is inserted to to draw up sample. It that works well for a short period of time, but is prone to breaking down quickly. When it starts to break down, standard leaks out of the cap and is lost. This poses a problem because it increases chances of exposure to hazardous chemicals. Also, our standards are very expensive, and any unnecessary loss should be avoided. By using the septa, I eliminated the issue of sample loss because they are essentially leak proof, and I eliminated the issue of potential breakdown over time by replacing them every time they were punctured with a syringe.

It was discovered by Sean Lawrence that the material the septa are made out of are prone to breaking down when exposed to caustic chemicals, such as the solvents we used to store our standards. Upon learning this, we reverted to using the Mininert Valves, and are now more diligent about replacing them. The septa contamination could be removed by again running the processed sample through acidified silica gel. The samples were rerun and no evidence of the septa contamination could be seen. Figure 2-6 shows one of the contaminated transitions as it aligned with an MeO-PCB congener in the calibration standard before it was run through acidified silica gel. Figure 2-7 is that same sample transition after performing cleanup with acidified silica gel.

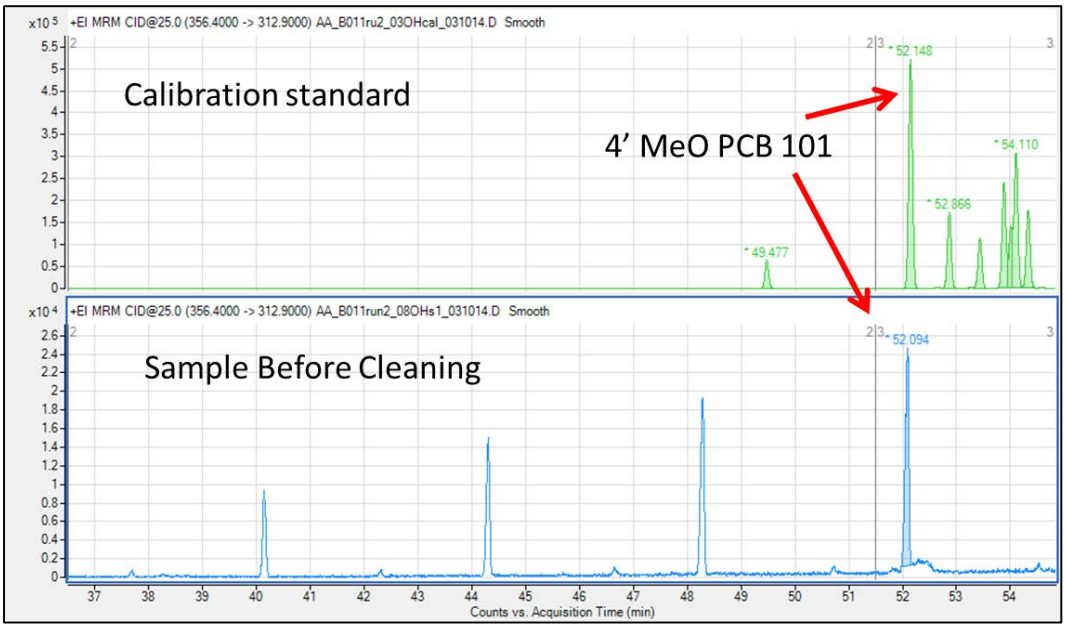

Figure 2-6: Chromatogram of a sample with the septa contamination prior to acidified silica gel cleaning

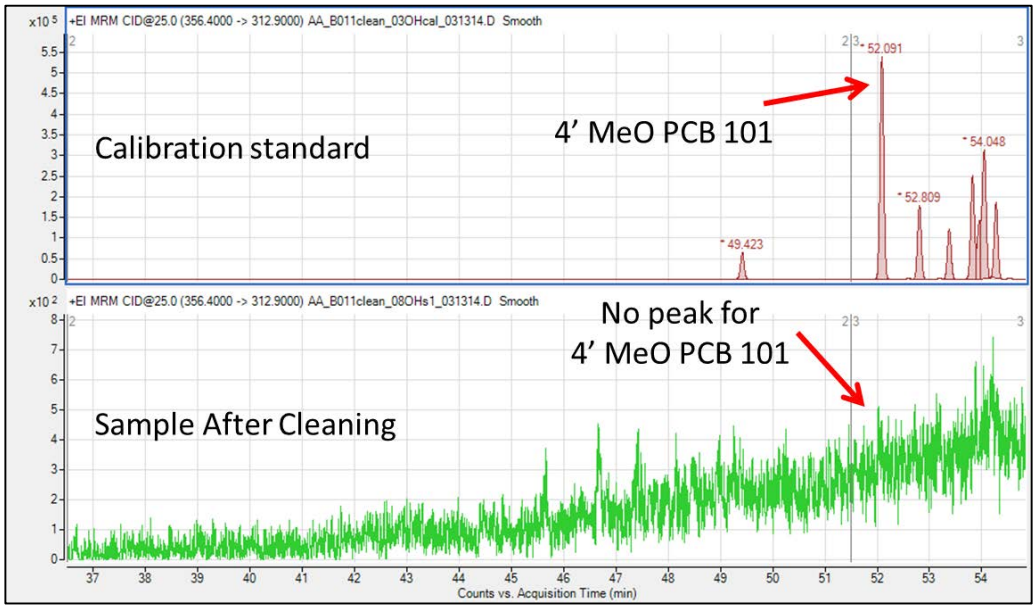

Figure 2-7: Chromatogram of the same sample shown in figure 2-6 after acidified silica gel cleaning

CHAPTER 3 RESULTS AND DISCUSSION

3.1. Introduction

Particulate and gas phase PCB and OH-PCB concentrations were measured at ten different elementary schools in Chicago: Adams, Carver, Guadalupe Reyes, Monroe, St. Columbanus, Zapata, Metcalf, Marquette, Owens, and Washington Park Academy. In total, thirty-one XAD resins were analyzed gas phase PCB and OH-PCB concentrations, and thirty QFF were analyzed for particulate phase PCB and OH-PCB concentrations. Among these, twenty-three corresponded to XAD and QFF pairs that were collected during a single sampling cycle. Samples were selected from a larger collection of samples that were collected as part of Project 4 of the Iowa Superfund Research Program. Weather data for each sampling period was obtained from historical weather records for Midway Airport in Chicago IL using weatherunderground.com. This website was chosen because it contains an easily accessible historical database of hourly weather conditions collected from Automated Surface Observation Systems maintained by the Federal Aviation Administration for over 2000 airports across the country [26].

3.2 Gas-Phase PCBs in Chicago Air

3.2.1 Gas-Phase PCB concentrations

Gas-phase PCBs account for the vast majority of airborne PCBs[26] and are the phase where where correlations in PCB concentrations with temperature, season, and location have been previously observed[8, 17, 27-32]. In total, thirty XAD resin samples from ten different locations were analyzed for gas-phase PCB concentrations. Concentrations ranged from 43.1 pg/m^3 to 2250 pg/m^3, with an average concentration of 594 pg/m^3 ± 445 pg/m^3. These values are in good agreement with values previously reported for Chicago, as well as other urban areas in North America using both active and passive sampling methods[8, 22, 31, 33-39]. Figure 3-1 below provides a summary of results for the ∑PCB concentrations from several different studies.

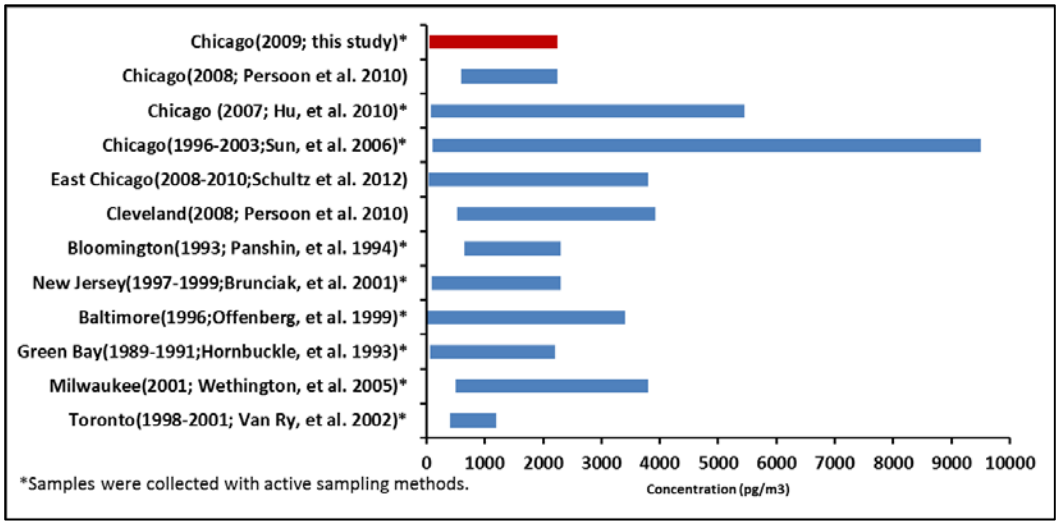

Figure 3-1: ∑PCB Concentration ranges reported in the air of urban areas in North America

3.2.2 Temporal Trends in Gas Phase PCBs

We observed large day to day variations in ∑PCB concentrations, as was predicted[40]. We found this variability to have a strong correlation to temperature. Figure 3-2 and Table 3-1 below show measured gas-phase PCB concentrations for the thirty XAD samples arranged by collections date, irrespective of the sampling locations. Also plotted is the average temperature (°C) over the sampling period of each sample.

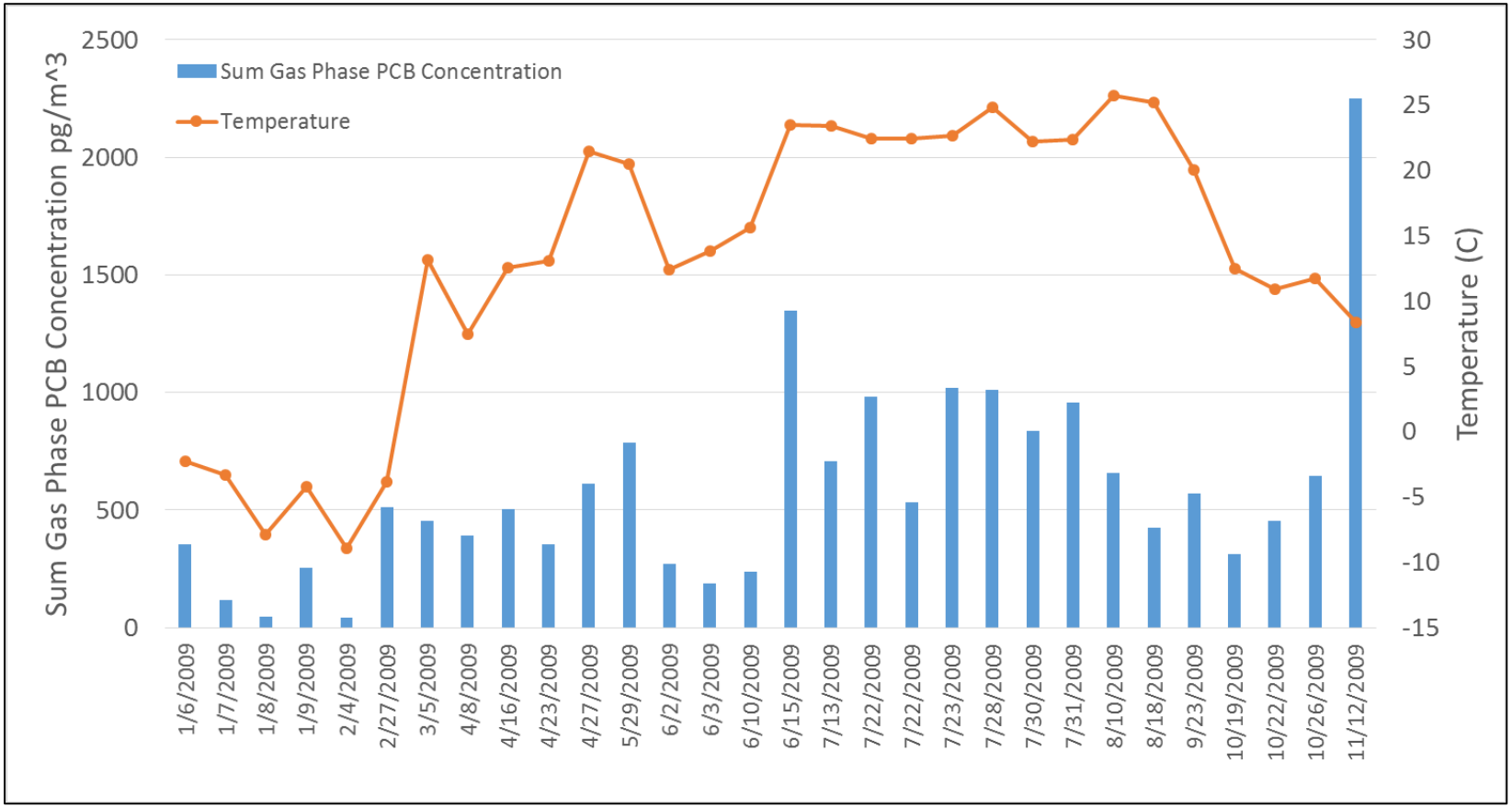

Figure 3-2: ∑Gas-phase PCB concentrations with temperatures and collection dates for the ten sites examined in this study

Table 3-1: ∑Gas-phase PCB concentrations and collection temperatures for the ten sties examined in this study

Collection Date	Location	∑ Gas-phase PCB Concentration pg/m3	Temperature °C
1/6/2009	Zapata	353.1	-2.3
1/7/2009	St. Columbanus	117.0	-3.3
1/8/2009	Monroe	46.8	-7.9
1/9/2009	Metcalf	253.1	-4.2
2/4/2009	Guad Reyes	43.1	-9.0
2/27/2009	Carver	511.2	-3.8
3/5/2009	Guad Reyes	452.0	13.2
4/8/2009	St. Columbanus	393.3	7.5
4/16/2009	Monroe	502.5	12.6
4/23/2009	Metcalf	356.0	13.1
4/27/2009	Carver	611.4	21.5
5/29/2009	Zapata	785.4	20.5
6/2/2009	Adams	272.4	12.4
6/3/2009	St. Columbanus	186.3	13.8
6/10/2009	Wash Park Acad	236.9	15.7
6/15/2009	Owens	1348.2	23.5
7/13/2009	Carver	707.2	23.4
7/22/2009	Monroe	981.2	22.4
7/22/2009	St. Columbanus	531.7	22.4
7/23/2009	Marquette	1019.0	22.6
7/28/2009	Monroe	1010.8	24.9
7/30/2009	Zapata	838.6	22.2
7/31/2009	Guad Reyes	955.6	22.4
8/10/2009	Guad Reyes	658.9	25.7
8/18/2009	Metcalf	425.2	25.2
9/23/2009	Carver	568.5	20.1
10/19/2009	St. Columbanus	312.4	12.5
10/22/2009	Zapata	452.9	10.9
10/26/2009	Monroe	646.5	11.7
11/12/2009	Metcalf	2251.9	8.4

There is a general trend between measured ∑gas-phase PCB concentrations and temperature between these Chicago sites (figure 3-2, table 3-1). With the exception of one unusually high sample collected in mid-November and a few unusually low samples collected in early June, gas phase PCB concentrations are higher when temperatures are higher.

3.2.3 Temporal Trends in Gas-Phase PCBs Specific to Site

Previous research suggests that although PCB congener profiles across Chicago share many similarities among different sampling sites, the temperature dependence of ∑PCBs can vary significantly[8]. Of the ten total sites we looked at, six had samples collected from at least three different dates throughout the year. Using temperature data obtained from an Automated Surface Observation Systems maintained by the Federal Aviation Administration for Midway Airport in Chicago[26], we were able to look at temperature dependences and temporal trends for these six sites in Chicago. Figure 3-3 and Table 3-2 below provide a summary of these six sites and their measured concentrations and average temperatures over the sampling period.

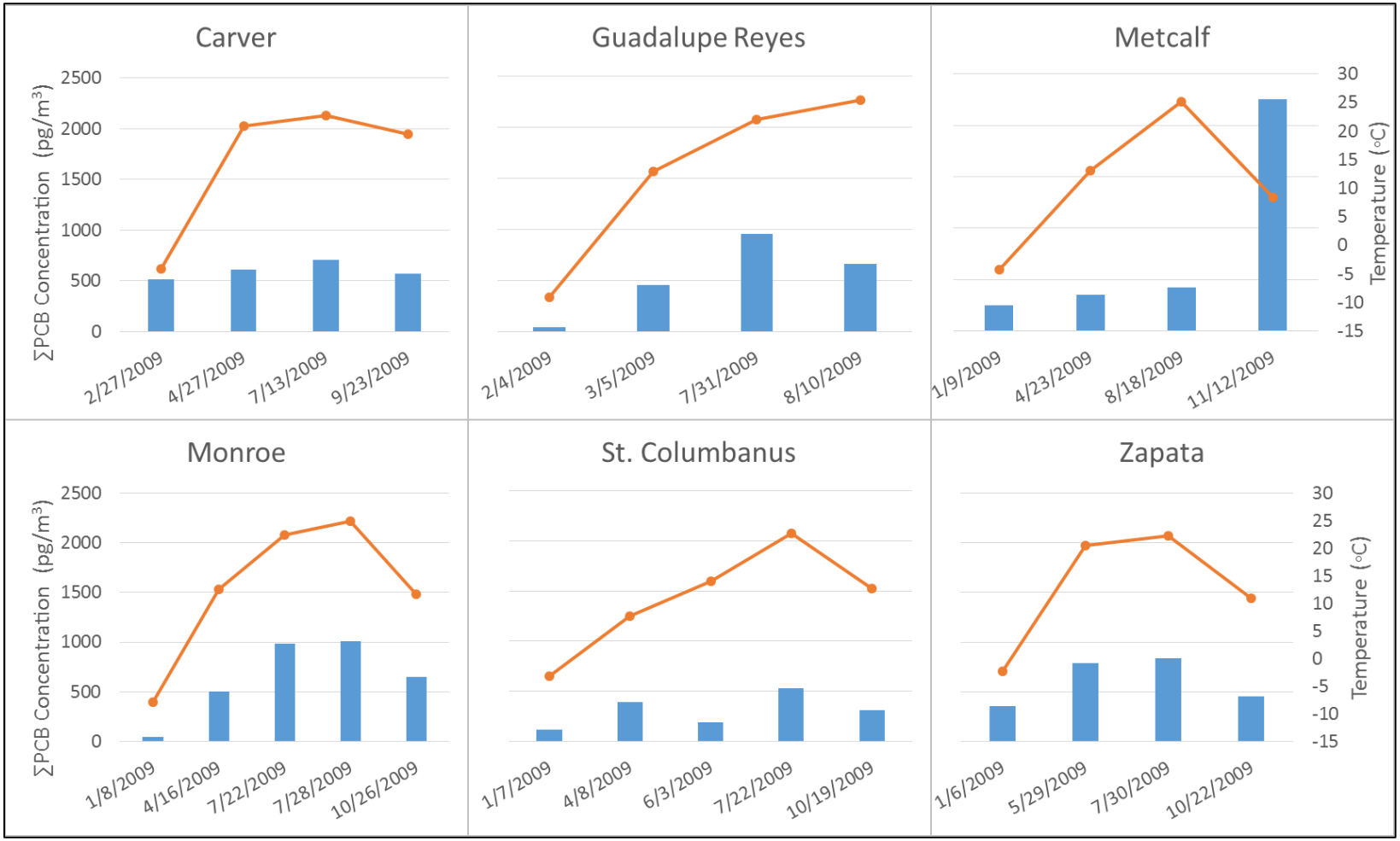

Figure 3-3: Gas-phase ∑PCB concentrations and temperatures for six locations in Chicago by collections date

Table 3-2: ∑Gas-phase PCB concentrations with collection date and temperatures for the six sties with at least 4 samples examined in this study

Location	Collection Date	∑ Gas-phase PCB Concnentration pg/m^3	Temperature °C
Carver	2/27/2009	511.2	-3.8
	4/27/2009	611.4	21.5
	7/13/2009	707.2	23.4
	9/23/2009	568.5	20.1
Guad Reyes	2/4/2009	43.1	-9.0
	3/5/2009	452.0	13.2
	7/31/2009	955.6	22.4
	8/10/2009	658.9	25.7
Metcalf	1/9/2009	253.1	-4.2
	4/23/2009	356.0	13.1
	8/18/2009	425.2	25.2
	11/12/2009	2251.9	8.4
Monroe	1/8/2009	46.8	-7.9
	4/16/2009	502.5	12.6
	7/22/2009	981.2	22.4
	7/28/2009	1010.8	24.9
	10/26/2009	646.5	11.7
St. Columbanus	1/7/2009	117.0	-3.3
	4/8/2009	393.3	7.5
	6/3/2009	186.3	13.8
	7/22/2009	531.7	22.4
	10/19/2009	312.4	12.5
Zapata	1/6/2009	353.1	-2.3
	5/29/2009	785.4	20.5
	7/30/2009	838.6	22.2
	10/22/2009	452.9	10.9

Data for the six sites shown in figure 3-3 and Table 3-2, shows that temperature plays a major role in gas phase ∑PCB concentrations when you consider samples on a site by site basis. For four of the six sites, the highest ∑PCB concentrations were measured on the date with the highest temperatures, and the lowest ∑PCB concentrations coincided with

the coldest collection temperatures for every site. For the majority of these sites, ∑PCB concentrations are almost always higher when temperatures are higher. For Carver, Monroe, and Zapata, it is always the case that higher air temperatures have higher ∑PCB concentrations. For Guadalupe Reyes, the sample collected on August 10, 2009 at an average collection temperature of 25.7 °C has ∑PCB concentration of 659 pg/m^3 while the sample collected on July 31, 2009 at an average collection temperature of 22.4 °C has a ∑PCB concentration of 956 pg/m^3. Of the four samples analyzed for Guadalupe Reyes, these were the two samples containing the highest ∑PCB concentrations and were sampled at the two warmest temperatures. Similarly, at St. Columbanus, there was not always a perfect correlation between ∑PCB concentrations and temperature. Among the five samples analyzed from St. Columbanus, the highest ∑PCB concentrations was measured on the day with the warmest temperature, and the lowest ∑PCB concentration was measured on the day with the coldest temperature. However, the other three samples collected from this site do not fit the trend as well. One of these samples was among those collected in early June, which, as mentioned above, seem to have unexpectedly low ∑PCB concentrations. Of all of the samples that were analyzed for gas-phase PCBs in the study, there is one that stands out among all of the others. Sample AA011-03, collected at Metcalf on November 12, 2009, has a total PCB concentration of 2252 pg/m^3. Not only is this is more than twice the concentration of the next highest samples, but it was collected on of the comparatively cooler temperatures of 8.4 °C, for which concentrations of other samples are more in the range of 500 pg/m^3.

3.2.4 The Clausius-Clayperon Relationship as it Applies to ∑PCBs

Assuming ideal gas behavior, gas-phase PCBs can be described thermodynamically by the Clausius-Claperyon equation[28]

$$lnP = \frac{-\Delta H_v}{RT} + const$$

where P is the gas-phase partial pressure (atm), ΔH_v is the enthalpy of vaporization, R is the gas constant (kJ/mol) and T is the average atmospheric temperature (Kelvin) over the sampling period. Figure 3-4 below shows the natural logarithm of the partial pressure (atm) of total PCBs (calculated by adding the partial pressures of all of the individual congeners) plotted against the inverse of the average temperature (Kelvin) recorded for the sampling period for the ten sites sampled in Chicago.

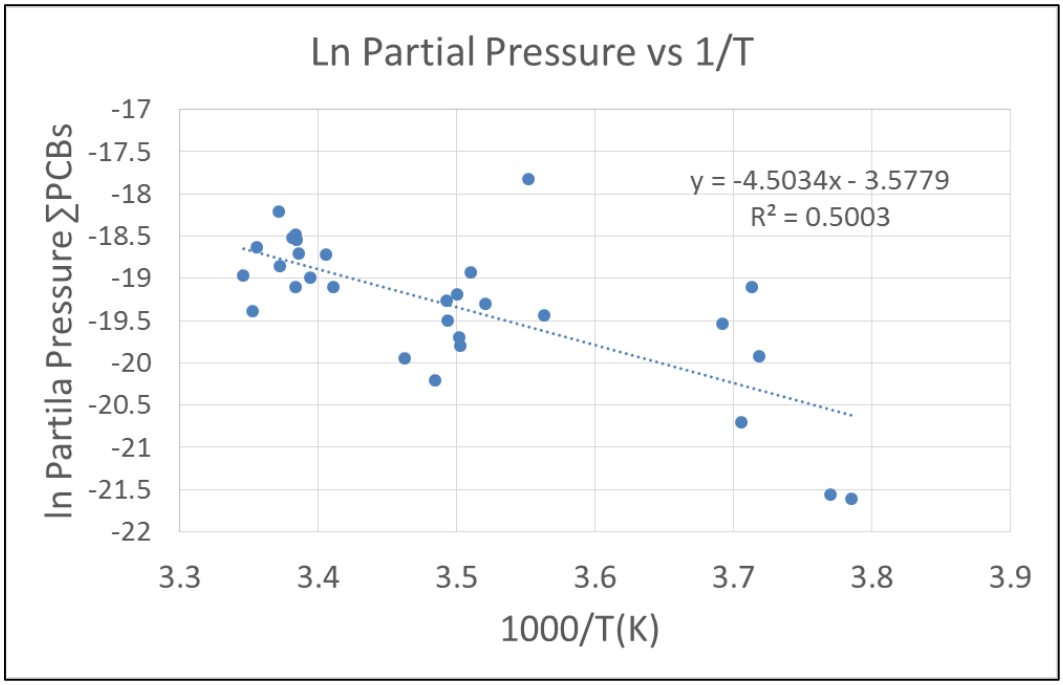

Figure 3-4: Clausius-Clayperon plots relating natural logarithms of partial pressure of ∑PCBs (atm) to the inverse of temperature (K)

Figure 3-4 shows that the natural logarithm of the partial ∑PCB decreases with the inverse of the temperature. The linear regression equation shown in figure 3-4, along with the Clausius-Clayperon equation, can be used to calculate the heat of vaporization for PCBs in Chicago. Applying these, we get a heat of vaporization of for Chicago of 37kJ/mol. This value agrees extremely well with the values reported for environmental samples by Hilery et al. (37 – 38 kJ/mol)[28] for samples collected on the shores of the Great Lakes, but are about half of the heats of vaporization for PCBs reported in controlled laboratory studies conducted by Falconer and Bidleman[41]. Falconer and Bidleman reported heats of vaporization ranging from 75 kJ/mol – 100 kJ/mol for trichlorinated biphenyls through octochlorinated biphenyls. Additionally, our value for heat of vaporization for PCBs is less than those reported in other environmental studies as well. Hoff et al.[42] reported heats of vaporization for atmospheric PCBs in Egbert, Ontario of 74 +/- 10 kJ/mol, and Panshin and Hites[36] gave a heat of vaporization for

atmospheric PCBs of 63 +/- 16 kJ/mol. Both of these studies share in common that they agree well with the laboratory values reported by Falconer and Bidleman, and that they were both carried out over land, far away from any large bodies of water. Similarly, Wania et al.[32] reported heats of vaporization for PCBs in the range of 45 – 74 kJ/mol. According to Hilery et al., atmospheric PCBs are predominately of the tri, tetra, and pentachlorinated homologue groups, and heats of vaporization for environmental samples would be expected to be at the lower end of the range reported by Falconer and Bidleman[28]. Still, this does not account for the large discrepancy between the laboratory values and the values reported in other studies. One possible explanation for this is that Chicago is located right on Lake Michigan. Our values for heat of vaporization of PCBs are consistent with those reported by Hilery et al., which were calculated from samples collected on the Shores of the Lake Superior, Lake Michigan, and Lake Erie. According to Hilery et al.[28] and Simick et al.[30], it is likely that factors related to air-water exchange of PCBs would result in lower heats of vaporization. Factors such as aqueous solubility of PCBs begin to affect the liquid to vapor phase transfer process. Because PCBs have such low affinity for water (solubilities of 10^{-5} – 10^{11} mol/L), the rejection of PCBs from water bodies could effectively lower the energy required for water-air phase transfer in comparison to land-air phase transfer.

Furthermore, Simick et al. say that in the real world heat of phase change is actually the energy needed to transfer from surfaces such as soil and vegetation, in addition to water in the atmosphere, and consequently the heat of phase transfer can be quite less than the heat of vaporization. They conclude that it is more appropriate to consider the enthalpy of surface-air exchange, $\Delta H_{sa,}$ instead of heat of vaporization. Considering this, our value for energy of phase transfer of 37kJ/mol seems more in agreement with what would be expected from environmental samples taken near a large body of water.

For six of the ten sites in this study, we measured gas phase PCB concentrations for at least four different dates throughout the year. We examined the relationship between partial pressure and temperature for these sites more closely. Figure 3-5 below shows the Clausius-Clayperon equation applied to these sites.

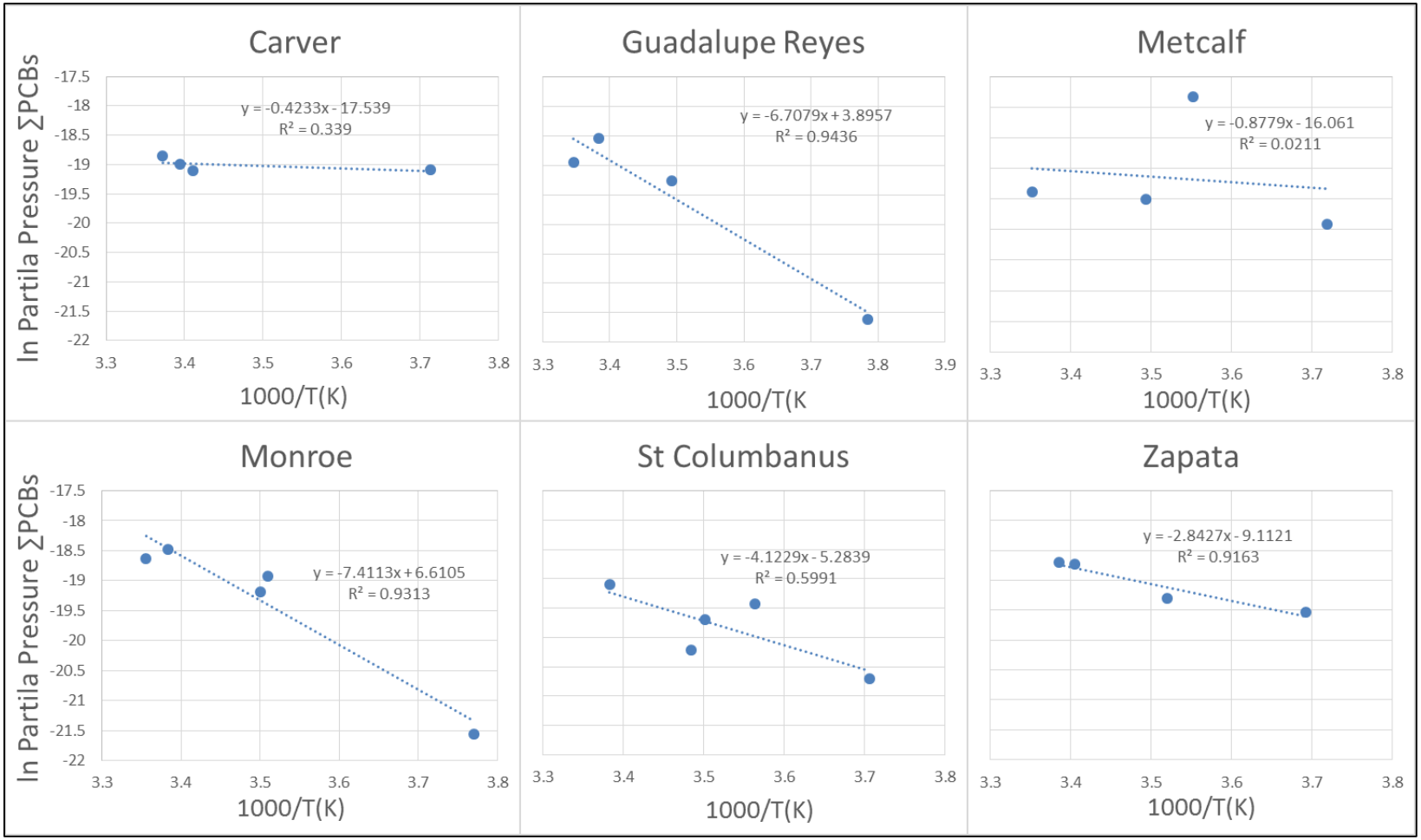

Figure 3-5: Clausius-Clayperon relationship applied to ∑PCBs for individual sites across Chicago. Plotted is the natural logarithm of the partial pressure contributed in the atmosphere from ∑PCBs against 1000 times the inverse of absolute temperature for the sampling period; also displayed are the equation for the linear regressions and the R^2 value

Figure 3-5 confirms that the correlation between temperature and partial pressure is stronger when looking at individual sites, which makes perfect sense considering that although similar, short range volatilization sources will be unique to each site. The Clausius-Clayperon relationship fits the data Guadalupe Reyes, Monroe, and Zapata remarkably well; all sites have R^2 values >0.91. At St. Columbanus, the R^2 vaule is 0.6, indicating that there is still a strong correlation, but it is not clear that volatilization is the only major source. Of the four samples collected at Carver, three were collected at very similar temperatures as opposed to the fourth, yet all samples contained very similar concentrations of total PCBs. The winter sample had much higher concentrations than expected of PCB3, comprising about half of the total PCBs in the sample, which could account for the poor fit of the model. In fact, when this sample is removed, the R^2 value for the Clausius-Clayperon model for Carver becomes 0.9996, which is extremely close to a perfect fit. This indicates that the unusually high level of PCB3 observed in that sample was from a unique source. (This is discussed in more detail in XXXXX Gas-Phase PCB profiles). At Metcalf, one of the four samples is a strong outlier, containing more than twice the concentration of total PCBs than any other samples analyzed in this study, and throws off the data set. Considering only the other three samples, the Clausius-Clayperon relationship fits quite well, yielding an R^2 value of 0.96. For the majority samples in this study, the Clausius-Clayperon relationship provides a good model for describing the relationship between partial pressure of total PCBs and absolute temperature, strongly suggesting their presence in the atmosphere is largely due to volatilization from local sources containing PCBs.

It is interesting to examine the variation in calculated values for heats of vaporization for each site, how those values relate to their R^2 values, and also how these parameters change if outliers are removed from the data set. Wania et al.[32] propose that the calculated value of ΔH_v is dependent on whether or not the source of PCBs to the

atmosphere at a site is controlled by long-range or short-range transport. They conclude that if the calculated ΔH_v is low compared to laboratory values, it is long-range transport that controls the levels of PCB concentrations. Conversely, if calculated values of ΔH_v are close to laboratory values, it is likely that the volatilization sources are near the vicinity of the site. Table 3-3 below summarizes the different enthalpies of vaporization calculated at each of the six sites in this study

Table 3-3: Calculated heats of vaporization and corresponding R^2 values specific to sampling sites in this study

Sampling Site	ΔH_v (kJ/mol)	R^2
Carver	3.5	0.34
Carver w/o outlier	53	0.9996
Guad Reyes	55	0.94
Metcalf	7.2	0.021
Metcalf w/o outlier	12	0.96
Monroe	61	0.93
St. Columbanus	34	0.60
Zapta	23	0.92

For this data set, three of the sampling sites, Carver, Guadalupe Reyes, and Monroe, have relatively high ΔH_v values, indicating short-range sources, while Metcalf, St. Columbanus, and Zapata all have comparatively low ΔH_v values, possibly suggesting long-range sources. The significance of this data is that it suggests that within the city of Chicago, a relatively small area, it is potentially possible for gas-phase PCB concentrations to be governed by either short-range or long-range sources. Still, the issue of identifying specific sources remains quite difficult, and that will continue to be the topic of more study.

It is interesting to note the dramatic effect removing the outlier sample from the Carver data set has on the value for H_v, changing it from 3.5 kJ/mol to 53 kJ/mol. The drastic change suggests that while the primary source of PCBs to the site throughout the year may be volatilization from a short-range source, there is also another, unidentified, source that contributed very high levels of PCB3 on February 27,2009; the day that sample was collected.

3.2.5 The Clausius-Clayperon Relationship as it Applies to PCB Homologue Groups

Wania et al.[32] report that the enthalpy of vaporization of a PCB dependent upon the number of chlorines it contains. Below are plots of the natural logarithm of PCBs by homologue group plotted as a function of the inverse of the temperature.

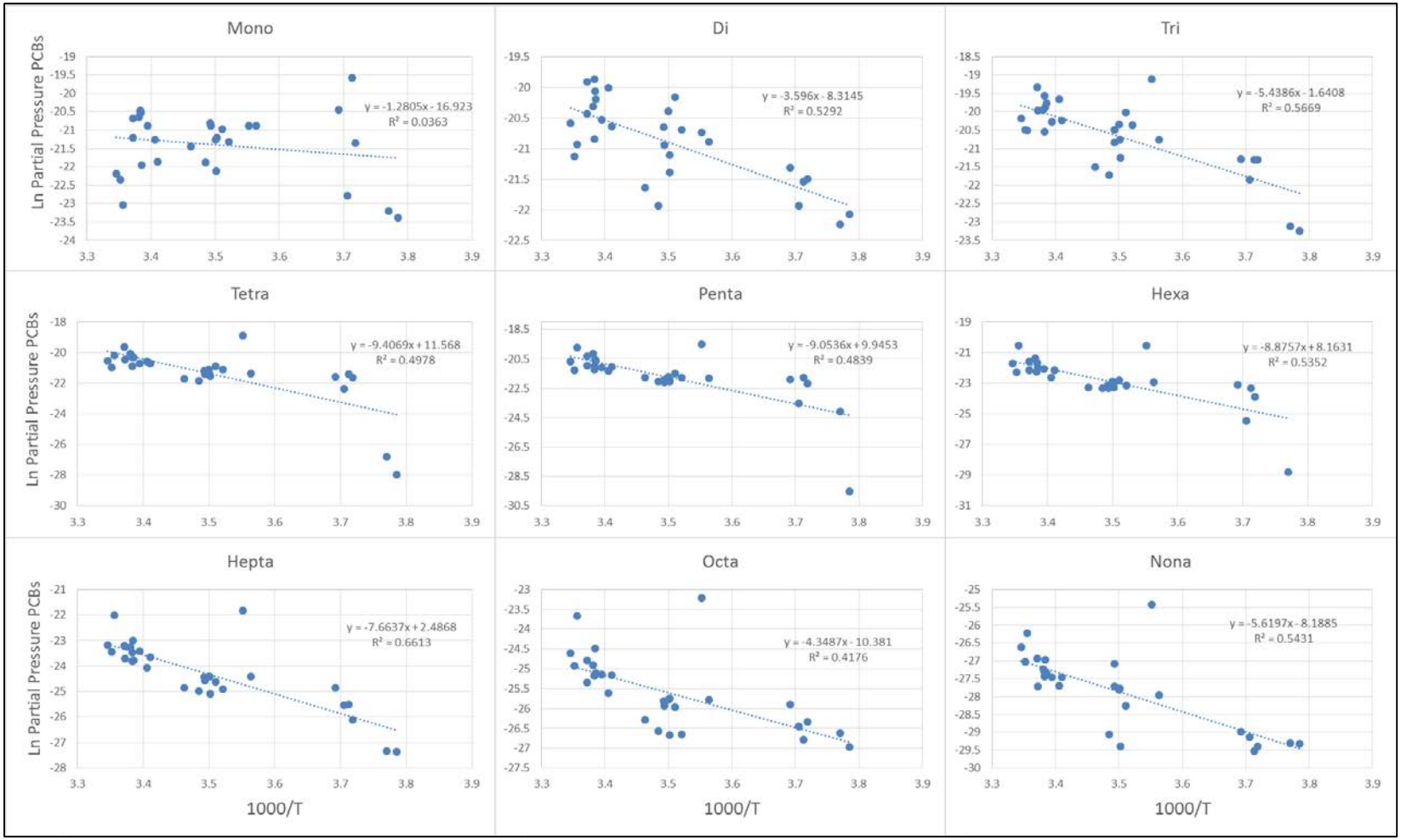

Figure 3-6: Clausius-Clayperon plots by homologue group for all of the 30 samples from the 10 sites analyzed in this study

From figure 3-6 above, it does in fact appear that slope of the Clausius Clayperon relationship is correlated to number of chlorines. There is no plot included for PCB 209 (ten chlorines) because it was only reported in 2 samples. The calculated values for the corresponding ΔH_v are summarized in table 3-4 below.

Table 3-4: Values for enthalpies of vaporization for gas-phase PCBs in Chicago by homologue group with R^2 values

Homologue	ΔH_v	R^2
mono	10.5	0.036
di	29.5	0.53
tri	44.6	0.57
tetra	77.2	0.50
penta	74.3	0.48
hexa	72.8	0.54
hepta	62.9	0.66
octa	35.7	0.42
nona	46.1	0.54

According to table 3-4, there is a clear dependence of enthalpy of vaporization values on number of chlorines. All of homologue groups appear to fit the model fairly well except for the monochlorinated biphenyls, suggesting that monochlorinated biphenyls in general cannot be modeled well by the Clasius-Clayperon relationship. Possible explanations are that monochlorinated biphenyls are present as a result of weathering processes or unidentified emissions sources[8].

3.3 Particulate Phase PCBs in Chicago Air

3.3.1 Particulate Phase PCB Concentrations

Particulate PCB concentrations were measured for a total of twenty-eight QFF samples from 10 different locations in Chicago. Particulate phase PCBs are known to account for a small fraction of total airborne PCBs – 4.3% on average – which makes them difficult to detect after applying an LOQ. After applying the LOQ to the QFF samples, twenty-two had detectable PCB concentrations, with an average ∑PCB concentration of 26.3 pg/m^3 and a standard deviation of ± 38.1 pg/m^3. ∑PCB concentrations ranged from 0.158 pg/m^3 to 123 pg/m^3. These values are shown as the blue portion of the bars in figure 3-7. Because such a high fraction of PCB congener were removed after LOQ application, the fraction removed was also considered in order to determine whether or not the LOQ had substantial effect on the sample set. This fraction is shown in purple in figure 3-7. Before taking the LOQ into account, particulate phase PCB concentrations ranged from 25.8 pg/m^3 to 142 pg/m^3. It is important to note that because the portion shown in purple represents the fraction removed with the LOQ, it has an inherently high level of uncertainty associated with it. Nonetheless, it is potentially useful in further determining if there are consistent trends related to particulate phase PCBs in the air and if further investigation, possibly utilizing more sophisticated particulate measurements, could prove to be a worthwhile future endeavor.

Figure 3-7 shows concentrations of particulate phase PCBs collected in Chicago organized by their collection date, irrespective of their location. The first thing that stands out is that the fraction of particulate PCB mass removed by the LOQ is quite large; with the exception of 6 QFF samples the fraction of PCB mass removed was larger than

the fraction not removed. Of these 6 QFF samples, 5 were collected in the summer when temperatures were comparatively warm, and 1 was collected in the fall when temperatures were slightly cooler. This data is consistent with the trend observed in gas phase PCBs, that when temperatures are warmer, PCB concentrations will be higher, with the exception of some outlier samples whose concentrations are predominantly not related to short range volatilization sources.

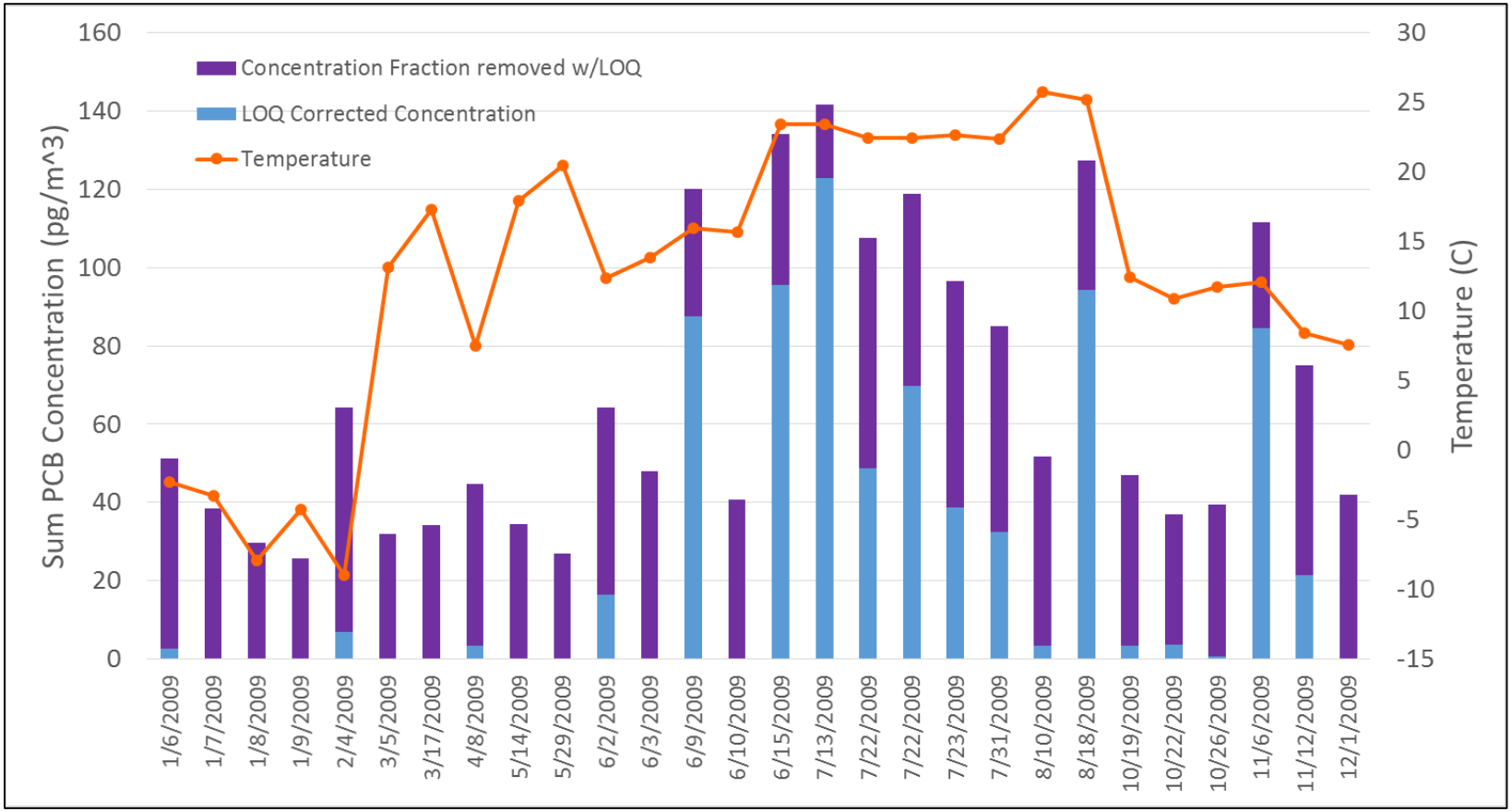

Figure 3-7: Particulate Phase PCB Sample Concentrations in Chicago Air Arranged by Collection Date

3.3.2 Particulate Phase PCBs in Relation to Total Particulates

Part of the analysis of the QFF filters included obtaining the total mass of particulates they collected (see QAQC section). Figure 3-8 below reports total particulate masses collected (g), total ∑PCB masses measured (ng) as particulates, and the fraction of PCBs of total particulates measured (ppb) along with the corresponding collection dates.

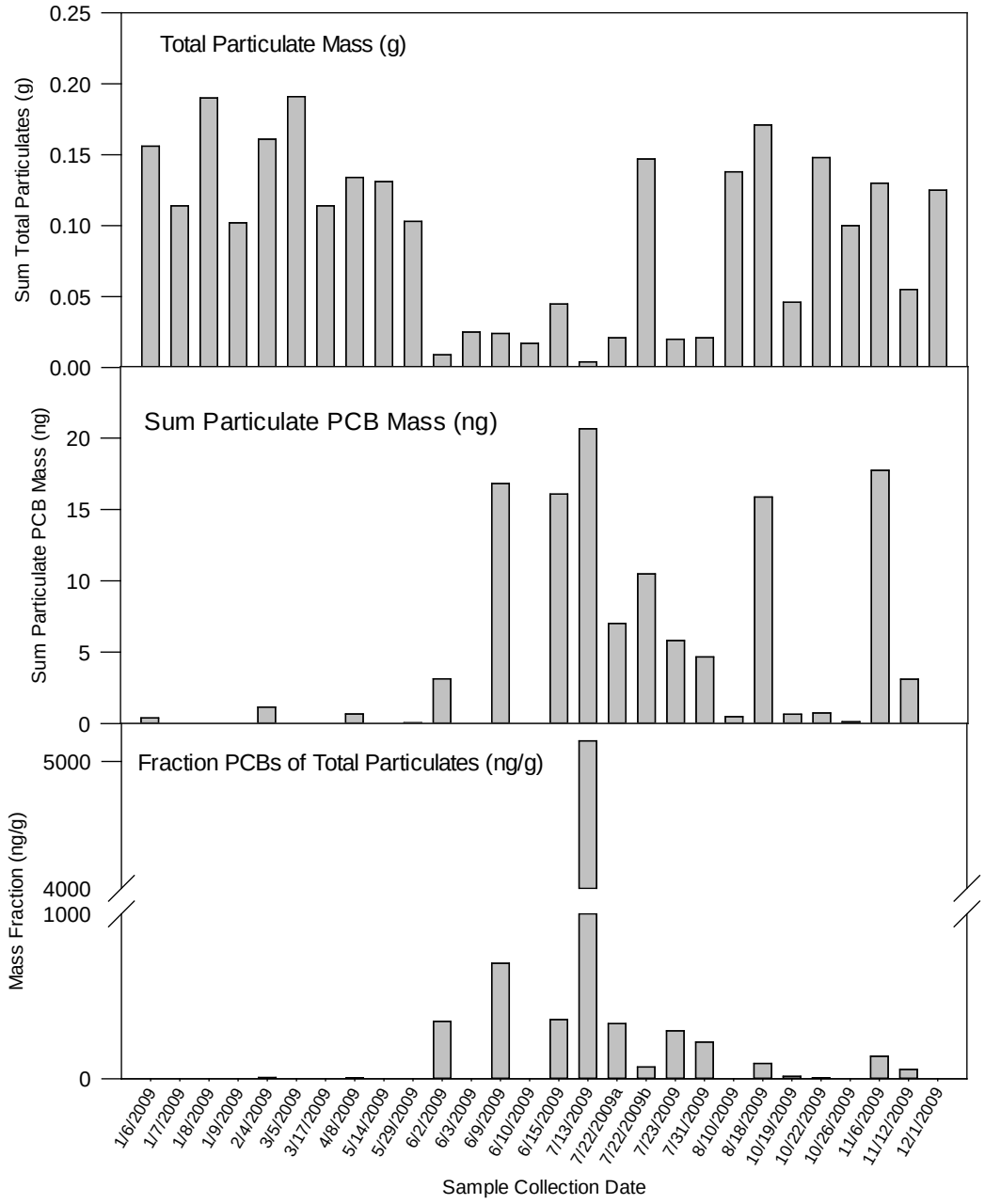

Figure 3-8: Masses of total particulates collected on filters (top), particulate phase PCBs measured, and the PCB fraction of total particulates

Figure 3-8 shows a few interesting trends. Starting with the top graph of total particulates collected, the first thing that stands out is that particulate masses for the warmer summer

months are substantially lower than those of the cooler winter, spring, and fall months. Of the twenty-eight total particulate mass measured, the nine lowest were measured between June 2nd, 2009 and July 31st, 2009. Also, in this time period, there was only one sample, collected on July 22nd that had levels comparable to the samples collected during the cooler months. From the data in this study, it appears that when temperatures are cooler, there are more particulates present in the air when temperatures are cooler. However, it appears to be the case that PCBs present in the particulate phase are more abundant during the warmer months, when particulates are lower and gas-phase PCB concentrations are higher. This is contrary to what was expected, which was to see a positive correlation between particulate masses and particulate phase PCB masses. One possible explanation for this has to do with the effect of local activity in an area on total particulate matter in the air. These sampling sites were all located at schools using high volume air samplers equipped with an exposed filter on top. That is, particulates were not selected by size or type, and all were collected on the filters. During the summer months, when particulates measured were low, there likely was limited activity in schools as the vast majority of students were on summer vacation. The reduction in student attendance means less traffic in parking lots and on nearby roads which would result in a reduction of road dust. Additionally, the lack of on-foot activity during outdoor activities such as recess would also result in a reduction of dust and total particulate levels in the air.

While the above hypothesis concerning the lower summer particulate levels makes sense, we still sought a means of confirming the validity of our method of measuring particulate levels. The EPA keeps daily records of PM 10 for the city of Chicago. While this is only accounts for one fraction of total PM levels, checking it was the best cross-reference I could find to compare against our values. The main thing I was looking for was to see if there was a similar trend of lower PM 10 levels in the summer as to what I saw in total

PM levels. Figure 3-9 below summarized the total PM levels we measured along with PM 10 levels reported by the EPA.

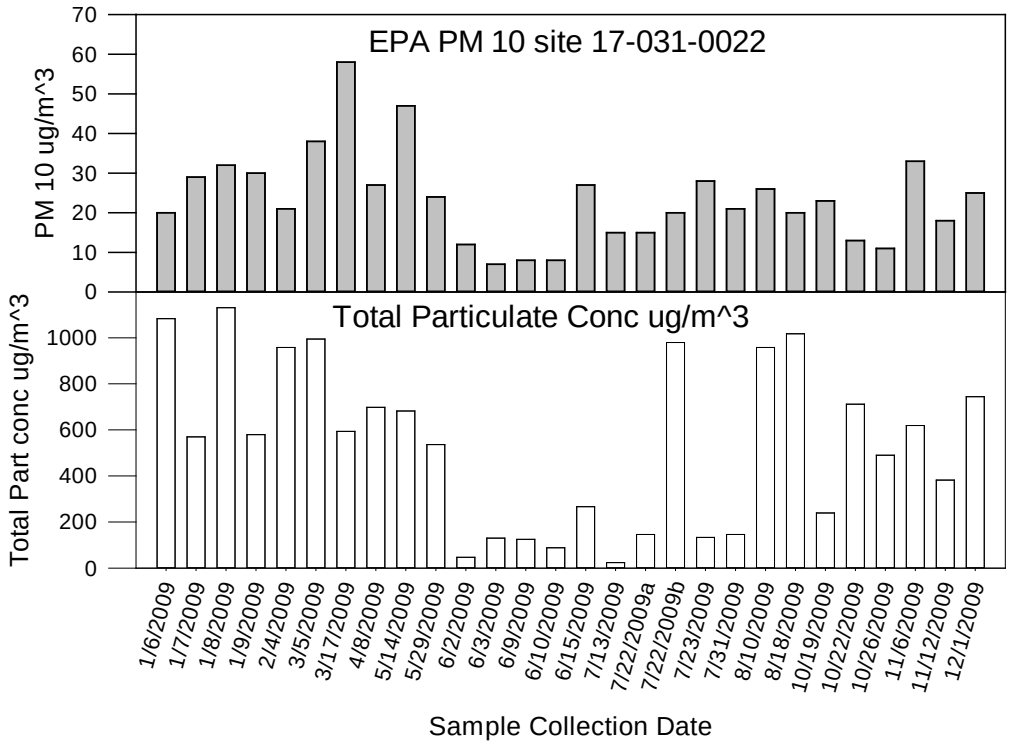

Figure 3-9: Concentrations of PM10 reported by the EPA and measured concentrations of total particulates for the sampling dates in this study

Looking at figure 3-9, one of the first things that stands out is that while both data sets don't have exactly the same characteristic relative high and low trends, they do have the same relative dip in concentration levels during the month of June. Both data sets have some of their lowest recorded particulate levels from 6/2/2009 to 6/10/2009. Also, a quick look at the figures shows that the EPA reported measurements are, on average,

about an order of magnitude lower than our reported values for the total particulates. While we are uncertain of the exact type of particulate matter collected on the filters, and this phenomenon needs more investigating, there are two seemingly logical conclusions that can be drawn from this study:

1: There is a strong correlation between temperature and PCB levels in the particulate phase. Even if total particulate levels are high, if temperatures are cool, we cannot expect to see a comparatively high level of particulate phase PCBs. Conversely, if total particulate levels are comparatively low, but temperatures are high, we can expect to see a higher fraction of PCBs present in the particulate phase, suggesting that PCBs have a higher affinity towards the particulate phase at warmer temperatures.. Figure 3-10 below summarizes the relationship of Particulate PCBs as the fraction total particulates in relationship to temperature.

2: Presence of PCBs as particulates are largely dependent on the type of particulate matter. At the sites chosen for this study, it appeared that much of the particulates collected on the sampling filters did not accumulate PCBs.

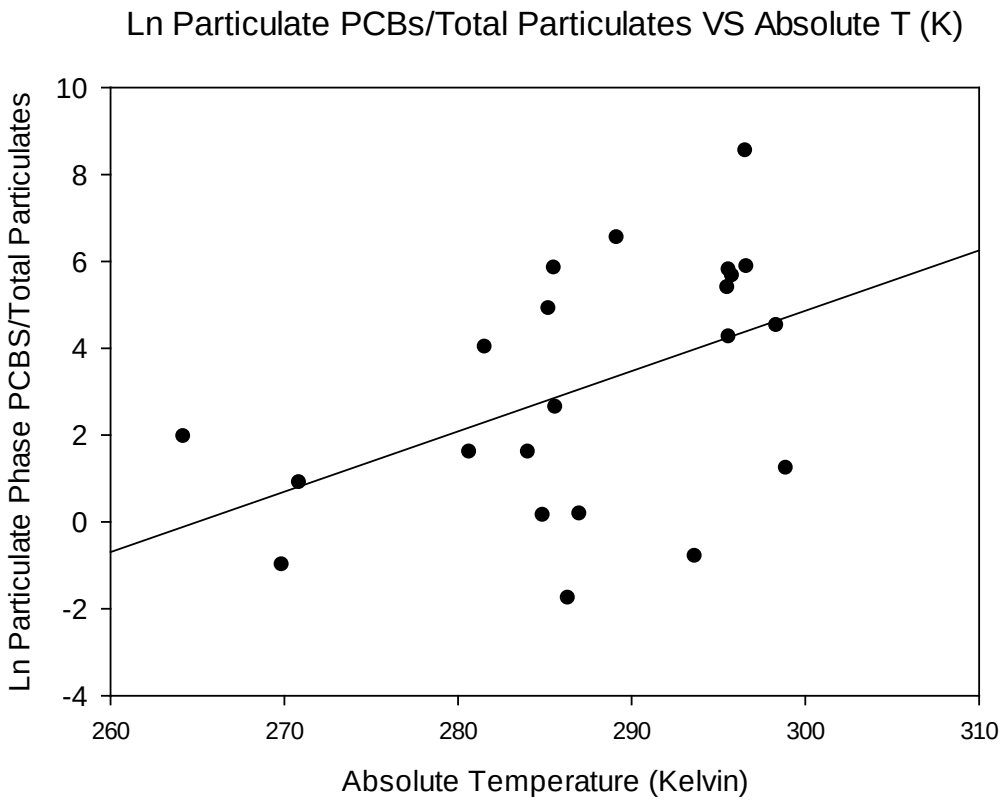

Figure 3-10: Natural logarithm of the fraction of particulate phase PCBs of total particulates plotted against absolute temperature in Kelvin

3.4 Gas Particle Partitioning of PCBs

3.4.1 Particulate PCBs as a Fraction of Total PCBs

Out of the thirty XAD samples and twenty-eight QFF samples analyzed in this study, there were twenty-two XAD and QFF sample pairs. The sample pairs were arranged by collection date to compare relative concentrations of gas-phase and particulate phase PCBs (figure 3-11). The concentration values for the QFF samples are after the LOQ application.

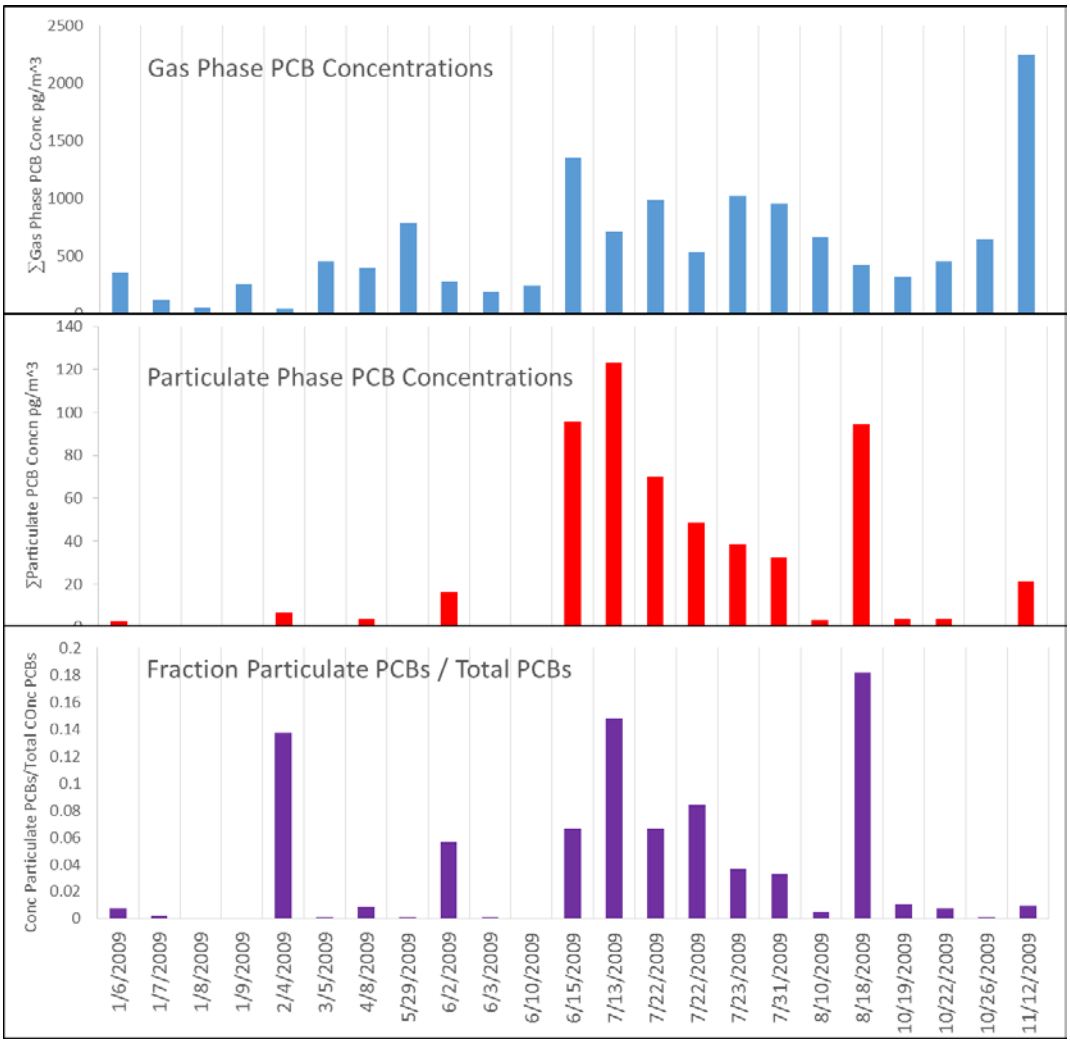

Figure 3-11: Gas phase (top) and particulate phase (middle) ∑PCB concentrations for XAD and QFF sample pairs and also fraction particulate PCBs of total PCBs by collection date.

PCBs are more abundant in the particulate phase when temperatures are warmer, and particulate phase PCBs account for a larger fraction of total PCBs when they are present at higher levels (figure 3-11). The relationship between PCBs in the gas and particulate

phase is best understood on a congener specific basis by calculating the gas/particle partitioning coefficient for each PCB congener.

3.4.2 Calculating Congener Specific Gas/Particle Partitioning Coefficients

Polychlorinated biphenyls are present in air as vapors as well as adsorbed/absorbed to particulate matter suspended in the air[41]. The fraction of PCBs present that associated with particulate matter is relatively small compared to the fraction present in the gas-phase, accounting for less than 5% of total airborne PCBs on average. Still, gas/particle partitioning is important to consider it plays an important role in wet and dry deposition as well as air-water exchange[43-45]. One way to better understand the relationship between these two phases is by calculating a particle/gas partitioning constant, K_P for each PCB congener, defined as:

$$K_P = {C_p}/{C_g}$$

Where C_p is defined as the concentration of a PCB congener on particles (ng/ug) and C_g is the gas-phase concentrations (ng/m^3) (figure 3-12). The value of doing this is that by calculating the values of K_P, one can estimate levels of total airborne PCBs by knowing only either the particulate phase or gas-phase concentrations, and subsequently calculating for the other. Discrepancies can arise from this method, as C_P is largely dependent on the nature of the particulate matters in the air. The affinity of a dust particle to allow organic molecules to adsorb to it is directly dependent on the organic composition of the particle, and how much of its organic content is available for

adsorption or absorption. Therefore, depending on what the particles in the air are comprised of, K_p values could vary significantly from study to study. This method is only valid if gas/particule equilibrium in the air is achieved. While the issue of gas/particle partitioning has been studied in detail, there is still uncertainty whether or not gas/particle equilibrium can be taken for granted[46]. Further, we saw from figure 3-10 that the fraction of PCBs in the particulate and gas-phase is related to air temperature. Therefore, it appears that K_P would vary with temperature. Nonetheless, computing rough K_P values is still useful in that it gives us a means to compare our results to those of others in the literature computed under similar conditions and in turn better understand the mechanisms and conditions that govern gas/particle partitioning of PCBs in Chicago.

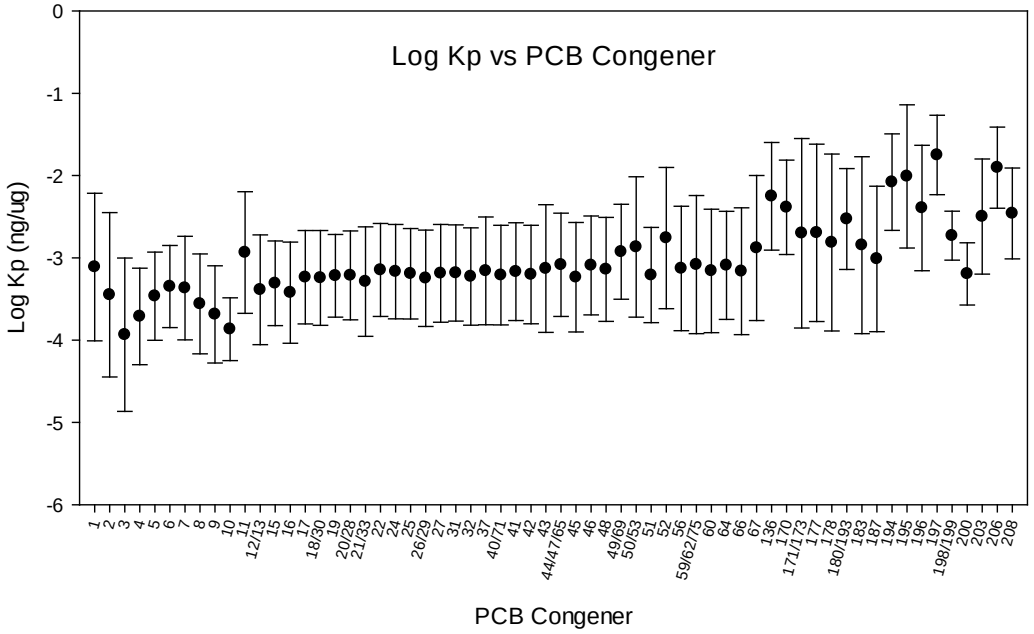

Figure 3-12: Calculated $\log_{10} K_P$ values for individual PCB congeners that were detected in both the gas and particulate phase

K_P values increase with PCB chlorination, which agrees with the observations of others[41, 47] (figure 3-12). All of the penta and hexachlorobiphenyls are missing from figure 3-12 because they were below the detection limit in the particulate phase. Despite the lower K_P values of lower chlorinated PCBs, they are still the prominent congeners present in the particulate phase due to their relatively high total concentrations in the air. Although the higher chlorinated PCBs are present in lower concentrations in the air, their higher K_P values give them a higher affinity for the particulate phase than the PCBs in the other homologue groups. The more "middle-weight" PCBs, however, are neither present in high concentrations nor have comparatively high K_P values. It is the combination of these two characteristics with an already difficult detection process that I believe is the reason why few particulate phase penta and hexachlorobiphenyls were detected.

3.4.3 Using Gas/Particle Partitioning in Conjunction with Octanol/Air Partitioning to Construct and Equilibrium Model for PCBs

Whether or not the dominant process governing gas/particle partitioning is adsorption to a solid organic particle or absorption to a thin viscous film coating a particle is not fully clear[46, 47], and models for both processes have been used to accurately describe the partitioning behavior of PCBs in the air[41, 46, 47]. Here, we will only examine the adsorption model proposed by Harner et al.[47] and Finizio et al.[46], as it has been shown to resolve discrepancies that arise between ortho-chlorine substituted PCBs within a homologue group when using the adsorption model[46, 47]. As mentioned, the absorption model assumes chemicals absorb into a thin, viscous organic film coating aerosol particles. The K_P values for each congener are plotted on a log/log scale versus their respective octanol-air partitioning coefficient. In theory, if equilibrium is reached, the slope of this plot will be equal to 1[46, 47]. Below is the log K_P – log K_{OA} plot constructed from the data in this study. The K_{OA} values used here were determined by Andres Martinez by using the following formula:

$$\log K_{OA} = logK_{OW} - logK_{AW} \quad (1)$$

Where K_{OW} and K_{AW} are the octanol-water and the air-water partitioning coefficients, repectively. K_{OW} values were determined by Hawker and Connell[48], and K_{AW} values were determined by Dunnivant et al.[49].

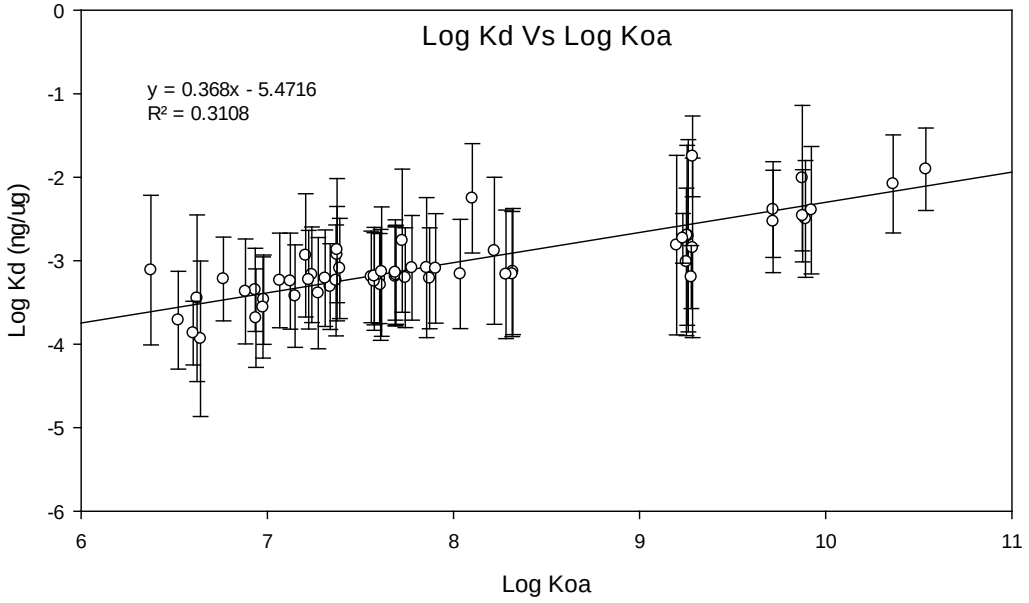

Figure 3-13: Log K_P per PCB congener plotted as a function of its log K_{OA}

Looking at figure 3-13, it is clear that there is a constant, linear relationship in the log-log plot of K_P and K_{OA}, however the slope 0.368 suggests that airborne PCBs are not in fact in gas/particle equilibrium (figure 3-13). This is similar to what Harner and Bidleman found in their study of gas/particle partitioning in Chicago air samples, however they calculated a slope of 0.654. The possible explanations for the differences in our slopes could be related to the temperature ranges our samples were collected over. Harner and Bidleman only looked at samples collected from February to March of 1995, whereas in this study we analyzed samples collected from January to December of 2009. As was noted in the general analysis of total particulates as a fraction of total PCBs, gas particle partitioning is temperature dependent. This difference in sampling temperatures could also help explain why the R^2 value for this figure is only 0.31.

3.5 PCB Profiles and Congener Detection Frequency

3.5.1 Gas-phase and Particulate Phase PCB Profiles and Detection Frequencies

Shown below (figure 3-14) is the average gas-phase mass fraction profile for the thirty XAD samples along with the average particulate phase profile for the twenty-eight QFF samples.

Aside from knowing the relative abundance of congeners in the air, it is also insightful to look at the relative frequency at which they are detected. It could be the case that a PCB congener accounts for a relatively small fraction of total PCB mass in the air, but that it is detected at a very high frequency. This could be a potential concern if a congener is one of those that is and exhibits toxic effects[6, 7]. Although it will not be discussed here, additional concern could also be attached to congeners present in the particulate phase if the size of the particulate matter is such that it can become lodged in the lungs during inhalation.

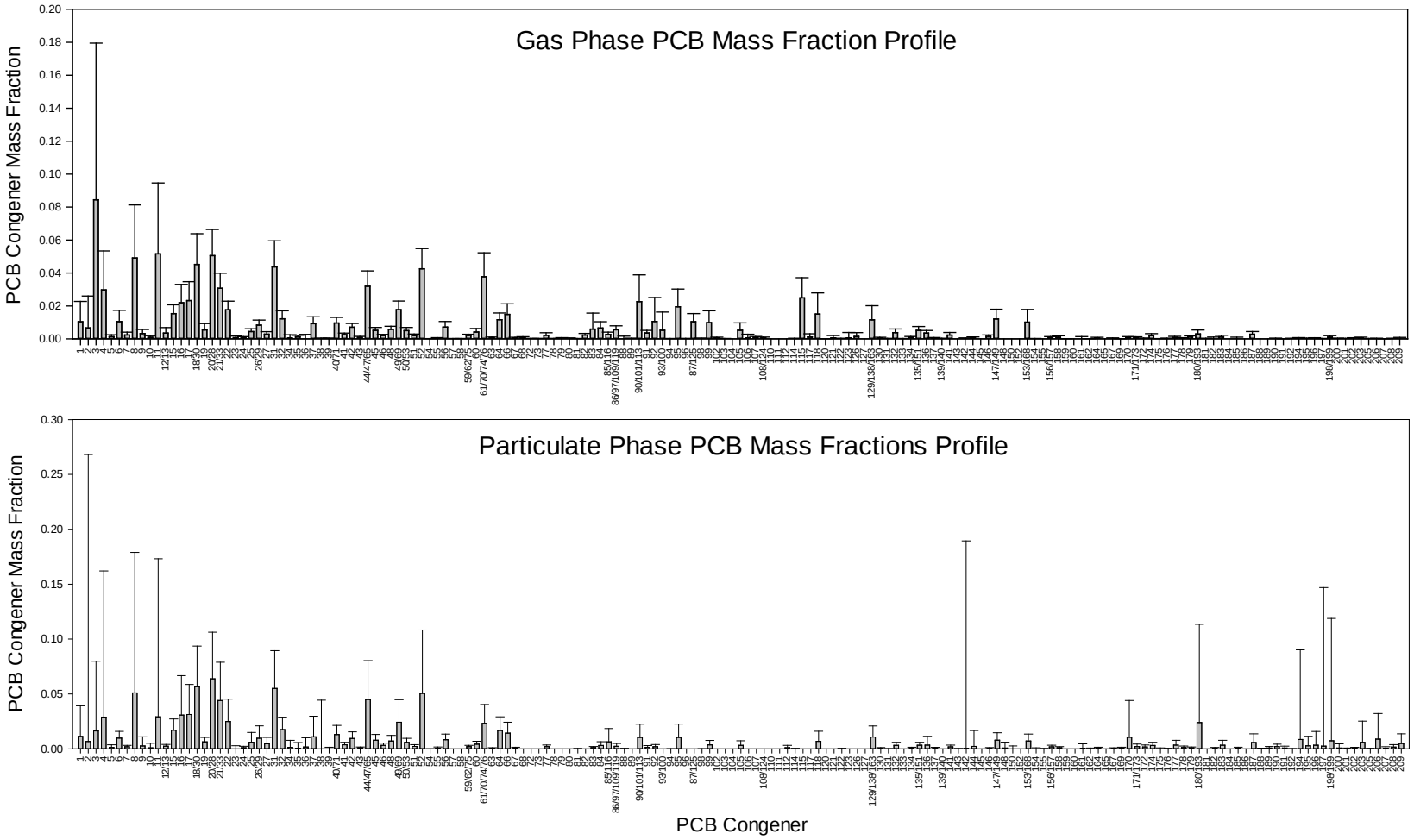

Figure 3-14: Average mass fraction profiles for gas-phase and particulate phase PCBs in Chicago air

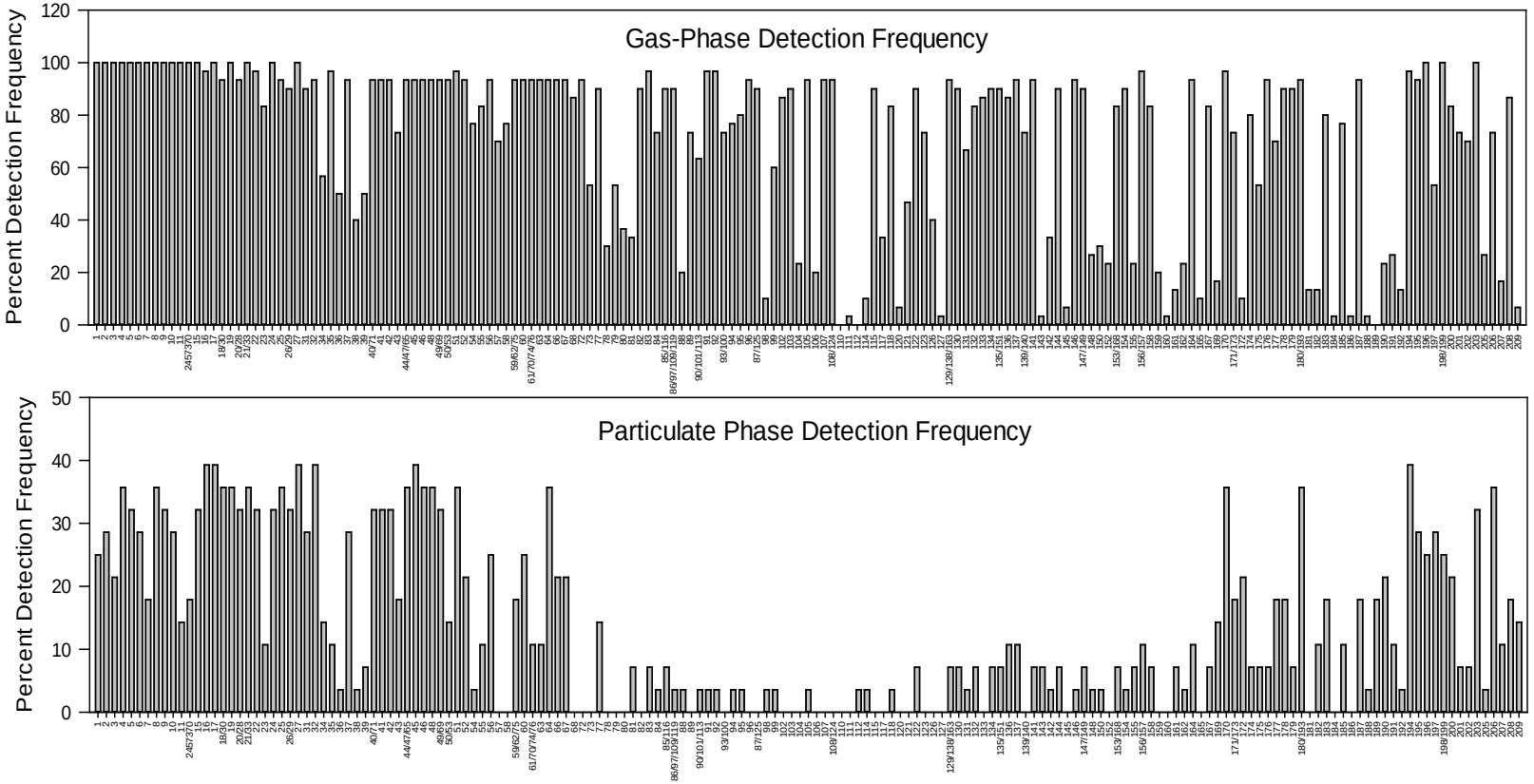

Figure 3-15: Relative detection frequencies of PCB congeners in the gas and particulate phase in Chicago air

Profiles for gas-phase and particulate phase PCBs in Chicago air are very similar (figure 3-14). Both profiles are heavily weighted towards the lower molecular weight congeners. This is significant, because although they are not the dioxin-like PCB congeners, many of the lower chlorinated PCBs are known to exhibit neurotoxic effects[6]. Further, lower chlorinated PCBs may pose significant risk to humans as they are readily metabolized and could be transformed into genotoxic or carcinogenic intermediates[7].

3.5.2 Gas-phase and Particulate Phase Profile Comparisons

Pentachlorobiphenyls constitute a larger fraction of total PCBs in the gas phase than in the particulate phase while the hepta, octa, nona, and decachlorobiphenyls constitute a higher fraction of total PCBs in the particulate phase. This relative distribution of PCBs according to their chlorination is exactly what we would expect to see based on the K_P values calculated in the previous section. This is also observed in the relatively low detection frequency of pentachlorobiphenyls in the particulate phase (figure 3-15).

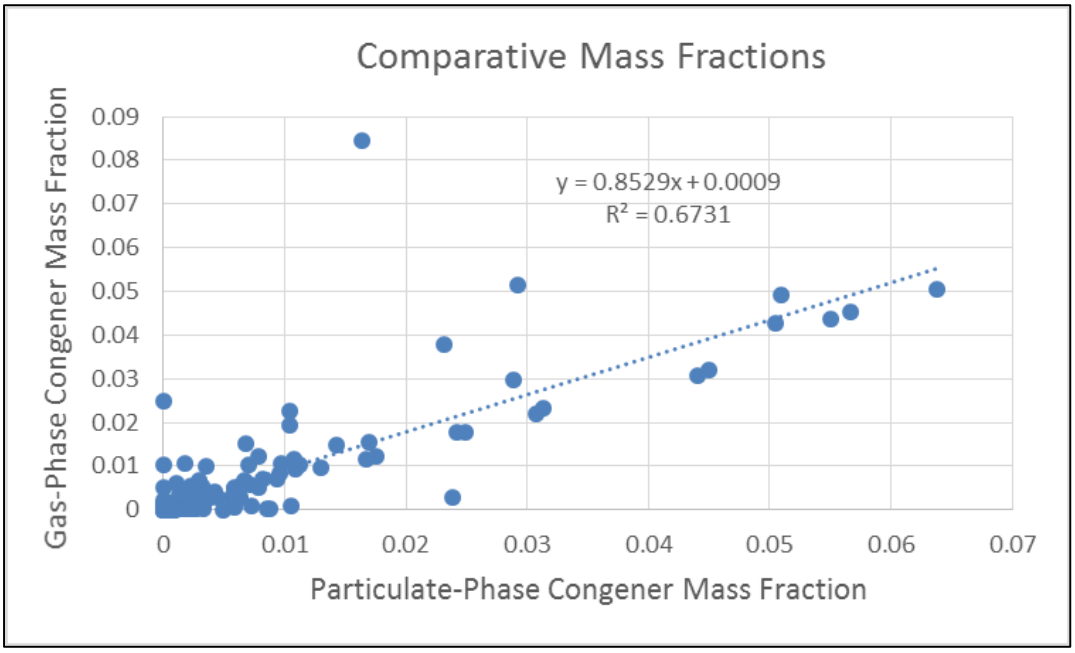

Figure 3-16: Comparison of relative gas-phase and particulate phase mass fractions of airborne PCBs in Chicago

Gas-phase and particulate phase PCBs exhibit similar distributions in Chicago (figure 3-16, $R^2 = 0.67$. The similarities and differences between profiles confirm the earlier observations made from analyzing the gas/particle partitioning of PCBs.

The minor contribution of particulate phase PCBs compared to gas-phase PCBs can be seen again by noting how little they change the overall profile of airborne PCBs. The gas phase mass fraction profile is very close to identical to the profile for the sum of the particulate and gas-phase PCBs (figure 3-17).

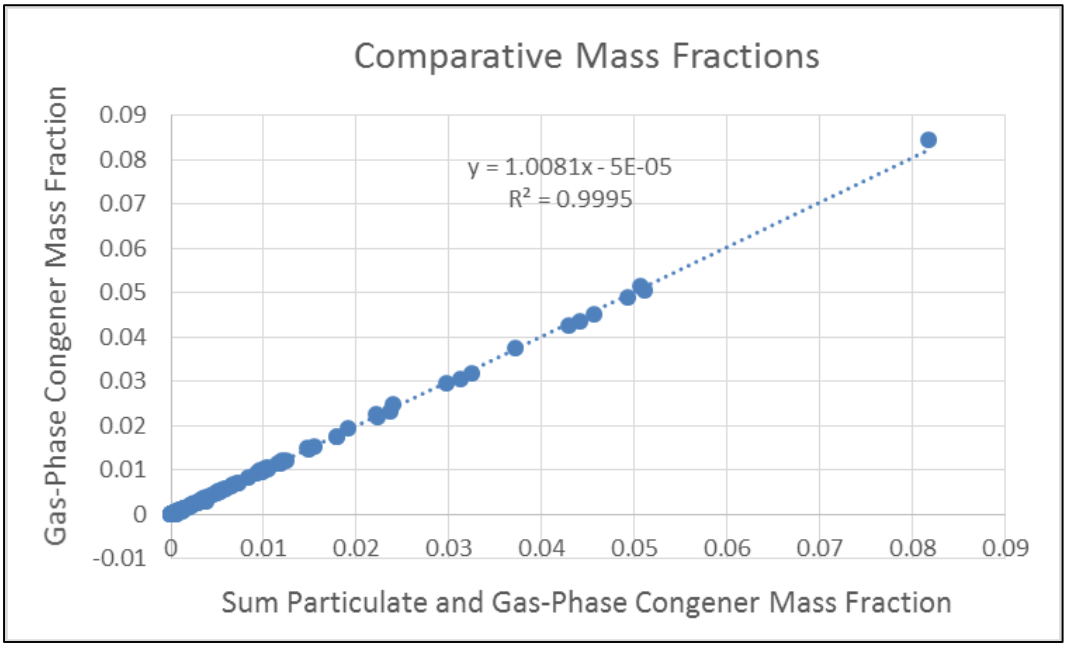

Figure 3-17: Comparison of relative gas-phase and ∑ gas and particulate phase mass fractions of airborne PCBs in Chicago

3.5.3 PCB 3 and PCB 11

The highest contributing congeners to the total mass of gas-phase PCBs in Chicago air are PCB 3 and PCB 11, accounting for ~8% and ~5% of the total gas-phase PCB mass in Chicago. Both are congeners of concern from a health standpoint due of their potential toxicological effects on humans[6, 7], and both congeners of interest due to their lack of connection to traditional Aroclor sources[17, 18, 50].

PCB 11 is a non-Aroclor PCB whose source has been directly linked to the production of paint pigments[17, 18]. It has been discussed elsewhere that emissions from paint are the primary contributor to airborne concentrations of

PCB11[17], and may play a significant role in contributing to airborne PCBs in general[18]. Hu et al. reported strong concentrations trends for PCB11 with temperature indicating volatilization from common outdoor surfaces[17], which was confirmed in this study. Figure 3-18 below shows the Clausius-Clayperon relationship for PCB 11, and the strong correlation between its concentration and temperature is observed in the linear fit with R^2 value of 0.55. Also worth noting is that the sample which proved to be a strong outlier for total PCB concentrations is not an outlier for concentrations of PCB 11, further suggesting that PCB 11 is in fact present due local volatilization surfaces.

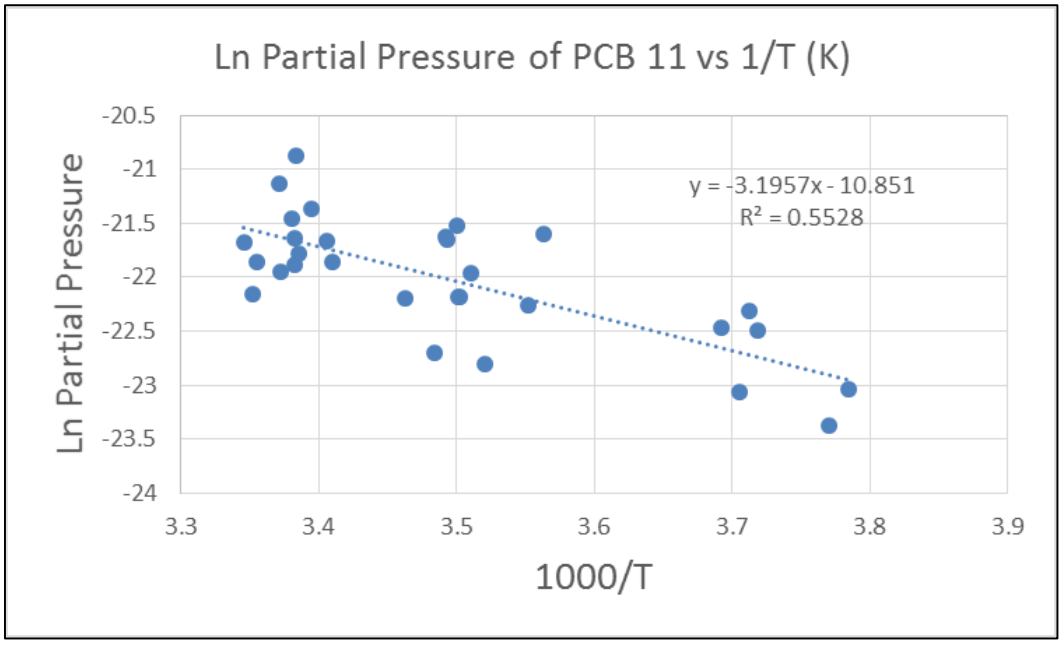

Figure 3-18: The Clausius-Clayperon relationship for PCB 11 exhibits a strong correlation to temperature, suggesting its presence in the air is from volatilization sources despite the fact that it is a non-Aroclor PCB

PCB 3 is present in Aroclors 1016 and 1242, but it accounts for an extremely low fraction of the masses of both of those (<0.5%), eliminating either Aroclor as the potential source of PCB3 in the air. Hu et al. did report PCB 3 detected in almost 50% of paint pigments analyzed. If this is the case, it would be expected that PCB 3 would exhibit the same type of temporal trend as PCB 11. Upon applying the Clausius-Clayperon relationship to PCB 3 however, it becomes clear that there is no apparent relationship between levels of PCB 3 in the air and temperature ($R^2 = 0.06$). This can be seen in figure 3-19 below. While a potential source is yet to be identified, it can be hypothesized that the high concentrations of PCB 3 are largely due to point source emissions that are common throughout Chicago.

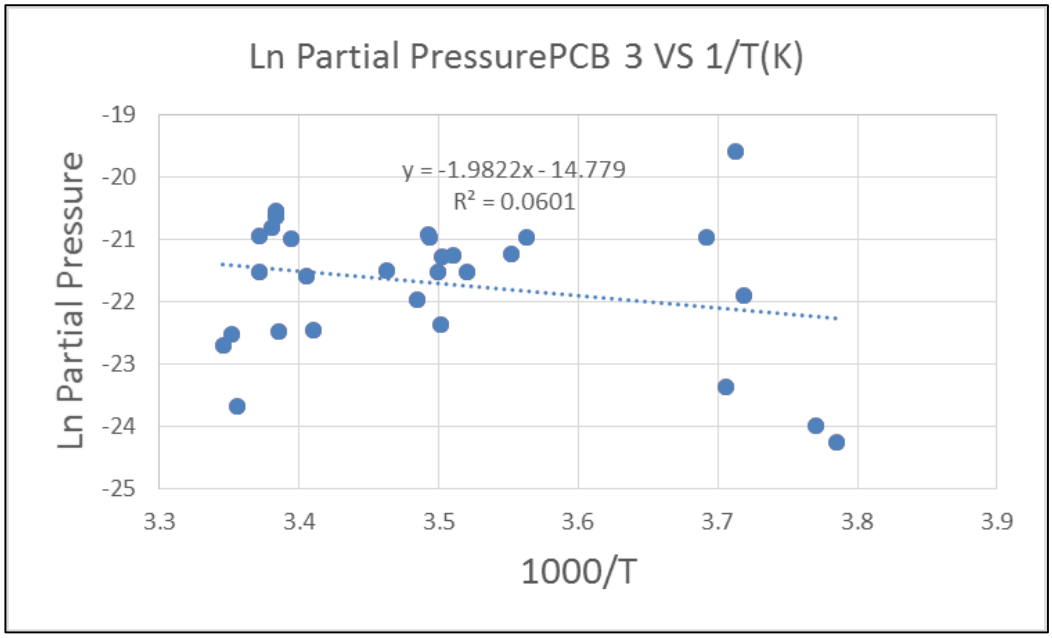

Figure 3-19: The Clausius-Clayperon relationship for PCB 3 exhibits almost no correlation to temperature, suggesting its presence in the air is not from volatilization sources

3.5.4 Congeners detected with 100% Frequency and Brief Discussion of Neurotoxicity

There were several congeners that were detected with very high frequency in the gas phase, as can be seen in figure 3-15. There were 24 congeners that were detected among 21 peaks with 100% frequency (there were three pairs of coeluting peaks). Of these 21 peaks, none corresponded to dioxin-like PCBs (discussed below), however 12 of them correlated to congeners that are known to be neurotoxic[6] (table 3-5).

Table 3-5: Mass fractions and neurotoxic/non-neurotoxic classification of congeners detected with 100 percent frequency in this study

Congeners Detected with 100% Frequency		
Congener	Mass Fraction	Neurotoxic
1	1.04E-02	No
2	6.67E-03	No
3	8.44E-02	No
4	2.97E-02	Yes
5	1.37E-03	Yes
6	1.05E-02	Yes
7	2.37E-03	No
8	4.91E-02	No
9	3.26E-03	Yes
10	1.03E-03	Yes
11	5.16E-02	Yes
12/13	3.55E-03	Yes
15	1.53E-02	No
17	2.33E-02	Yes
19	5.42E-03	Yes
21/33	3.08E-02	Yes
24	7.27E-04	Yes
27	2.89E-03	Yes
196	3.85E-04	No
198/199	1.04E-03	No
203	5.93E-04	No

3.5.5 Dioxin-like PCBs

While the emphasis of this report is not on the toxic equivalencies of PCBs, I do feel it is important to at least briefly address those compounds which have been shown to exhibit dioxin-like properties, and their relative abundance and detection frequency in these samples, as inhalation is an important exposure pathway. According to Patterson et al.[51], there are twelve PCBs that, due to the number and placement of their chlorines, are considered dioxin-like. Table 3-6 below summarizes these 12 congeners and their relative abundance and detection frequencies in both the gas and particulate phase.

Table 3-6: Dioxin-like PCBs and their relative abundance and detection frequency in Chicago air samples

Dioxin-Like Congener(s)	Gas-Phase PCBs		Particulate Phase PCBs	
	Mass Fraction (%)	Detection Frequency (%)	Mass Fraction (%)	Detection Frequency (%)
77	0.21	90	.020	14
81	0.012	33	0.017	7
105	0.53	93	0.31	4
114	0.017	10	0.021	4
118	1.5	83	0.68	4
123	0.056	73	0	0
126	0.14	40	0	0
156/157	0.072	97	0.18	11
167	0.030	83	0.045	7
169	4.5E-3	17	0.054	14
189	0	0	0.074	18
∑ Congeners	2.6	n/a	1.4	n/a

While it is apparent that Dioxin like PCBs don't contribute to a very large fraction of total airborne PCBs (~2.6% in the gas-phase and ~1.4 in the particulate phase), they are

not insubstantial to the total concentrations of PCBs, and should be taken into consideration when evaluating potential consequences of exposure to airborne PCBs in Chicago. Also, it is clear that the PCBs that are dioxin like exhibit the same type of temporal trends as were observed for total PCBs. This is seen in the Clausius-Clayperon diagram for Dioxin like PCBs below.

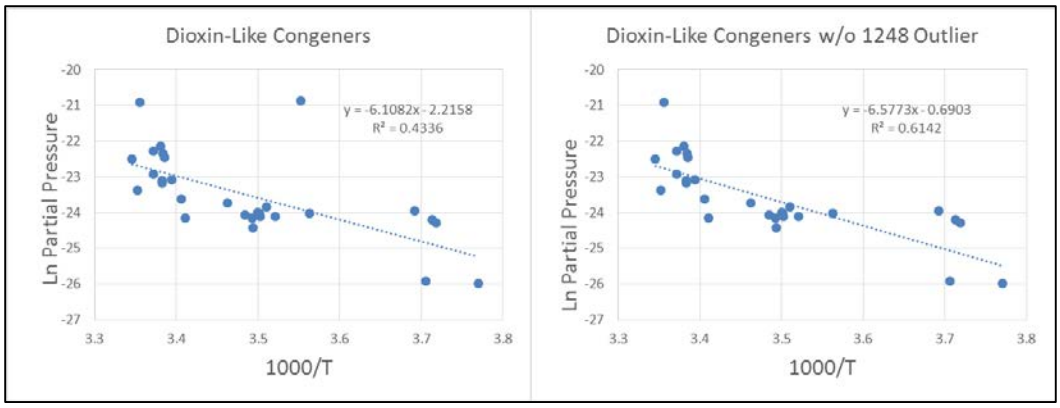

Figure 3-20: Clausius-Clayperon relationship with and without 1248 outlier for dioxin-like PCBs

Figure 3-20 shows the Clausius-Clayperon relationship for total dioxin-like PCBs both with and without the Metclaf outlier (referred to here as the 1248 outlier because of the strong similarities between its profile and that of Aroclor 1248) sample that has already been discussed previously. Notice the change in R^2 squared value for the fit of 0.43 to 0.61 in the regression formula when the outlier is removed from the data set. Recall that the profile for this sample most closely resembled that of Aroclor 1248, whereas the majority of samples resembled that of Aroclor 1242. Also, note that the most abundant dioxin-like PCB in Chicago air in both the gas and particulate phase is PCB 118,

accounting for approximately half of the total mass of dioxin-like PCBs in both phases. According to Frame et al.[50], Aroclor 1248 contains about 3.5 as much PCB 118 by mass as Aroclor 1242 does. Clausius-Clayperon relationships were plotted for PCB 118 both with and without the 1248 outlier (figure 3-21). As expected, figure 3-21 shows that the fit of the Clausius-Clayperon relationship improves significantly when the 1248 outlier is removed from the data set.

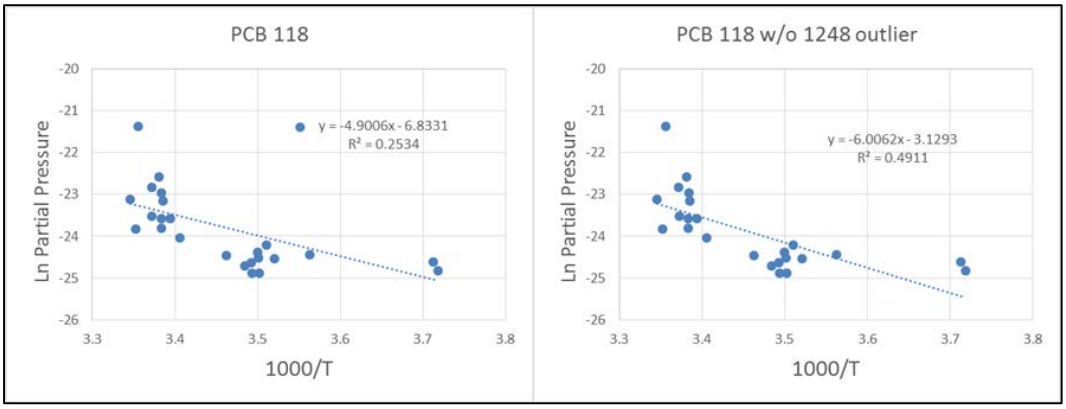

Figure 3-21: Calusius-Clayperon relationship with and without the 1248 outlier for PCB 118, the most abundant dioxin-like PCB in Chicago air

3.6 Gas-phase Profile Comparison to Previous Studies

3.6.1 Comparison to Reported Mass Fractions for Aroclor by Frame et al., 1996

The gas-phase PCB profile for the samples in this study was compared to the profiles of five Aroclor mixtures published by Frame et al.[50] (figure 3-22). For Aroclors 1248 and 1254, Frame et al. published relative mass fractions for two separate stock mixtures. For the comparisons in this study, I used the average mass fractions of the two values they reported for each Aroclor.

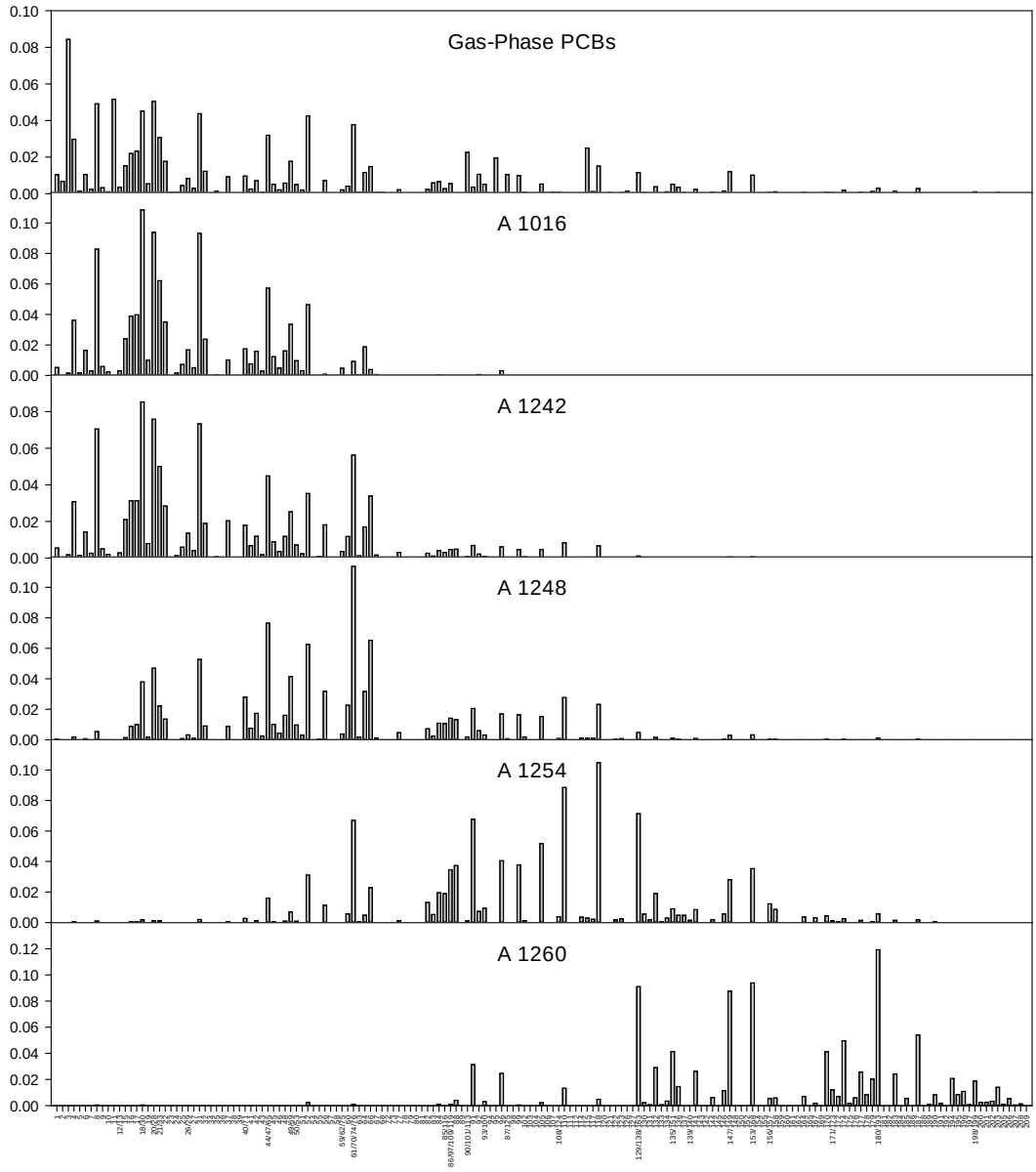

Figure 3-22: Congener mass fraction profiles for gas-phase PCBs measured in Chicago in this study and for 5 Aroclor mixtures reported by Frame et al.[50]

A qualitative look at the profiles between gas phase PCBs and the Aroclors shows strong similarities to A 1016 and A 1242 for the lower molecular weight congeners, and some resemblance to middle molecular weight congeners found in A 1248 and 1254, but

almost no resemblance to higher molecular weight congener distribution of A1260. Correlations were made between the gas-phase PCB profile and all of the 5 Aroclor profiles. The gas-phase PCBs correlated most strongly with A 1242 with an R^2 value of 0.53. The correlation with A 1016 was close to that of A 1242, with an R^2 value of 0.48. The corresponding R^2 values for the correlations to Aroclors 1248, 1254, and 1260 were 0.30, 0.04, and 1×10^{-5}, respectively. It is important to note that because the air profile correlates most strongly with the lower chlorinated Aroclor mixtures does not necessarily mean that other Aroclor mixtures can be entirely eliminated as potential contaminants to a site. Mixtures such as 1254 and 1260, composed of predominantly middle and higher chlorinated compounds, would need to be present in higher amounts in order to have as strong of a signal in the air as the lower chlorinated mixtures due to the lower tendency of the higher chlorinated congeners to volatilize. It is worth noting that although present in relatively small abundance in these air samples, (0.24% and 0.16%, respectively) congeners 180/193, and 187 are the most abundant hepta chlorinated congeners that were detected. While these congeners are present in Aroclors 1248 and 1254 at very low concentrations (~ <0.05%), they account for a rather large fraction of Aroclor 1260 (180/193 ~ 12%, 187 ~ 5%). The low tendency of these congeners to volatilize, and their comparative abundance in the air to their levels in Aroclors 1248 and 1254, suggest the presence of Aroclor 1260 despite the overall poor correlation of its profile with that of Chicago air.

3.6.2 Comparison to Mass Fractions for Chicago Air by Hu et al., 2010

Plotted below (figure 3-23) is the gas-phase PCB profile reported for this study (samples collected in 2009) alongside the gas-phase PCB profile reported by Hu et al.[8] (samples collected in 2007), data comparison courtesy of Nick Herkert.

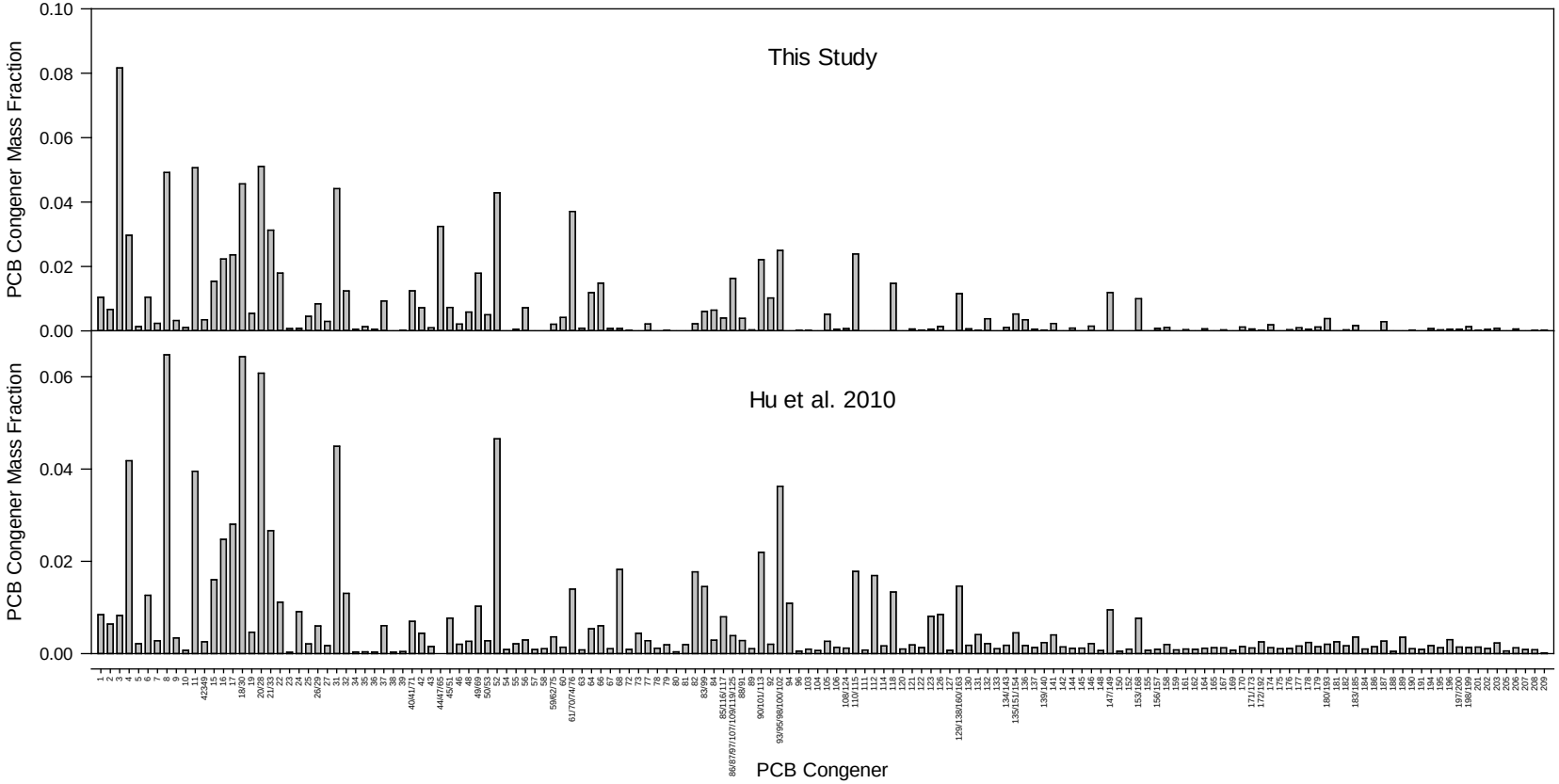

Figure 3-23: Average gas-phase mass fraction profiles for gas-phase and particulate phase PCBs in Chicago air from this study and Hu et al.[8]

There are many similarities between the congener profile reported by Hu et al. and the congener profile for the samples in this study. Both are weighted most heavily toward the lower chlorinated congeners, and they share many of same prominent peaks in the tetra, penta, and hexa homologue groups. Hu et al. reported average concentrations for several more of the higher chlorinated compounds than were detected in this study, however. While I am not certain why this is, a simple explanation could be that it is possible for source signals in a location to change over time. There is a time span of two years between when the samples analyzed by Hu et al. (2007) and the samples analyzed in this study (2009) were collected. The values for those higher chlorinated congeners reported by Hu et al., but not here, are all relatively low, and it is quite possible that in the time span of two years they could have fallen below the detection limits of this study. Further analysis of these differences may be done in the future, but is not the object of this study.

Another, more interesting observation between the two studies is the difference in abundance of PCB3. Hu et al. reported that PCB accounted for <1% of gas-phase PCBs. Here, PCB 3 accounts for <8% of total PCBs in Chicago, and is the single highest contributing PCB congener to total PCB mass in Chicago air. It is really quite interesting that such a dramatic change would occur in the span of two years. While PCB3 is detected in some Aroclors it accounts for only a small fraction of the total PCB masses (<0.2%), and it is highly unlikely that Aroclors are its predominant source in the samples from 2009 analyzed in this study. It is known that PCB3 has been found in paint pigments[18], but, as already noted, it does not fit the Clausius-Clayperon relationship well at all, which would be expected if it were a volatilization source. Without further speculation, it appears that the presence of PCB3 in the air is from an as of yet unidentified point emission source. Exploring potential non-volatilization sources of

PCB3, and PCBs in general, will likely be a point of study in the future that will extend the work begun here.

3.7 Discussion of Gas-Phase Profiles by Site

In addition to analyzing total PCB concentration by sampling date and examining correlations with temperature, samples were analyzed by specific congener to create a mass fraction congener profile. The advantage of doing this is it allows us to see exactly what the composition by mass is for PCBs in Chicago air. By doing this, we can compare our sample profiles to known profiles of other environmental samples as well as the known original Aroclor profiles, looking for potential sources. Additionally, it allows us to look at trends beyond anomalies in the Clausius-Clayperon relationship; aside from looking for unusually high concentrations that are possible due to non-volatilization sources, we can look at sample specific profiles and compare to potential sources specific to each site and each sample collected on a given day. Because the vast majority of airborne PCBs are in the gas phase, and particulate PCB levels are typically related to gas phase concentrations, sample specific profiles were only calculated for XAD samples. These are discussed in detail below. Profiles for each site are shown, in relation to each other, in figure 3-24 below.

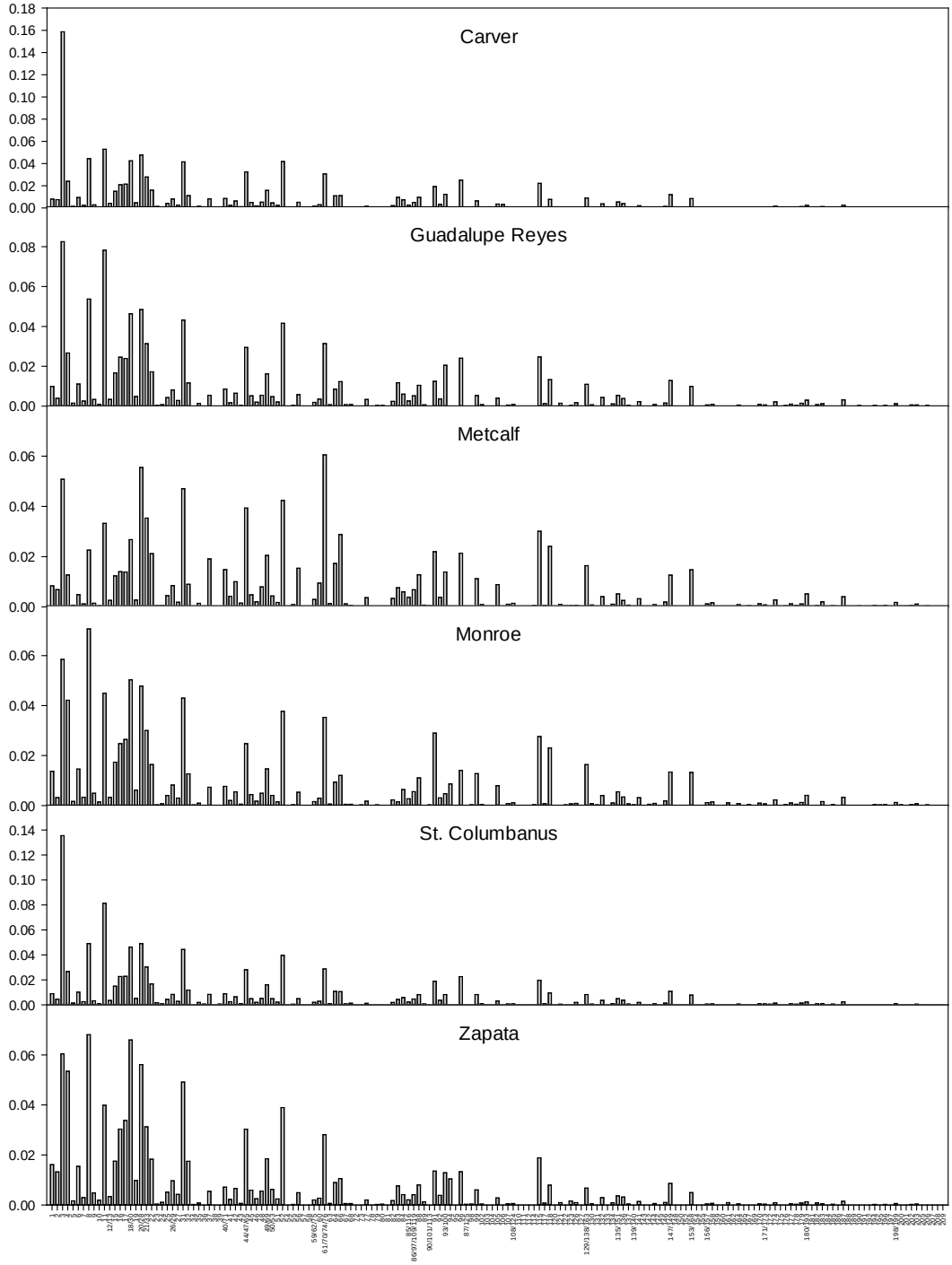

Figure 3-24: Average congener mass fraction profiles for gas-phase PCBs measured in Chicago for the six sites in this study having four or more samples

3.7.1 Guadalupe Reyes, St Columbanus, Zapata

The samples collected at Guadalupe Reyes, St. Columbanus, and Zapta all showed no dramatic differences between the samples within a site. Profiles from the three sites all correlated most strongly with Aroclor 1242, although the correlation for St. Columbanus is rather weak. With an R^2 value of only 0.31, it is the site in this study that most weakly correlates to a single Aroclor. The R^2 value for the correlation between Zapata and Aroclor 1242 was 0.69, making it the most highly correlated site in this study with a single Aroclor. Correlations for these sites are shown in figures 3-25, 3-26 and 3-27 below.

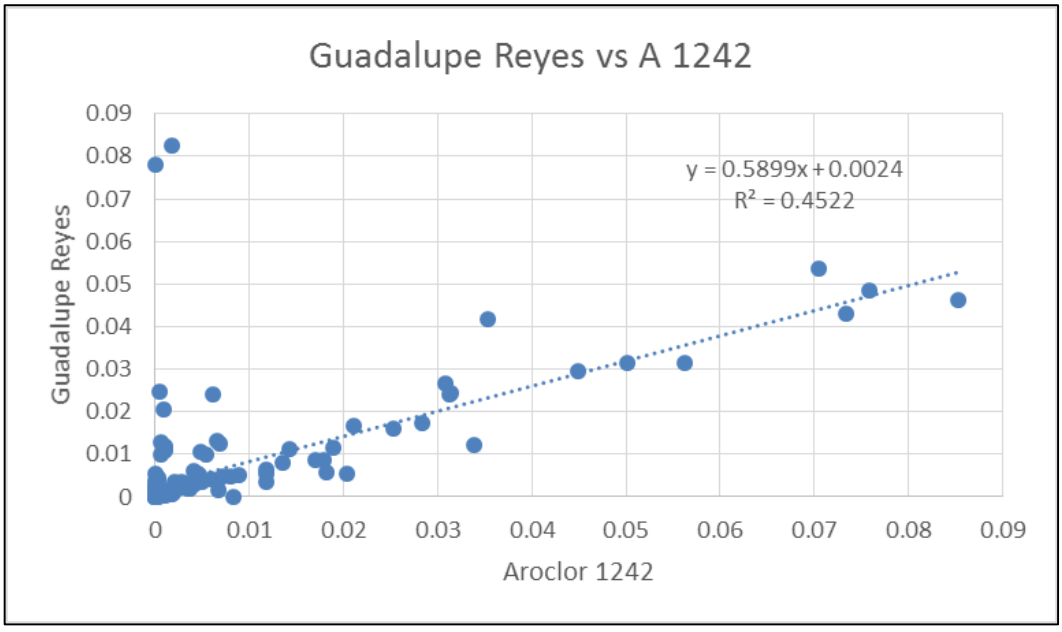

Figure 3-25: Comparison of mass fractions for gas-phase PCBs at Guadalupe Reyes and Aroclor 1242

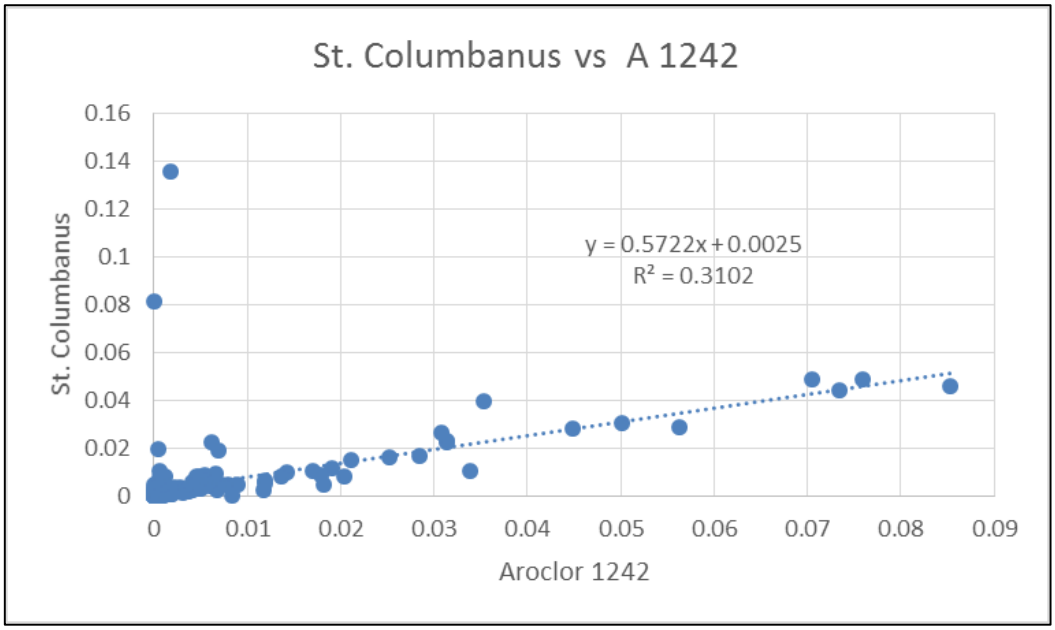

Figure 3-26: Comparison of mass fractions for gas-phase PCBs at St. Columbanus and Aroclor 1242

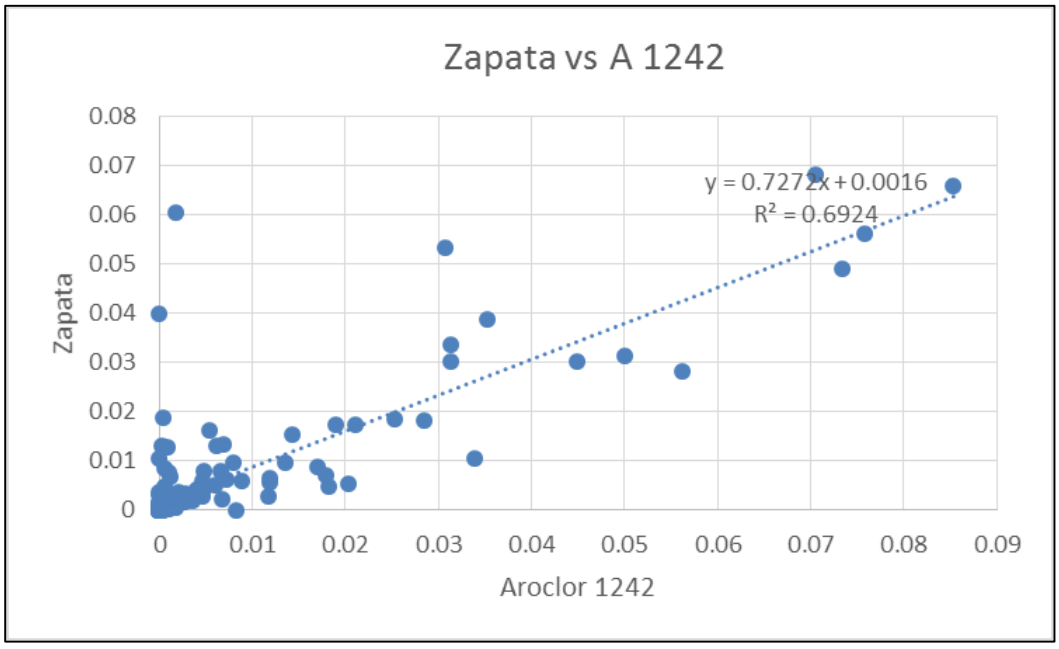

Figure 3-27: Comparison of mass fractions for gas-phase PCBs at Zapata and Aroclor 1242

3.7.2 Carver

Perhaps the most striking observation concerning the samples from Carver is that PCB3 constitutes such a large fraction of the total mass of PCBs in the samples. This contribution is largely due to one sample. In sample AA011-04, collected on 2/27/2009, the measured concentration for PCB3 was 262 pg/m^3. For comparison, this is roughly 18% of the total PCB3 detected in all of the thirty XAD samples in this study, and more than 5.5 times the average PCB 3 level of 47 pg/m^3 for all of the thirty samples analyzed in this study. It is very difficult to determine what the source of such a high concentration of just one PCB congener could be, and at this time I don't have any propositions. PCB 3 however is a congener of much interest as it appears that it's levels in Chicago are increasing since the study by Hu et al.[8], and will certainly be looked at further. Because the concentration for that one sample was so high for PCB 3, the other 3 samples were used to do a comparison to Aroclors. The Aroclor match was Aroclor 1242. The three Carver samples matched A1242 with an R^2 value of 0.62. This is seen in figure 3-28 below.

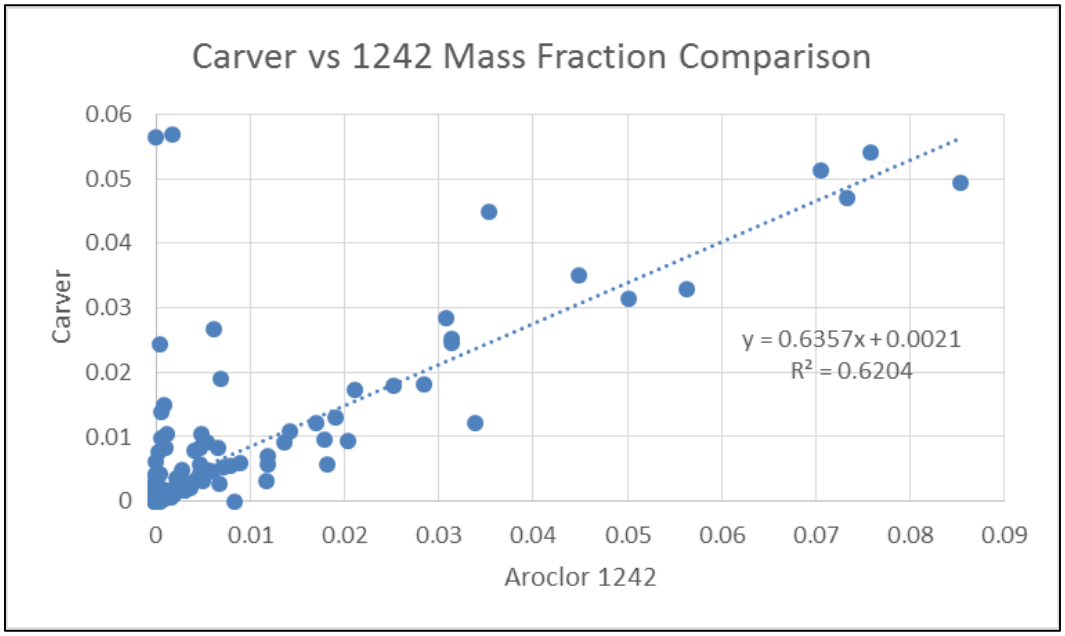

Figure 3-28: Comparison of mass fractions for gas-phase PCBs at Carver and Aroclor 1242

3.7.3 Metcalf

The samples from Metcalf are quite interesting. Looking at the profile for the samples as a whole, Metcalf is the only site in Chicago that has the highest correlation to Aroclor 1248, and not 1242. Also, recall that Metcalf was the site where the highest concentration sample was collected, and it was a strong outlier when modeling with the Clausius-Clayperon relationship. To look into this further, the samples from Metcalf were compared as a group without outlier and the outlier sample was compared individually. When this was done, it was found that the "normal", so to say, samples correlated most strongly with Aroclor 1242, and the outlier corresponded most strongly with Aroclor 1248. These results are shown below in figures 3-29 and 3-30.

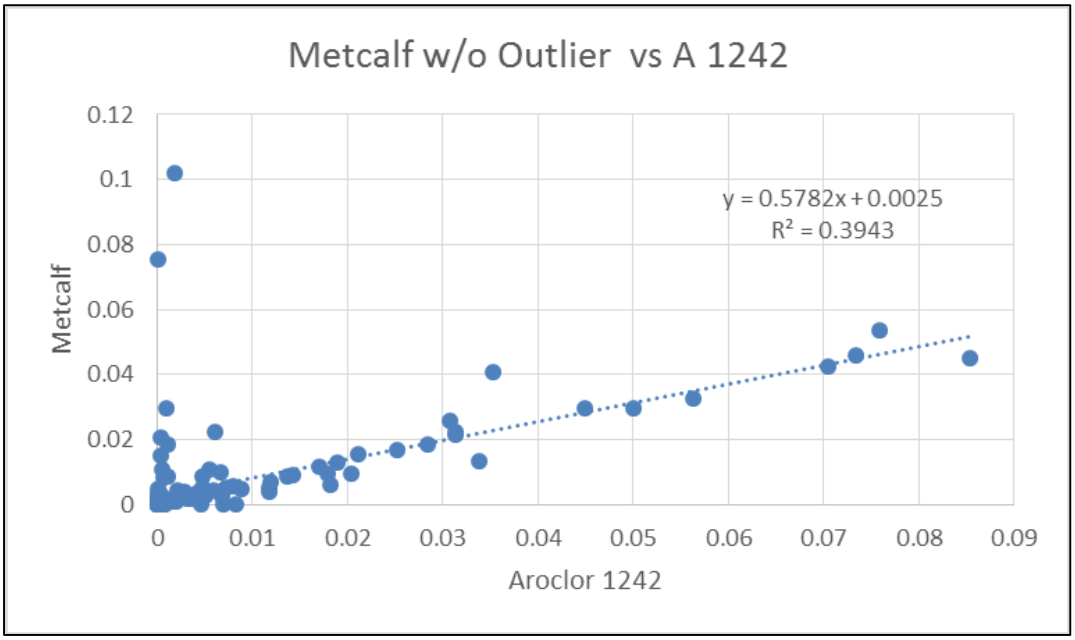

Figure 3-29: Comparison of mass fractions for gas-phase PCBs at Metcalf without the outlier sample and Aroclor 1242

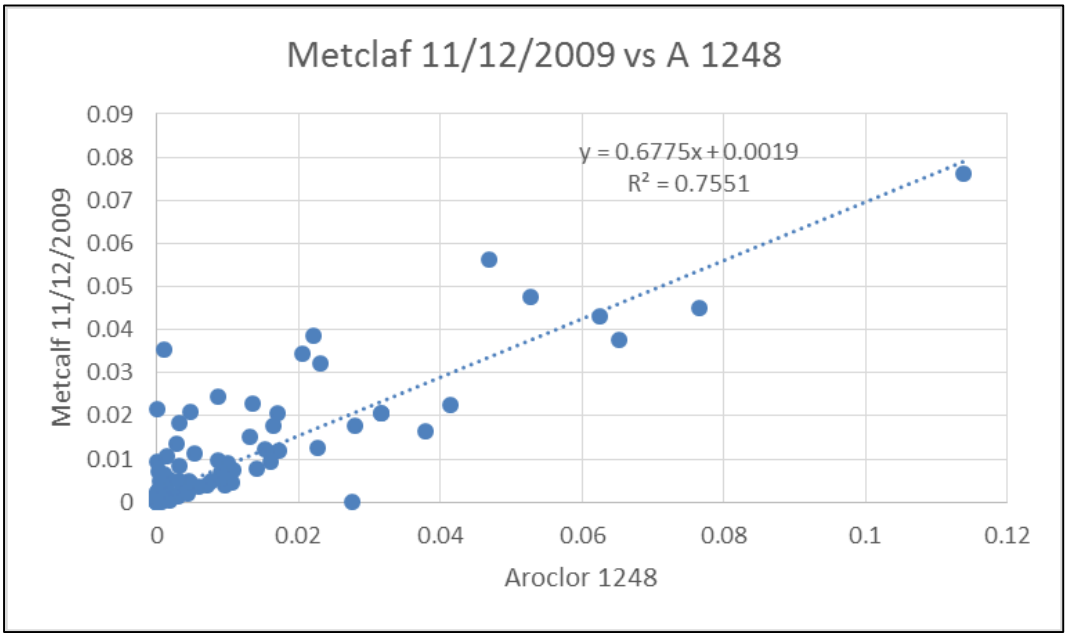

Figure 3-30: Comparison of mass fractions for Metcalf sample collected on 11/12/2009 and Aroclor 1248

Even though the samples correlate most strongly with Aroclor 1242 when the outlier is removed, the correlation, with an R^2 value of 0.39, is not very strong. The outlier however, has a very strong correlation to Aroclor 1248, with an R^2 value of 0.75, which is very high for the samples considered in this study. The fact that the outlier sample does not fit the Clausius-Clayperon relationship is further supported here because not only is it so much higher than expected, but the source seems to be something entirely different. While it is difficult to speculate as to what this would be exactly, one possible explanation could be if the wind were blowing strongly from one direction over a long period of time. It is known that atmospheric PCBs can be from long range or short range sources[28, 30], and it is entirely conceivable that at one site, at any given time, sources of atmospheric PCBs could be from both short range and/or long range sources. If the wind were blowing consistently over a long enough period of time from the direction of a source that with a strong signal for Aroclor 1248, it could be strong enough to overcome any local source and explain both why the concentration is so unexpectedly high and the sample has a distinct profile from all of the others.

3.7.4 Monroe

Of the five total samples collected at Monroe, 4 of them correlate strongly with Aroclor 1242, while one of them, collected on 7/28/2009, did not correlate well with Aroclor 1242 (R^2=0.16), but correlated most strongly with Aroclor 1254. The plots showing these correlations are shown in figure 3-31 and 3-32 below.

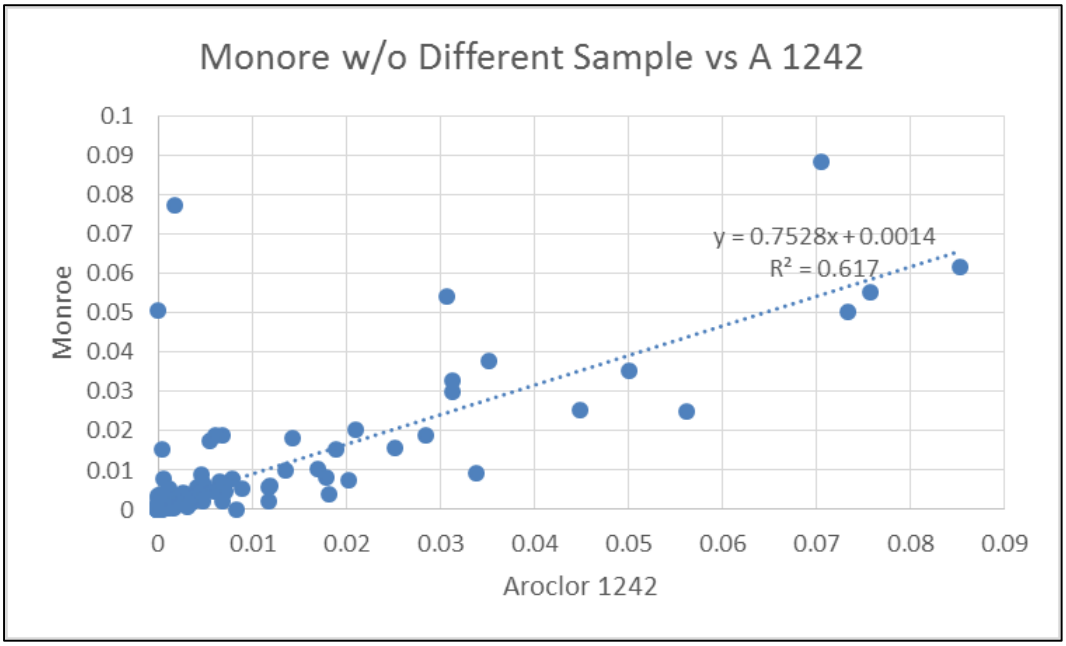

Figure 3-31: Comparison of mass fractions for gas-phase PCBs at Monroe without the outlier sample and Aroclor 1242

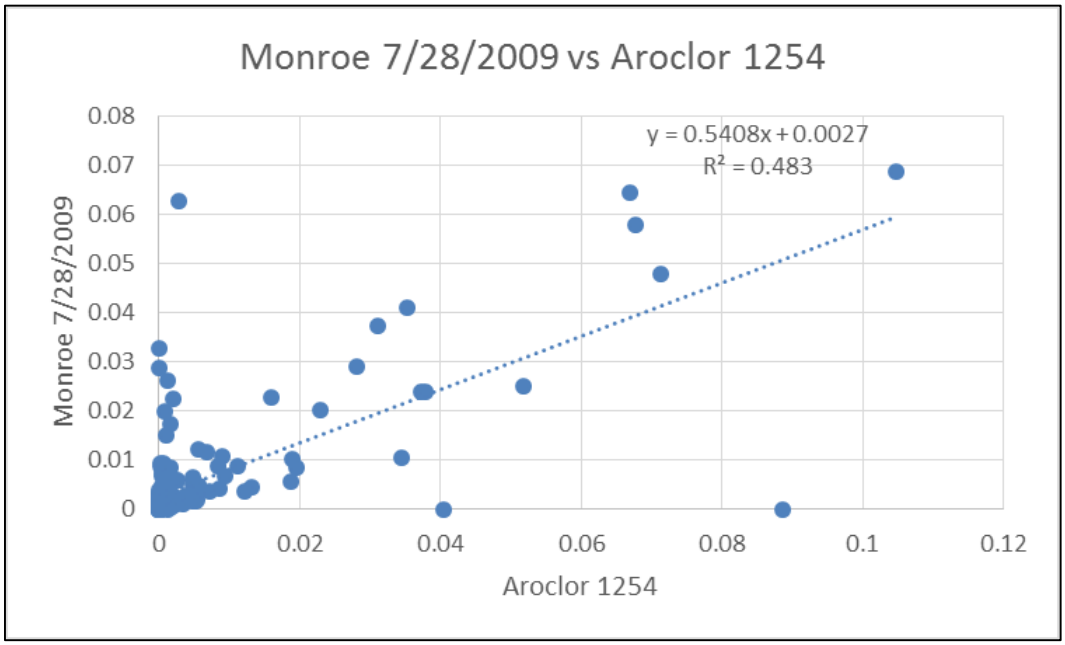

Figure 3-32: Comparison of mass fractions for Monroe sample collected on 7/28/2009 and Aroclor 1254

The difference in profiles between the one sample collected on 7/28/2009 from the other samples from Monroe suggests, again, that while the local source at Monroe likely resembles Aroclor 1242, it is occasionally possible for a long range source with a different characteristic profile to dominate the airborne PCB concentrations.

3.8 Spatial Distributions of ∑ PCBs in Chicago Air

An important element of this study was to analyze spatial distributions of PCBs in Chicago. The sample sites used were selected so that they, more or less, were uniformly spaced and formed a north to south transect through the city. The primary intention behind selecting the sites like this was, apart from the possibility of identifying one or more surprisingly high concentration sites, to determine if there was a tendency towards higher PCB concentrations between northern and southern Chicago.

The results from this study confirm what has been previously reported by Hu et al.[8], that PCB congeners are distributed throughout the city of Chicago, and exhibit a very small fraction of comparatively small fraction of sources that contribute to higher concentrations. Even then, these high concentration samples appear variable, as seen in the seasonal analysis at each site. Perhaps the most interesting observation is not that these sample maps don't point to one higher concentration area, but that the relative concentrations between sites appear to vary throughout the year. This indicates that while temperature is a dominant factor in dictating PCB concentrations, there are still other day to day factors that have an important influence on PCB concentrations. Figure 3-33 below shows the average ∑PCB concentration distribution for the six sites with

multiple samples considered in this study while figure 3-34 shows their seasonal ∑PCB concentrations.

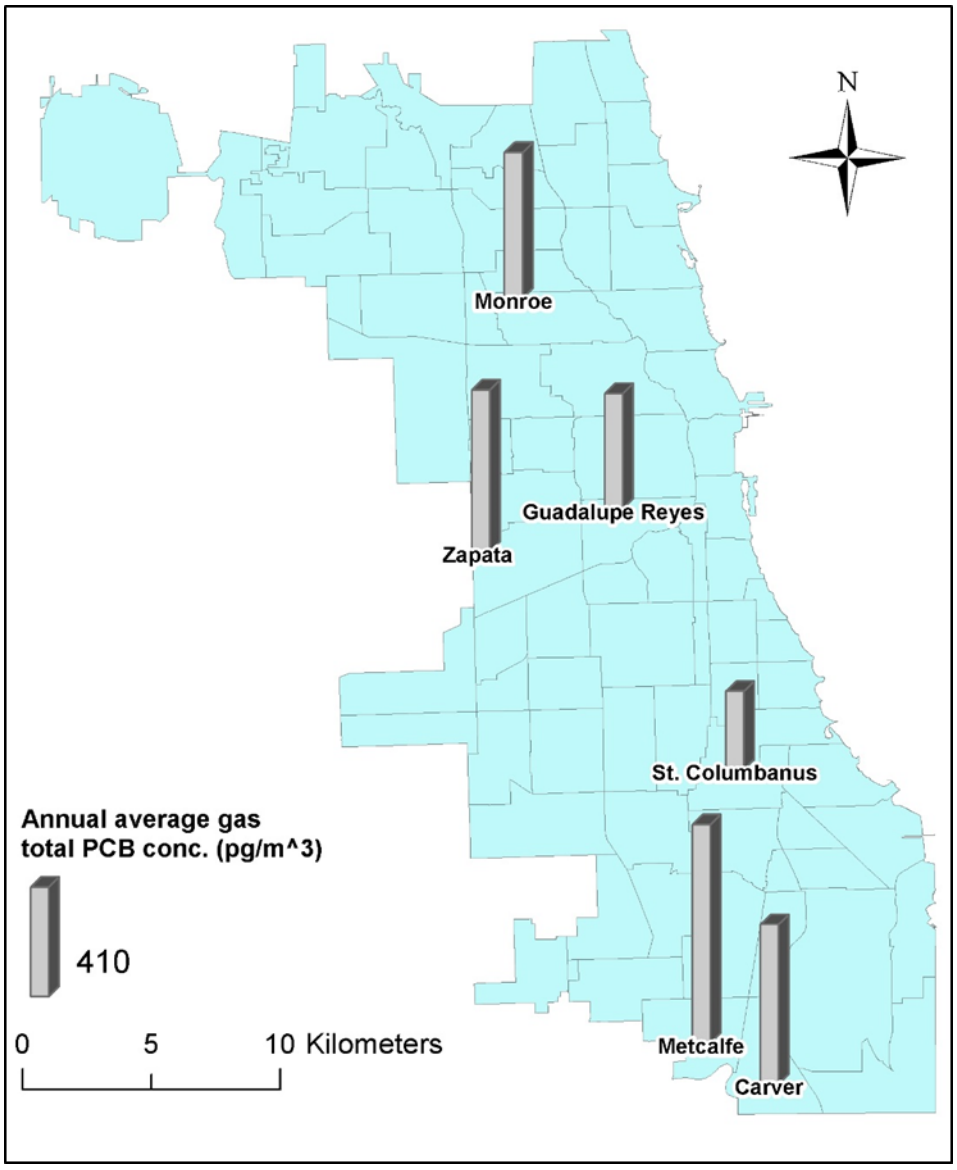

Figure 3-33: Average concentrations of ∑PCB for the six Chicago sites analyzed in this study

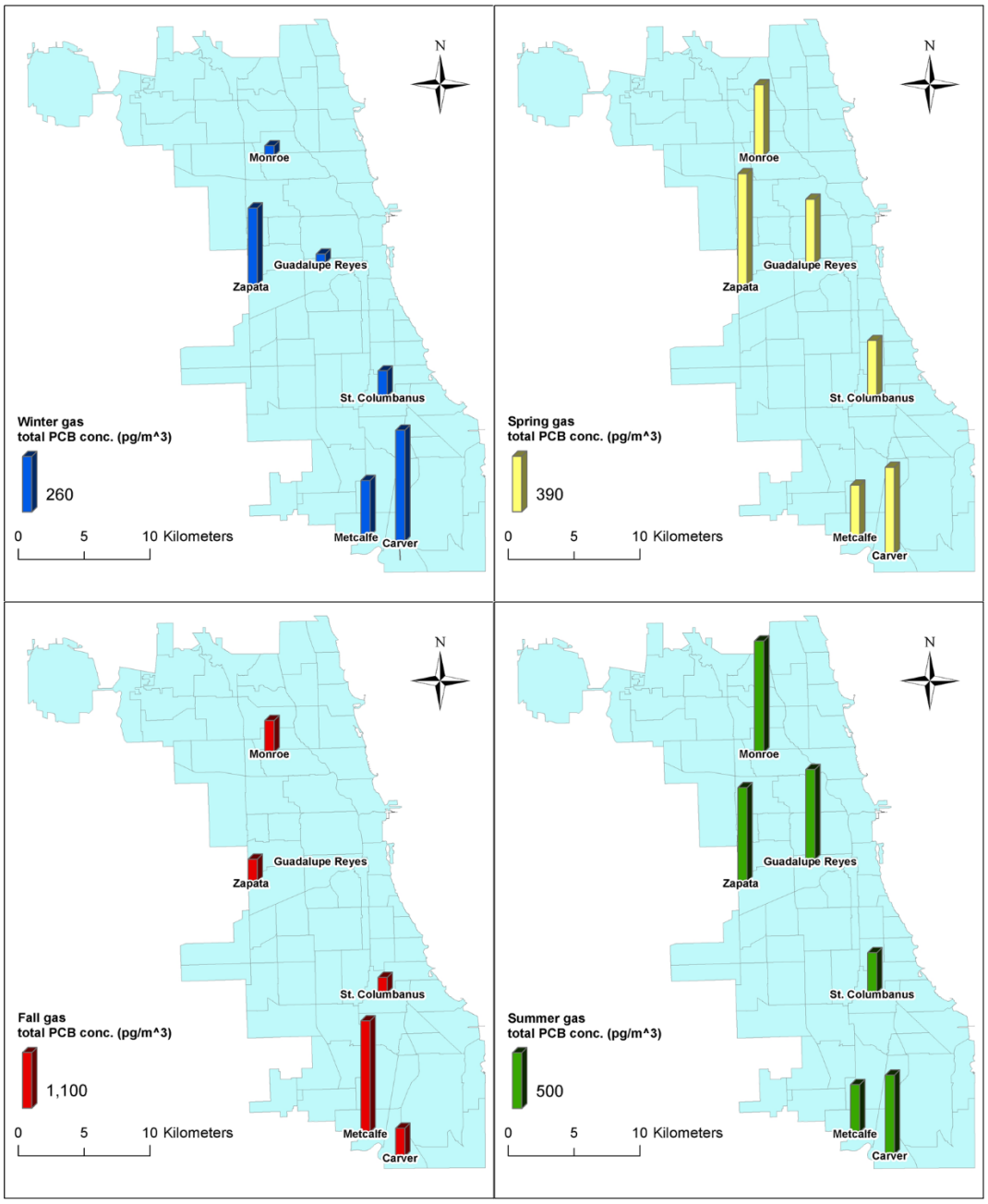

Figure 3-34: Seasonal distributions of ∑PCB concentrations for the six Chicago sites analyzed in this study

Perhaps a better method to observe spatial distributions would be to employ the use of passive samplers, as they are much less subject to the day to day variations at a site. Currently, Nick Herkert is in the middle of a study that involves the analysis of over 100 passive PUF samples. When the anlysis on this is complete, we will be better able to discuss spatial distributions throughout the city. As of now, however, if there is a trend, it is not yet clear to us. Below are maps, constructed by Andres Martinez, that show the yearly average gas-phase PCB concentrations at the sites we looked at in detail as well as their seasonal concentrations.

3.9 OH-PCBs in Chicago Air

One of the major objectives of this study was to discover whether or not we could detect the presence of OH-PCBs in air. While their presence in the atmosphere has been hypothesized as a result of reactions between PCBs and the hydroxyl radical[12-14], and the reason for observed diurnal variations in atmospheric PCB concentrations[13, 14], they have yet to be directly measured in atmospheric samples. We began this study with the hope to be the first to do so; and we did. In this study we detected 2 OH-PCBs in the gas phase, and 2 OH-PCBs in the particulate phase. At first, this was a little surprising to me, because previous studies have suggested the potential presence of many atmospheric OH-PCBs from several homologue groups[12-14]. However, considering there are 837 known monohydroxylated PCBs alone[15], and we only have the capacity to measure for 65 of those, the likelihood that we would happen to have standards for the same OH-PCBs that would be present in air is not necessarily very high. In the chromatograms I analyzed, there were many peaks that did not correspond to any of the 65 peaks in our

calibration standard. These peaks could very well represent OH-PCBs that we just are not able to verify.

3.9.1 Particulate phase OH-PCBs

In the particulate phase, we detected the presence of 6OH-PCB 2 and 3'OH-PCB65. Of the thirty QFF samples I analyzed, 6OH-PCB2 was only found above our LOQ in 6 samples, which were all collected in the summer months. Particulate phase concentrations of 6OH-PCB 2 ranged from 0.33 pg/m^3 on August 18, 2009 to 2.6 pg/m^3 on July 30, 2009, and had an average value of 0.90 +/- 0.85 pg/m^3. Values for 3'OH-PCB 65 in the particulate phase ranged from 0.039 pg/m^3 on May 29, 2009 to 0.26 pg/m^3 on June 15, 2009 with an average value of 0.13 +/- 0.071 pg/m^3. Figures 3-35 and 3-36 below show the measured concentrations for these congeners plotted in order of their collection date along with the average temperatures during the sampling period.

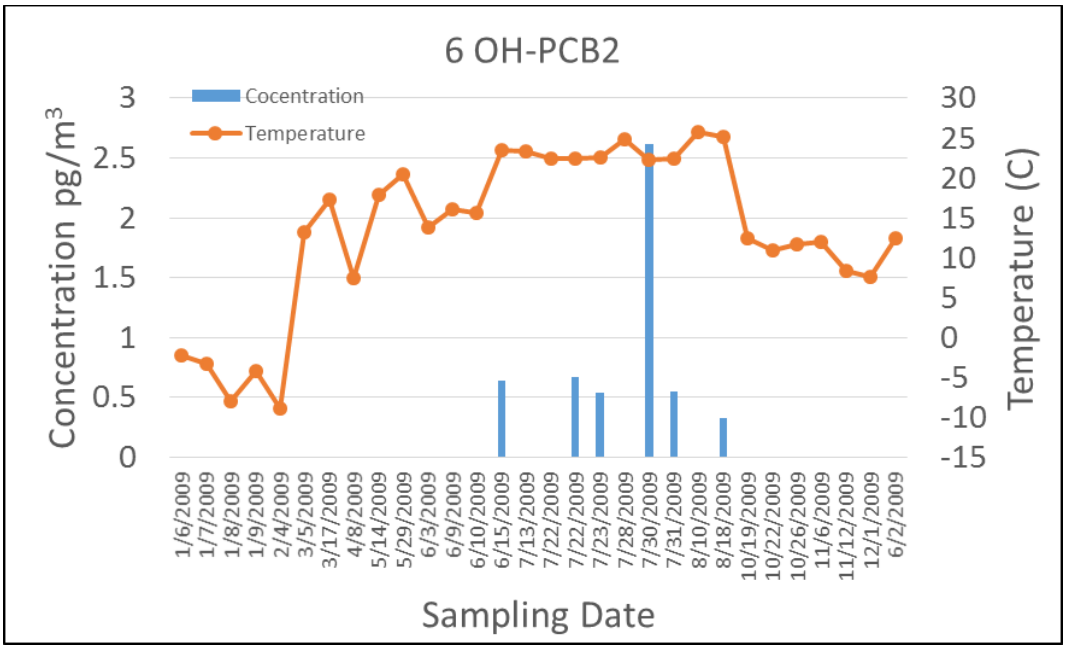

Figure 3-35: Particulate phase concentrations of 6OH-PCB2 in Chicago air samples plotted alongside the air temperatures they were collected at in order of their collection date.

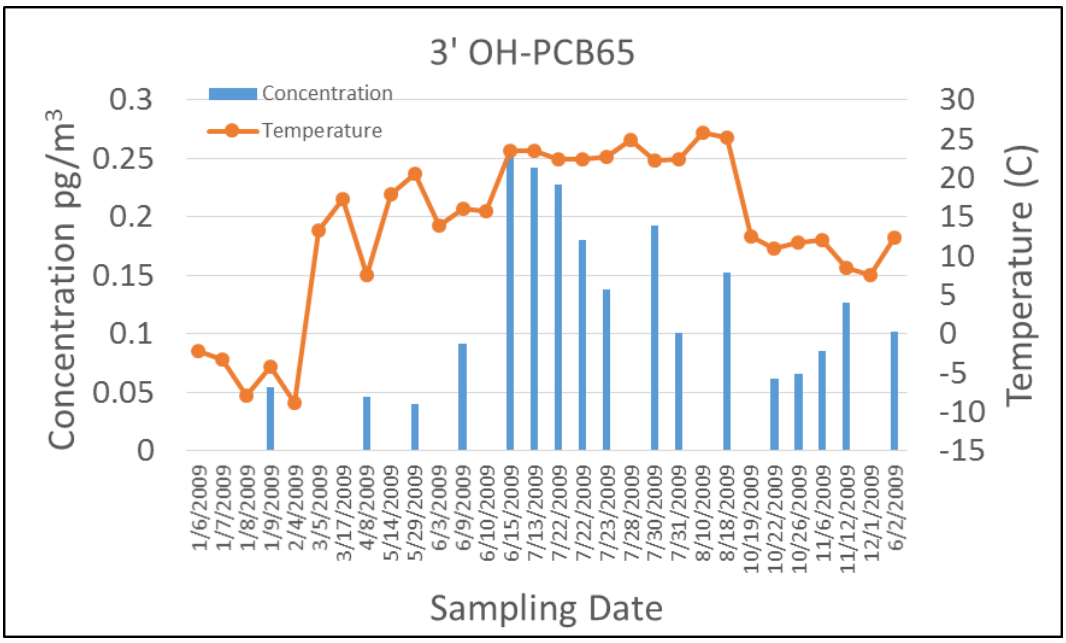

Figure 3-36: Particulate phase concentrations of 3'OH-PCB65 in Chicago air samples plotted alongside the air temperatures they were collected at in order of their collection date.

Looking at figures 3-35 and 3-36 it appears that, as for PCBs, it is difficult to measure OH-PCBs in the particulate phase. Many of the samples, especially in the case of 6OH-PCB2, were below our LOQ values. If there is a trend to be observed, it is not very evident from this sample set. Still, it can be seen that concentrations for both congeners were highest in the warmer summer months, as was expected.

Although the concentrations for 3'OH-PCB65 are overall very low, there does appear to be an overall trend to higher concentrations during the warmer months. Because this compound was detected in the particulate phase and therefore doesn't have a partial pressure associated with it, the Clausius-Clayperon relationship cannon be aplite to it. However, it can still be insightful to simply look for a trend between the congener's concentration and temperature, even if it is only qualitative.

3.9.2 Gas-Phase OH-PCBs in Chicago Air

In the gas phase, I detected 4OH-PCB2, and 6OH-PCB2. Figures 3-37 and 3-38 below show the concentrations of 4OH-PCB2 and 6OH-PCB2 by order of their sample collection date plotted against the average air temperatures over their sampling period, respectively.

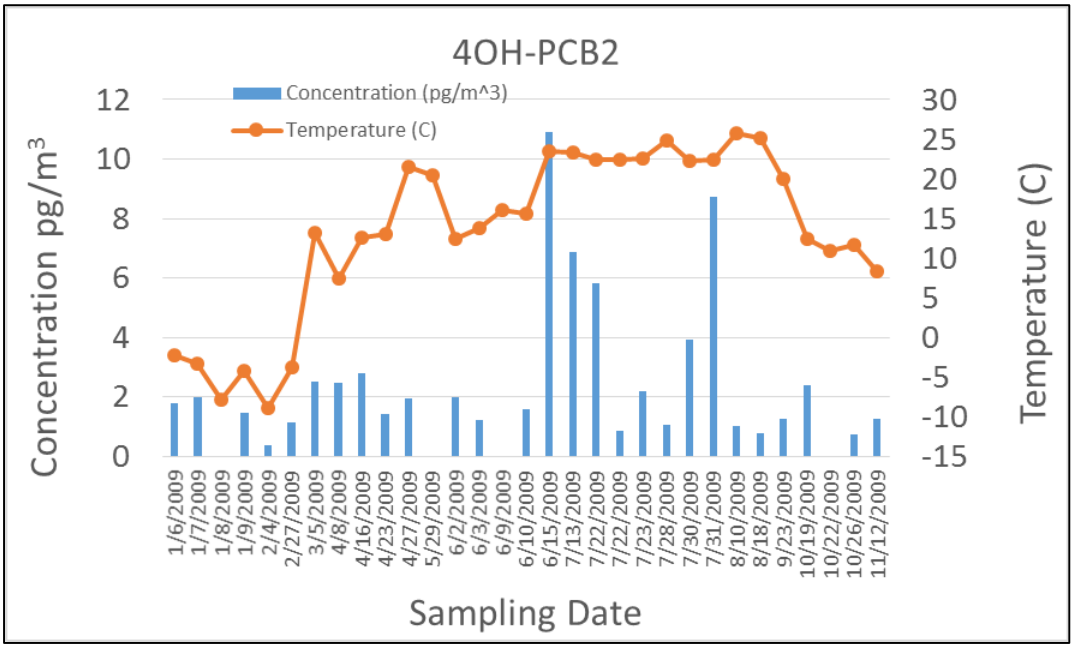

Figure 3-37: Gas-phase concentrations of 4OH-PCB2 in Chicago air samples plotted alongside the air temperatures they were collected at in order of their collection date.

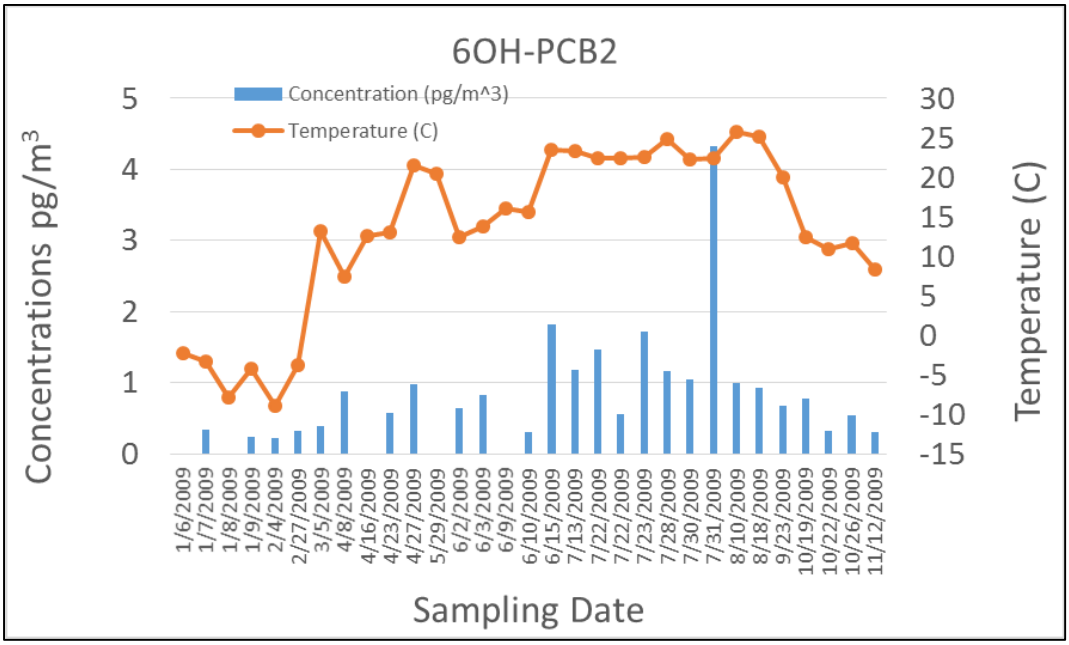

Figure 3-38: Gas-phase concentrations of 6OH-PCB2 in Chicago air samples plotted alongside the air temperatures they were collected at in order of their collection date.

While both congeners may exhibit some trend towards seasonality, 6OH-PCB2 has a much stronger correlation with temperature than 4OH-PCB2 (figure 3-37, figure 3-38). A more conclusive way to demonstrate this is to apply the Clausius-Clayperon model to both data sets to look for a relationship between congener partial pressure and temperature. This is examined for 4OH-PCB2 and 6OH-PCB2 in figures 3-39 and 3-40 below, respectively.

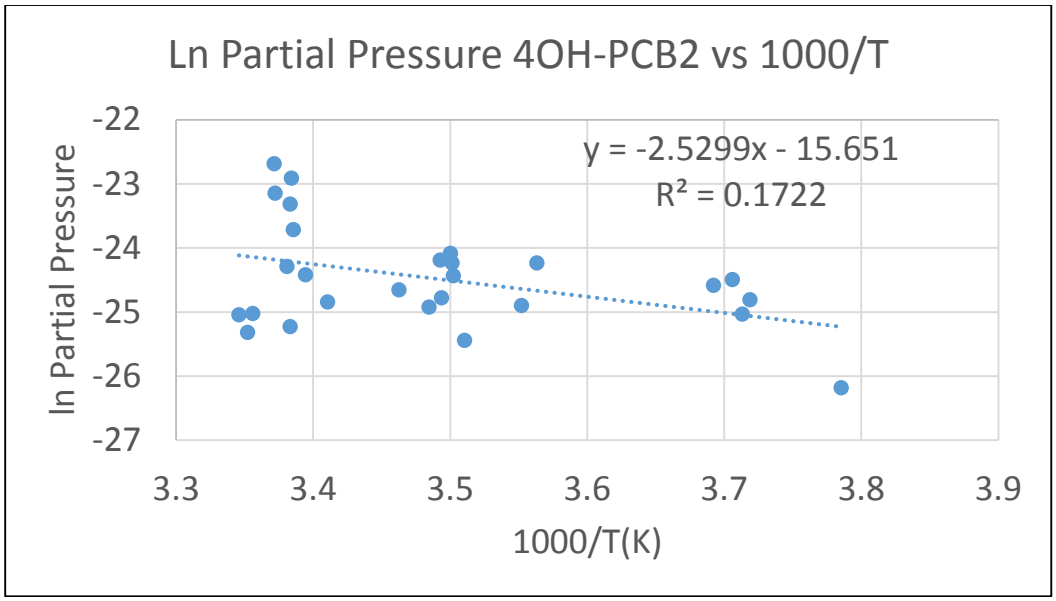

Figure 3-39: Clausius-Clayperon relationship applied to 4OH-PCB2. Plotted is the natural logarithm of the partial pressure contributed in the atmosphere from 4OH-PCB2 against 1000 times the inverse of absolute temperature for the sampling period. Also displayed are the equation for the linear regressions and the R^2 value.

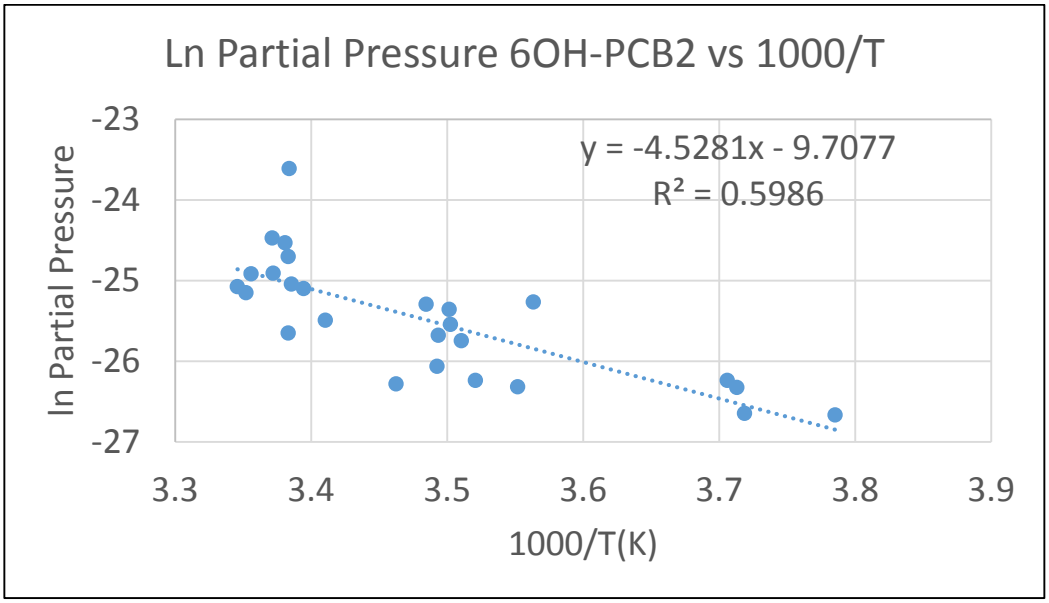

Figure 3-40: Clausius-Clayperon relationship applied to 6OH-PCB2. Plotted is the natural logarithm of the partial pressure contributed in the atmosphere from 6OH-PCB2 against 1000 times the inverse of absolute temperature for the sampling period. Also displayed are the equation for the linear regressions and the R^2 value.

Concentrations of 6OH-PCB2 show a much stronger correlation with temperature than concentrations of 4OH-PCB2 (figure 3-39, figure 3-40). As noted in the discussion of PCBs, application of the Clausius-Clayperon relationship can be a good indication as to whether or not the source of a compound in the atmosphere is in fact primarily due to volatilization. A good linear fit indicates that volatilization could in fact be a primary source to atmospheric concentrations, while a poor linear regression fit indicates that other sources, possibly emissions, contribute more to atmospheric concentrations. Looking at the Clausius-Clayperon relationship for 4OH-PCB2, it is obvious that the data doesn't fit the regression model very well. With an R^2 value of only 0.17, it can be concluded that the Clausius-Clayperon relationship is insufficient in indicating volatilization as a primary source of 4OH-PCB2 in the air. However, for 6OH-PCB2, this is not the case. The data set for 6OH-PCB fits the regression model quite nicely with an R^2 value of 0.60. This is especially good considering this data is for several sites throughout Chicago, each presumably with a unique source for volatilization. Also of worth mentioning is that when I calculated the value for the heat of vaporization for 6OH-PCB2 I got a value of 37 kJ/mol; almost exactly the same value I obtained for the sum of PCB congeners.

Additionally, concentrations of 6OH-PCB2 were examined by sampling site and compared to average temperatures over the sampling period. As for PCBs, the Clausius-Clayperon relationship was also applied to all of the sites with 3 or more samples with detectable gas-phase concentrations of 6OH-PCB2. Similarly to looking at the PCB samples by their collection site, in most cases the relationship between congener concentration and temperature was stronger on an individual site basis than for the combined sites. Three of the five sites with at least three samples had data that fit the linear regression for the Clausius-Clayperon model with R^2 values greater than 0.91. Figure 3-41 below shows concentrations of 6OH-PCB2 for each site plotted alongside the

average sampling temperature and figure 3-42 is of the Clausius-Clayperon relationship applied to the partial pressure contribution of 6OH-PCB2 in the atmosphere for each sampling site.

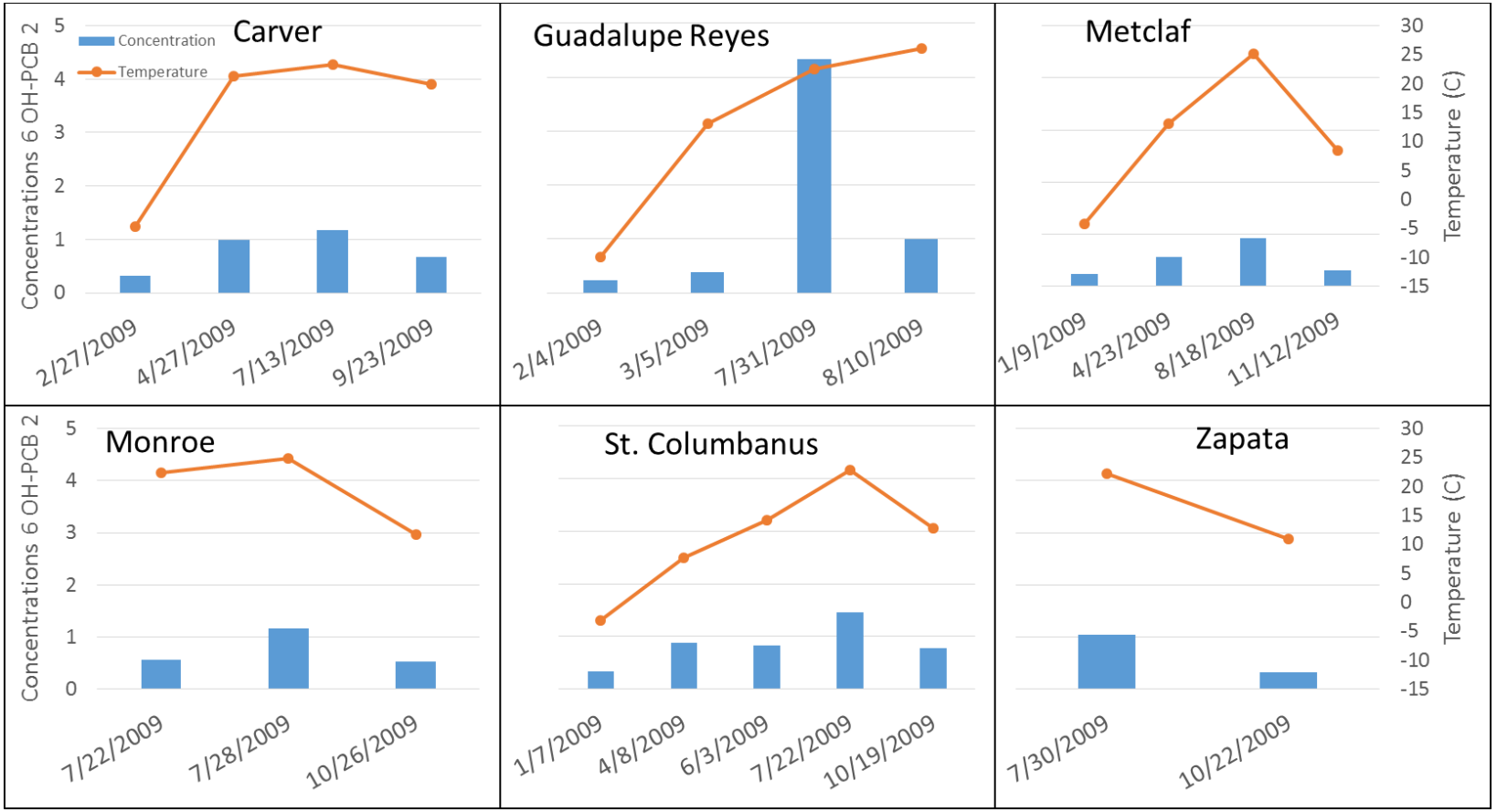

Figure 3-41: Site specific concentrations of 6OH-PCB2 in Chicago air samples plotted alongside the air temperatures they were collected at in order of their collection date.

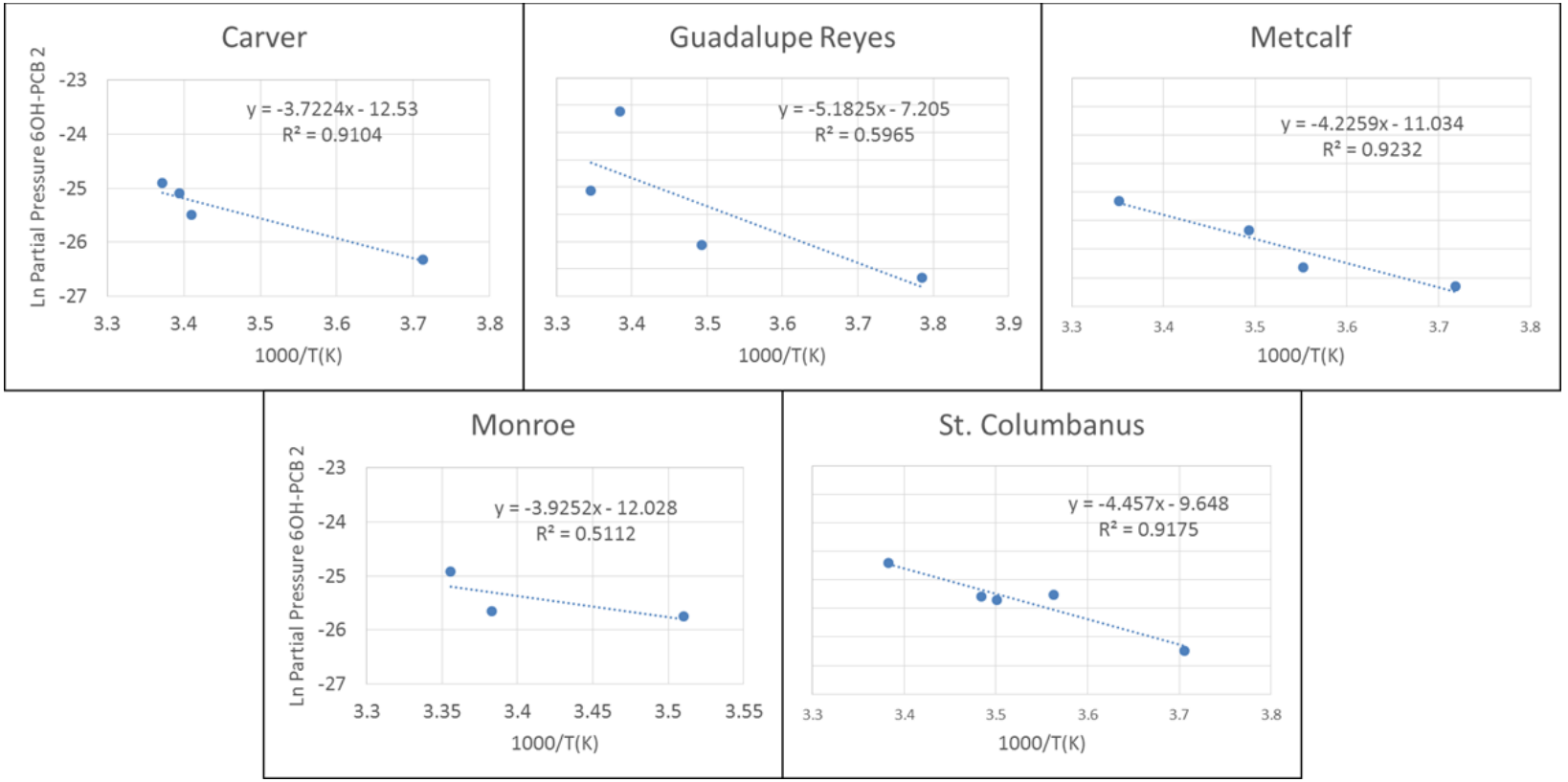

Figure 3-42: Clausius-Clayperon relationship applied to 6OH-PCB2 for individual sites across Chicago. Plotted is the natural logarithm of the partial pressure contributed in the atmosphere from 6OH-PCB2 against 1000 times the inverse of absolute temperature for the sampling period. Also displayed are the equation for the linear regressions and the R^2 value.

Figures 3-41 and 3-42 confirm what we would expect from looking at the data for all of the sites combined: The correlations between temperature and concentration, and temperature and partial pressure, are stronger when looking at individual sites. The Clausius-Clayperon relationship fits the data for Carver, Metcalf, and St Columbanus remarkably well. At the other two sites, Guadalupe Reyes and Monroe, the model still fits well, but it is not clear that volatilization is the only major source. One of the samples collected at Guadalupe Reyes is a strong outlier, containing several times the concentrations of 6OH-PCB2 of any of the other samples, and throws off the data set. At Monroe, 6 OH-PCB2 was only measured in three samples, two of which were collected in the summer at similar temperatures, making it a far from ideal data set to apply the Clausius-Clayperon relationship. For the majority of the data points however, the Clausius-Clayperon relationship provides a good model for describing the relationship between partial pressure of 6OH-PCB2 and absolute temperature, strongly suggesting its presence in the atmosphere is largely due to volatilization from a contaminated source.

Worth noting here is that the 3 sites that the Clausius-Clayperon relationship fit the data for 6OPH-PCB2 well are the 3 sites that it didn't work so well for ∑PCBs. Interestingly enough, the converse is also true; it fit the data for ∑PCBs well for the sites that it did not fit so well for 6OH-PCB2. While it is still early on, this data suggests that the potential source of gas-phase 6OH-PCB2 may be different than for the majority of gas-phase PCBs.

3.10. Exploring Hydroxyl Reactions as a Potential Source of Gas-phase OH-PCBs

I found the data for 6OH-PCB2 somewhat surprising based on the fact that the monochlorinated PCBs for the same sample set did not fit the Clausis-Clayperon relationship very well when examined as either the sum of the homologue group or as individual congeners. This, along with the fact that 4OH-PCB2 also did not fit the Clausius-Clayperon relationship, suggests that while volatilization may be a primary source of 6OH-PCB2 in the atmosphere, the presence of 4OH-PCB2 is potentially from a different source. While it is difficult to pinpoint an exact source to either hydoxylated compound in the atmosphere because little is understood about the origins of both of them, we can return to our original hypotheses to better understand where they may be coming from. Recall our hypotheses for OH-PCBs state that they can be present in the atmosphere by one of two means:

1.) Volatilizing from an environmental source such as Aroclors or sediment[16].
2.) As a result of reactions between PCBs and the hydroxyl radical[12, 20] .

Hypothesis 1 seems to confirm the presence of 6OH-PCB2, but not 4OH-PCB2. We can conclude that volatilization is likely not a primary source of 4OH-PCB2 in the atmosphere, but without further investigation, it would be premature to conclude that it is therefore a product from reactions between the hydroxyl radical and PCBs.
Before going on, it is important to understand the origins of the hydroxyl radical in the atmosphere. In the atmosphere, the hydroxyl radical forms from the photolytic degradation of ozone in the presence of water vapor according to the following reaction:

$$O_3 + h\nu(\lambda < 320nm) \rightarrow O(1D) + O_2$$

$$O(1D) + H_2O \rightarrow \cdot OH + \cdot OH$$

In the atmosphere, the hydroxyl radical in known to readily react with many organic pollutants, often times serving as the first step in their removal from the atmosphere. It is worth noting that the photons needed in order for this reaction to proceed are in the ultra violet (UV) part of the radiation spectrum. The amount of UV radiation that is able to penetrate to the troposphere (and consequently the production of the hydroxyl radical) is highly dependent on the level of cloud cover.

The only problem with confirming this hypothesis is that literature on the processes that govern these reactions, to the best of my knowledge, is not readily available. In an attempt to proceed with examining this hypothesis, I decided to assume the simplest hydroxyl radical and PCB reaction I could think of and proceed from there. Such a reaction would have the following characteristics:

1.) The reaction between a PCB congener and a hydroxyl radical will be simple. The hydroxyl radical will replace one of the constituent hydrogen ions with a hydroxide ion, leaving all of the constituent chlorines in the same location on the biphenyl molecule.
2.) Reactions between hydroxyl radicals and PCBs in the atmosphere occur at environmentally significant rates. Therefore, we can expect a consistent relationship observed between the concentration of an OH-PCB congener and its parent PCB congener across the sample set.

3.) In the atmosphere, there is one most likely reaction between a PCB congener and hydroxyl radical that will occur.

With these assumptions as a basis, I was able to narrow down the possible parent compound of any OH-PCB2 congener that is the product of hydroxyl reactions to PCB2. Although I still don't know all of the potential OH-PCB2 compounds, or their likelihood or forming from the reaction between a hydroxyl radical and PCB2, I could at least confirm or eliminate 4OH-PCB2 and 6OH-PCB2 as potential products of the reaction based on whether or not their concentrations demonstrated a trend compared with PCB2 concentrations.

I examined the relationship between gas-phase concentrations of PCB2 to gas-phase concentrations of 6OH-PCB2, and 4OH-PCB2, respectively. I did this by plotting values for the parent PCB congener (PCB 2) side by side with the two potentail daughter compounds in separate graphs (figure 3-43, figure 3-44).

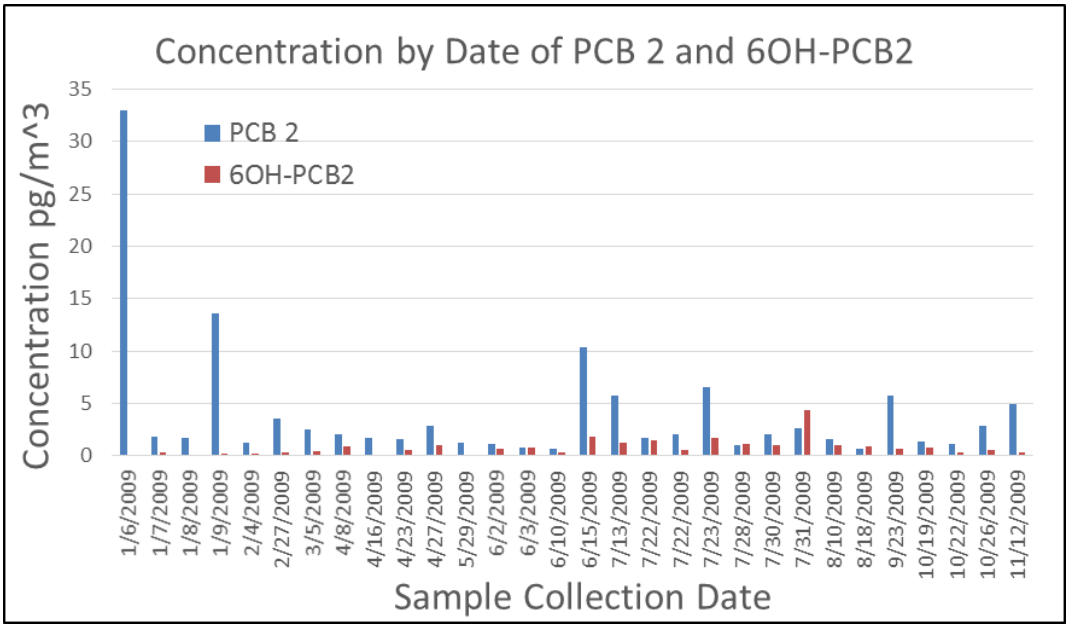

Figure 3-43: Concentrations of PCB2 and 6OH-PCB2 for samples collected in Chicago arranged according to their sampling date (values that appear as 0's for the hydoxylated compounds in the figures were below the LOQ)

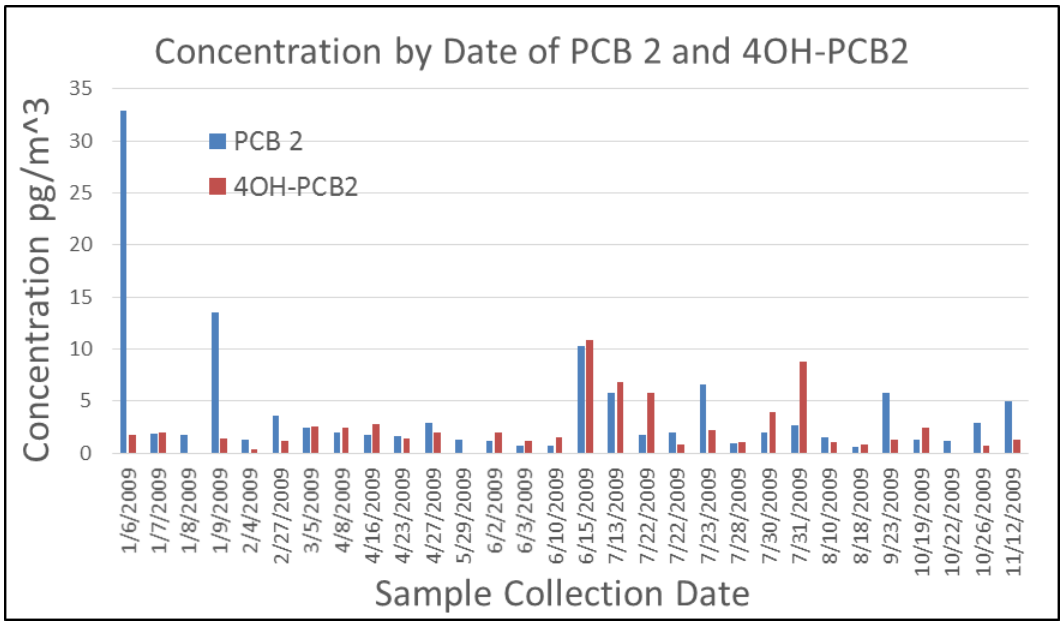

Figure 3-44: Concentrations of PCB2 and 4OH-PCB2 for samples collected in Chicago arranged according to their sampling date (values that appear as 0's for the hydoxylated compounds in the figures were below the LOQ)

It is striking how closely concentrations of 4OH-PCB2 correlate to concentrations of PCB2 compared to concentrations of 6OH-PCB2 (figure 3-43, figure 3-44). From a quick qualitative analysis it is clear that while concentrations of 6OH-PCB2 are on the same order as PCB2 for a few samples (primarily some of the summer samples), concentrations of 4OH-PCB2 are regularly comparable to levels for PCB2 concentrations. The similarities in levels was at first very surprising to me, because I saw absolutely no reason why the concentrations between these two compounds should be so close. However, after considering some of the results discussed by Totten et al.[14], this began to make more sense. While Totten et al. did not report a value for the diurnal variations in monochlorinated biphenyl congeners in Chicago, they did report that daytime concentrations, computed from a six-day average during July of 1994 in Chicago, for dichlorobiphenyl and trichlorobiphenyl are on average 58% and 55% of night time concentrations, respectively, with daytime PCB concentrations continuing to decrease with increasing chlorination for the higher chlorinated compounds[14]. Assuming that this decrease is solely due to hydroxyl reactions, we can expect concentrations of OH-PCBs to be comparable to their parent PCBs in daytime samples, potentially being a little higher. Further, if we assume reaction rates for monochlorobiphenyl are on the same order as for dichlorbiphenyl and trichlorobiphenyl, we can expect levels of PCB2 to be comparable to the hydorxlated compounds it forms. This is indeed what we see in the case of PCB2 and 4OH-PCB2.

It is evident that PCB2 and 4OH-PCB2 are not always present at similar concentrations (figure 3-44). Two samples in particular stand out. On January 6, 2009, and January 9, 2009, concentrations of PCB2 were several times higher than concentrations of 4OH-PCB2, for both samples. On both of these days light snow was reported in the forecast[26]. Totten et al. state that precipitation events can account for muted diurnal variations they observed in some of their samples[14]; this indeed appears to be the case

for our samples as well. Additionally, based on the reduced OH radical produced under overcast conditions, this is what we could expect to see. Further, it could account in part for the unusually high concentrations of PCB2 for these samples. Although temperatures were comparatively cold, levels of PCB2 could be higher than average in part due to reduced reaction with the hydroxyl radical. There are a five additional samples that contain significantly higher levels of PCB2 than 4OH-PCB2, but not to the same extent as the two samples discussed previously. Still, these samples warrant a closer look. In order of collection date they were sampled on 2/27/2009, 7/23/2009, 9/23/2009, 10/26/2009, and 11/12/2009. On three of these dates, there was precipitation recorded. On 2/27/2009 there was a rain and snow; on 7/23/2009 there was rain; on 10/26/2009 there was rain. On 9/23/2009, no precipitation was recorded, but the weather was overcast throughout the majority of the day, and there was rainfall recorded the day before, on 9/22/2009. On 11/12/2009, other than becoming overcast in the late afternoon, the weather appeared to be fairly mild.

3.11 Determining a Rate Constant for PCB2

In the laboratory experiments conducted by Anderson and Hites[12], and Atkinson and Aschmann[20], rate constants of reaction, k_{OH} were determined were determined for several different congeners, including 3-chlorobypenyl (PCB2). Anderson and Hites calculated temperature dependent rate constants for 14 congeners between temperatures that ranged from 323K to 363K, and then estimated K_{OH} values at 298K. For PCB2 they obtained a k_{OH} value at 298K of 5.0×10^{-12}molecules^{-1}cm^{3}s^{-1} with a 95% confidence interval of 4.4 – 5.7 x1 0^{-12}molecules^{-1}cm^{3}s^{-1}. Atkinson and Aschmann reported a value of $5.4 \pm 0.8 \times 10^{-12}$molecules^{-1}cm^{3}s^{-1} at a temperature of 295 ± 1K for PCB2. In the

environmental experiments conducted by Totten et al.[14] and Mandalakis et al.[13], environmental values were calculated for k_{OH} and compared to literature values, however, they did not report any k_{OH} values for PCB2, or any other monochlorinated PCBS.

In the studies mentioned above, reaction rate constants were calculated based on initial and final concentrations of PCB congeners, and using either a known or estimated OH radical concentration. Second order rate constants were then calculated according to the second order rate equation:

$$k_{OH,environment} = \frac{\ln \frac{C_{PCBi,final}}{C_{PCBi,initial}}}{t[OH]}$$

Where $C_{PCBi,initial}$ and $C_{PCBi,final}$ refer to the average PCB congener concentrations before and after reacting with the hydroxyl radical, respectively, and *t* is equal to the sampling time.

In this experiment, we did not have initial and final concentrations of PCBs at the start and end of the sampling period, but rather we calculated an average concentration over the sampling period. However, initial and final concentrations could be estimated based on the same assumption made by the other environmental studies discussed here[13, 14]; that all loss of a PCB in the atmosphere is due to its conversion to an OH-PCB by way of the second order reaction with the hydroxyl radical, according to

$$PCB_i + \cdot OH \rightarrow OH - PCB_i$$

where PCB_i is and $OH\text{-}PCB_i$ refer to a specific PCB congener. From this, a few basic consequences follow:

1.) Assuming that the overnight levels of the hydroxyl radical are negligible and PCB concentrations are able to increase as they continue to volatilize from their sources, we can reason that PCB concentrations will reach their peak levels at early morning, right before OH radical production begins.
2.) PCB levels during the day time will decrease by the same amount that their hydroxylated byproducts are produced.
3.) In the absence of the hydroxyl radical reaction, OH-PCB levels will dramatically fall overnight as a result of atmospheric dissipation; to levels that can be considered negligible to their daytime levels, and they will be lowest first thing in the morning, when PCB levels are highest.

Combining these assumptions with those made earlier, namely that there is one most likely reaction that takes place in the atmosphere between a PCB congener and the hydroxyl radical and that the reaction takes place at a relatively constant rate, we can reason that the initial concentration of a PCB congener in equations xxxx is equal to the average measured concentration of that congener plus the average measured concentration of its hydroxyl reaction product, and that the final concentration of a PCB congener in equation xxx then is approximately equal to its measured average concentration. Working with these assumptions as our presence, it follows that for PCB2

$$k_{OH,environment} = \frac{ln\frac{C_{PCB2,final}}{C_{PCB2,initial}}}{t[OH]}$$

Where $C_{PCB2,\,initial} = [PCB2] + [4OHPCB2]$

and $C_{PCB2,final} = [PCB2]$

Finally, following in the steps of Totten et al., we can assume an approximate value for [OH] for urban areas of 3 x 10^{-6} molecules cm^{-1}, as established by Howard et al.[52]. In the final analysis, when all of these things are considered, we can calculate a rate constant for the reaction and end up with a value of 8.03 ± 5.62 x 10^{-12} $molecules^{-1}cm^3s^{-1}$. This value is in good agreement with literature values, which are summarized in table 3-7 below.

Table 3-7: reported rate constants for reaction between PCB2 and OH radical

Study	K_{OH} $10^{-12}molecules^{-1} \times cm^3 \times s^{-1}$	Temp (K)	Type of study
This study (2015)	8.03 ± 5.62	287 ± 11	Environmental
Anderson, Hites (1996)	5.0 (95% CI, 4.4 – 5.7)	298	Laboratory
Atkinson, Aschmann (1985)	5.4 ± 0.8	295 ± 1	Laboratory

There are no other environmental studies to report rate constants for any monochlorinated PCBs to compare their value to. However, the value calculated here is closer to the literature values than many of the values calculated by Totten et al. using the similar method of approximating hydroxyl radical concentrations.

CHAPTER 4 SUMMARY AND CONCLUSIONS

PCBs were found to be more or less ubiquitously distributed throughout the city of Chicago, with no strong spatial trends among the sampling sites considered in this study, confirming the results previously reported by Hu et al.[8]. In the gas-phase, there was an average ∑PCB concentration of 594 pg/m^3 ± 445 pg/m^3 and ranged from 43.1 pg/m^3 to 2250 pg/m^3. As was expected there was a strong temporal relationship among ∑PCBs, and the fit the Clausius-Clayperon model very well, indicating that local volatilization sources play a major role in determining ∑PCB concentrations.

Although the vast majority of Chicago samples obey the Clausius-Clayperon equation and have PCB mass fraction profiles resemble that of Aroclor 1242, there are a few that more closely resemble other Aroclors and are outliers in the Clausius-Clayperon equation, indicating that although short range volatilization sources generally dominate airborne PCB distributions, it is possible for other factors to have larger contributions to airborne PCB levels.

The highest contributing congener to gas-phase PCBs was PCB 3, contributing to over 8% of total gas-phase PCBs by mass. Although an Aroclor congener, the mass fraction contribution is high enough such that it rules out Aroclors as a potential source. Concentrations of PCB3 also do not obey the Calusius-Clayperon relationship indicating it is likely present from an as of yet unidentified point emission source.

Particulate phase PCBs were found, on average, to contribute to 4.3% of total airborne PCBs by mass. ∑Particulate phase PCB concentrations averaged 26.3 pg/m^3 with a standard deviation of ± 38.1 pg/m^3 and ranged from 0.158 pg/m^3 to 123 pg/m^3.

Gas/particle partitioning coefficients, K_d were calculated for 77 PCB congeners. It was observed that K_d values increase with increasing PCB chlorination.

This study was successful in identifying OH-PCBs in both the gas and particulate phases. Contrary to our initial hypothesis, OH-PCBs were detected more frequently in the gas-phase than the particulate phase, although only slightly. In the gas-phase, 6OH-PCB2 exhibited temporal trends consistent with those of local volatilization sources, while 4OH-PCB2 exhibited traits indicative of a byproduct of the reaction between PCB2 and the hydroxyl radical. The calculated rate constant of $8.03 \pm 8.03 \pm 5.62 \times 10^{-12}$ molecules^{-1}cm^{3}s^{-1} for this reaction agrees well with rate constants determined by laboratory studies for the reaction of PCB2 with the hydroxyl radical[12, 20].

CHAPTER 5 FUTURE WORK

Anderson and Hites state that OH radical PCB reactions appear to be the major permanent loss process for PCBs from the atmosphere[12]. If this is indeed true, and the reactions happen at an environmentally significant rate as stated by Totten et al.[14], we should expect to see substantial amounts of OH-PCBs in the atmosphere – comparable to the concentrations of PCBs in the atmosphere. In this study, we found evidence to support this claim. Measured concentrations of PCB2 and 4OH-PCB2 suggest that this is happening, but we were unable to find conclusive evidence for other PCB congeners. A major issue hindering this is the sheer magnitude of possible OH-PCBs. With so many possible compounds and the ability to detect only a fraction of them, it is quite possible that the compounds we have standards for may not be the same compounds produced from reactions between OH radical and PCB congeners in the atmosphere. It would be beneficial if the mechanisms of the reactions were studied further so we could have a concrete idea of which congeners to look for in the air. Then we could potentially either obtain or synthesize standards for those compounds, develop analytical methods for their detection in environmental samples, and conduct a chamber experiment similar to that of Anderson and Hites to see if the proposed mechanisms of OH-PCB formation are accurate by seeing if they are in fact detected. The work conducted by Totten et al. suggests that removal rates in the environment are highest for di and trichlorobiphenyl. Perhaps reactions for these two homologue groups, in addition to the monochloroinated biphenyls, would be a good place to begin studying the reaction mechanisms between the hydroxyl radical and different PCBs.

REFERENCES CITED

1. Hornbuckle, K., et al., *Polychlorinated Biphenyls in the Great Lakes*, in *Persistent Organic Pollutants in the Great Lakes*, R. Hites, Editor. 2006, Springer Berlin Heidelberg. p. 13-70.
2. Erickson, M. and R. Kaley, II, *Applications of polychlorinated biphenyls.* Environmental Science and Pollution Research, 2011. **18**(2): p. 135-151.
3. Registry, A.f.T.S.D. *Toxic Substances Portal - Polychlorinated Biphenyls (PCBs): Health Effects*. [cited 2014 12/16/2014]; Available from: http://www.atsdr.cdc.gov/toxprofiles/tp.asp?id=142&tid=26.
4. USEPA, *Health Effects of PCBs*.
5. Giesy, J.P. and K. Kannan, *Dioxin-Like and Non-Dioxin-Like Toxic Effects of Polychlorinated Biphenyls (PCBs): Implications For Risk Assessment.* Critical Reviews in Toxicology, 1998. **28**(6): p. 511-569.
6. Kodavanti, P.R.S., *Molecular neurotoxicaology: Environmental Agents and Transcription-Transduction Coupling*. 2004. p. 151.
7. Ludewig, G., et al., *Metabolic activation of PCBs to carcinogens in vivo—A review*. Environmental Toxicology and Pharmacology, 2008. **25**(2): p. 241-246.
8. Hu, D., et al., *Atmospheric PCB congeners across Chicago.* Atmospheric Environment, 2010. **44**(12): p. 1550-1557.
9. Marek, R.F., et al., *PCBs and OH-PCBs in Serum from Children and Mothers in Urban and Rural U.S. Communities.* Environmental Science & Technology, 2013. **47**(7): p. 3353-3361.
10. Park, J.-S., et al., *Polychlorinated Biphenyls and Their Hydroxylated Metabolites (OH-PCBs) in Pregnant Women from Eastern Slovakia.* Environmental Health Perspectives, 2007. **115**(1): p. 20-27.
11. Kunisue, T. and S. Tanabe, *Hydroxylated polychlorinated biphenyls (OH-PCBs) in the blood of mammals and birds from Japan: Lower chlorinated OH-PCBs and profiles.* Chemosphere, 2009. **74**(7): p. 950-961.
12. Anderson, P.N. and R.A. Hites, *OH Radical Reactions: The Major Removal Pathway for Polychlorinated Biphenyls from the Atmosphere.* Environmental Science & Technology, 1996. **30**(5): p. 1756-1763.
13. Mandalakis, M., H. Berresheim, and E.G. Stephanou, *Direct Evidence for Destruction of Polychlorobiphenyls by OH Radicals in the Subtropical Troposphere.* Environmental Science & Technology, 2002. **37**(3): p. 542-547.
14. Totten, L.A., S.J. Eisenreich, and P.A. Brunciak, *Evidence for destruction of PCBs by the OH radical in urban atmospheres.* Chemosphere, 2002. **47**(7): p. 735-746.
15. Ueno, D., et al., *Detection of Hydroxylated Polychlorinated Biphenyls (OH-PCBs) in the Abiotic Environment: Surface Water and Precipitation from Ontario, Canada.* Environmental Science & Technology, 2007. **41**(6): p. 1841-1848.

16. Marek, R.F., A. Martinez, and K.C. Hornbuckle, *Discovery of Hydroxylated Polychlorinated Biphenyls (OH-PCBs) in Sediment from a Lake Michigan Waterway and Original Commercial Aroclors.* Environmental Science & Technology, 2013. **47**(15): p. 8204-8210.
17. Hu, D., A. Martinez, and K.C. Hornbuckle, *Discovery of Non-Aroclor PCB (3,3'-Dichlorobiphenyl) in Chicago Air.* Environmental Science & Technology, 2008. **42**(21): p. 7873-7877.
18. Hu, D. and K.C. Hornbuckle, *Inadvertent Polychlorinated Biphenyls in Commercial Paint Pigments†.* Environmental Science & Technology, 2009. **44**(8): p. 2822-2827.
19. Atkinson, R., et al., *Kinetics and Products of the Gas-Phase Reactions of OH Radicals and N2O5 with Naphthalene and Biphenyl.* Environmental Science & Technology, 1987. **21**(10): p. 1014-1022.
20. Atkinson, R. and S.M. Aschmann, *Rate constants for the gas-phase reaction of hydroxyl radicals with biphenyl and the monochlorobiphenyls at 295 .+-. 1 K.* Environmental Science & Technology, 1985. **19**(5): p. 462-464.
21. Petrich, N.T., et al., *Simulating and Explaining Passive Air Sampling Rates for Semivolatile Compounds on Polyurethane Foam Passive Samplers.* Environmental Science & Technology, 2013. **47**(15): p. 8591-8598.
22. Schulz, T.J., *Comparison of PCBs in East Chicago, Indiana and Columbus Junction, Iowa in Indoor and Outdoor air.* 2012.
23. USEPA, *Method 1668C Chlorinated Biphenyl Congeners in Water, Soil, Sediment, and Tissue by HRGC/HRMS.* 2010.
24. Martinez, A., et al., *Polychlorinated biphenyls in the surficial sediment of Indiana Harbor and Ship Canal, Lake Michigan.* Environment International, 2010. **36**(8): p. 849-854.
25. Buser, H.R., D.R. Zook, and C. Rappe, *Determination of methyl sulfone-substituted polychlorobiphenyls by mass spectrometric techniques with application to environmental samples.* Analytical Chemistry, 1992. **64**(10): p. 1176-1183.
26. Underground, W. *Chicago Illinois, 2009*. [cited 2014 12/22/2014]; Available from: http://www.wunderground.com/.
27. Carlson, D.L. and R.A. Hites, *Temperature Dependence of Atmospheric PCB Concentrations.* Environmental Science & Technology, 2004. **39**(3): p. 740-747.
28. Hillery, B.R., et al., *Temporal and Spatial Trends in a Long-Term Study of Gas-Phase PCB Concentrations near the Great Lakes.* Environmental Science & Technology, 1997. **31**(6): p. 1811-1816.
29. Hornbuckle, K.C. and S.J. Eisenreich, *Dynamics of gaseous semivolatile organic compounds in a terrestrial ecosystem—effects of diurnal and seasonal climate variations.* Atmospheric Environment, 1996. **30**(23): p. 3935-3945.
30. Simcik, M.F., et al., *Temperature Dependence and Temporal Trends of Polychlorinated Biphenyl Congeners in the Great Lakes Atmosphere.* Environmental Science & Technology, 1999. **33**(12): p. 1991-1995.
31. Sun, P., I. Basu, and R.A. Hites, *Temporal Trends of Polychlorinated Biphenyls in Precipitation and Air at Chicago.* Environmental Science & Technology, 2006. **40**(4): p. 1178-1183.

32. Wania, F., et al., *Temperature Dependence of Atmospheric Concentrations of Semivolatile Organic Compounds.* Environmental Science & Technology, 1998. **32**(8): p. 1013-1021.
33. Brunciak, P.A., et al., *Atmospheric polychlorinated biphenyl concentrations and apparent degradation in coastal New Jersey.* Atmospheric Environment, 2001. **35**(19): p. 3325-3339.
34. Hornbuckle, K.C., D.R. Achman, and S.J. Eisenreich, *Over-water and over-land polychlorinated biphenyls in Green Bay, Lake Michigan.* Environmental Science & Technology, 1993. **27**(1): p. 87-98.
35. Offenberg, J.H. and J.E. Baker, *Influence of Baltimore's Urban Atmosphere on Organic Contaminants over the Northern Chesapeake Bay.* Journal of the Air & Waste Management Association, 1999. **49**(8): p. 959-965.
36. Panshin, S.Y. and R.A. Hites, *Atmospheric Concentrations of Polychlorinated Biphenyls in Bloomington, Indiana.* Environmental Science & Technology, 1994. **28**(12): p. 2008-2013.
37. Persoon, C., et al., *Spatial Distribution of Airborne Polychlorinated Biphenyls in Cleveland, Ohio and Chicago, Illinois.* Environmental Science & Technology, 2009. **44**(8): p. 2797-2802.
38. Van Ry, D.A., et al., *Wet Deposition of Polychlorinated Biphenyls in Urban and Background Areas of the Mid-Atlantic States.* Environmental Science & Technology, 2002. **36**(15): p. 3201-3209.
39. Wethington, D.M. and K.C. Hornbuckle, *Milwaukee, WI, as a Source of Atmospheric PCBs to Lake Michigan.* Environmental Science & Technology, 2004. **39**(1): p. 57-63.
40. Green, M.L., et al., *Regional Spatial and Temporal Interpolation of Atmospheric PCBs: Interpretation of Lake Michigan Mass Balance Data.* Environmental Science & Technology, 2000. **34**(9): p. 1833-1841.
41. Falconer, R.L. and T.F. Bidleman, *Vapor pressures and predicted particle/gas distributions of polychlorinated biphenyl congeners as functions of temperature and ortho-chlorine substitution.* Atmospheric Environment, 1994. **28**(3): p. 547-554.
42. Hoff, R.M., D.C.G. Muir, and N.P. Grift, *Annual cycle of polychlorinated biphenyls and organohalogen pesticides in air in southern Ontario. 2. Atmospheric transport and sources.* Environmental Science & Technology, 1992. **26**(2): p. 276-283.
43. Franz, T.P., S.J. Eisenreich, and T.M. Holsen, *Dry Deposition of Particulate Polychlorinated Biphenyls and Polycyclic Aromatic Hydrocarbons to Lake Michigan.* Environmental Science & Technology, 1998. **32**(23): p. 3681-3688.
44. Hoff, R.M., et al., *Atmospheric deposition of toxic chemicals to the Great Lakes: A review of data through 1994.* Atmospheric Environment, 1996. **30**(20): p. 3505-3527.
45. Holsen, T.M., et al., *Dry deposition of polychlorinated biphenyls in urban areas.* Environmental Science & Technology, 1991. **25**(6): p. 1075-1081.
46. Finizio, A.M., Donald; Bidleman, Terry; Harner, Tom, *Octanol-Air Partitioning Coefficient as a Predictor of Partitioning of Semi-Volatile Organic Chemicals to Aerosols.* Atmospheric Environment, 1997. **31**(15): p. 2289 - 2296.

47. Harner, T. and T.F. Bidleman, *Octanol−Air Partition Coefficient for Describing Particle/Gas Partitioning of Aromatic Compounds in Urban Air*. Environmental Science & Technology, 1998. **32**(10): p. 1494-1502.
48. Hawker, D.W. and D.W. Connell, *Octanol-water partition coefficients of polychlorinated biphenyl congeners.* Environmental Science & Technology, 1988. **22**(4): p. 382-387.
49. Dunnivant, F.M., et al., *Quantitative structure-property relationships for aqueous solubilities and Henry's law constants of polychlorinated biphenyls.* Environmental Science & Technology, 1992. **26**(8): p. 1567-1573.
50. Frame, G.M., J.W. Cochran, and S.S. Bøwadt, *Complete PCB congener distributions for 17 aroclor mixtures determined by 3 HRGC systems optimized for comprehensive, quantitative, congener-specific analysis.* Journal of High Resolution Chromatography, 1996. **19**(12): p. 657-668.
51. Patterson Jr, D.G., et al., *Total TEQ reference range (PCDDs, PCDFs, cPCBs, mono-PCBs) for the US population 2001–2002.* Chemosphere, 2008. **73**(1, Supplement): p. S261-S277.
52. Philip H. Howard, R.S.B., William F. Jarvis, William M. Meylan, Edward M. Michalenko, *Environmental Degradation Rates*. 1991: Lewis Publishers.

APPENDIX OF RAW DATA

Table A-1 Raw data for sample batch AA008 showing necessary metadata and uncorrected congener masses for PCBs and OH-PCBs (ng)

Batch ID	AA008-01	AA008-02	AA008-03	AA008-04	AA008-06	AA008-07	AA008-08	AA008-09	AA008-11	AA008-12	AA008-10	
Sample ID	AV 0675	AV 0725	AV 0746	AV 0726	AV 0745	AV 0704	AV 0700	AV 0722	AV 0701	AV 0747		
Sampling Location	Adams	Carver	Guadalupe Reyes	Marquette	Monroe	Owens	St. Columbanus	St. Columbanus	Washington Park Academy	Zapata	Batch Blank	
Sampling Date	6/2/2009	7/13/2009	7/31/2009	7/23/2009	7/28/2009	6/15/2009	6/3/2009	7/22/2009	6/10/2009	7/30/2009		
Sampling Start Time	7:30	7:30	6:30	7:30	7:00	7:30	7:30	7:30	7:30	6:30		
Sampling Stop Time	15:30	14:30	12:30	13:45	12:30	14:30	15:30	13:30	15:30	12:30		
Sampling rate (m3/min)	0.4	0.4	0.4	0.4	0.4	0.4	0.4	0.4	0.4	0.4		
Air Volume (m^3	192	168	144	150	132	168	192	144	192	144		
Mean Temp (K)	286	297	296	296	298	297	287	296	289	295		
PCB Congener												LOQ (ng)
1	0.473	1.22	1.03	1.07	0.362	1.56	0.329	0.372	0.38	1.09	0.0715	0.0803
2	0.224	0.965	0.381	0.988	0.128	1.74	0.138	0.251	0.134	0.291	0.0413	0.0169
3	8.77	5.82	12.4	10.5	0.524	10.4	4.41	13.2	6.96	1.92	0.132	0.0912
4	1.44	4.24	2.93	3.16	0.976	5.88	0.732	1.23	0.808	6.69	0.0945	0.309
5	0.114	0.205	0.173	0.165	0.0695	0.307	0.0337	0.0796	0.0401	0.162	0.0166	0.0139
6	0.444	1.48	1.35	1.37	0.5	2.22	0.257	0.567	0.272	1.42	0.0391	0.22
7	0.103	0.326	0.331	0.286	0.116	0.452	0.0673	0.142	0.078	0.276	0.0261	0.0353
8	2.01	6.5	6.43	6.16	2.66	9.78	1.18	2.87	1.23	6.54	0.125	0.691
9	0.119	0.439	0.386	0.4	0.147	0.622	0.074	0.171	0.0731	0.423	0.0186	0.0501
10	0.0489	0.145	0.0994	0.101	0.0334	0.203	0.0289	0.0439	0.0317	0.164	0.00999	0.0167
11	4.24	4.5	11.4	6.61	3.85	10.3	2.5	5.32	4.12	4.6	0.182	0.33
12/13	0.206	0.551	0.405	0.477	0.177	1.23	0.101	0.192	0.146	0.324	0.0694	0.0606
15	0.674	2.16	2.16	2.1	1.19	3.57	0.42	1.03	0.439	1.96	0.0626	0.159
16	0.00723	3.15	3.16	2.8	1.25	5.77	0.576	1.42	0.735	3.61	0.0792	0.336

17	1.13	3.44	2.94	2.81	1.13	6.19	0.627	1.4	0.749	4.59	0.0739	0.419
18/30	2.26	6.45	6.15	5.41	2.3	11.5	1.29	2.76	1.44	8.03	0.152	0.944
19	0.319	0.875	0.491	0.567	0.224	1.3	0.171	0.265	0.216	1.3	0.0222	0.0964
20/28	2.19	6.73	6.38	6.31	3.51	13.2	1.39	3.41	1.77	6.33	0.148	0.715
21/33	2.49	3.75	3.92	3.82	2.02	6.64	0.803	2.04	0.929	3.12	0.108	0.356
22	1.22	2.19	2.31	2.16	1.24	4.35	0.433	1.19	0.572	1.89	0.0566	0.21
23	0.0194	0.062	0.0977	0.0704	0.0224	0.148	0.000174	0.147	0.000466	0.0459	0.012	0.00591
24	0.0328	0.109	0.09	0.0918	0.0447	0.191	0.0189	0.0361	0.0275	0.122	0.00963	0.0129
25	0.47	0.624	0.61	0.531	0.258	1.14	0.144	0.266	0.185	0.715	0.03	0.0946
26/29	0.0334	1.18	1.1	1.05	0.481	2.3	0.24	0.546	0.324	1.17	0.0547	0.135
27	0.163	0.433	0.333	0.326	0.163	0.88	0.0855	0.167	0.122	0.608	0.017	0.0497
31	0.2	5.94	5.61	5.69	2.99	11.1	1.28	2.98	1.6	5.74	0.133	0.683
32	0.504	1.88	1.43	1.49	0.651	3.57	0.329	0.745	0.411	2.21	0.0518	0.237
34	0.606	0.0403	0.000449	0.0381	0.0109	0.0611	0.000108	0.000213	0.000321	0.0245	0.014	0.00711
35	0.0872	0.172	0.208	0.178	0.0731	0.371	0.0446	0.143	0.0938	0.00017	0.022	0.0075
36	0.607	0.0003	0.000361	0.000403	0.0000873	0.0377	0.0000489	0.000624	0.0329	0.000298	0.0224	0.00668
37	0.34	0.963	1	1.08	0.899	2.12	0.215	0.624	0.284	0.000402	0.0501	0.0749
38	0.000384	0.054	0.0566	0.0159	0.000131	0.118	0.0427	0.000364	0.000122	0.000498	0.0171	0.00577
39	0.00026	0.000291	0.0396	0.0235	0.0000631	0.0691	0.0000245	0.0341	0.0641	0.000145	0.0218	0.00753
40/71	0.504	1.16	1.26	1.28	0.8	3.04	0.304	0.71	0.391	0.392	0.0533	0.129
41	0.121	0.306	0.231	0.366	0.142	0.692	0.0756	0.18	0.0884	0.174	0.0192	0.045
42	0.365	0.866	0.911	0.925	0.527	2.11	0.206	0.5	0.27	0.926	0.035	0.0929
43	0.0601	0.153	0.0771	0.156	0.00105	0.404	0.049	0.0849	0.049	0.00102	0.0126	0.0272
44/47/65	1.68	4.77	4.36	5.09	3.05	9.07	1.27	2.17	1.3	4.68	0.192	0.521
45	0.271	0.77	0.739	0.686	0.261	1.82	0.149	0.344	0.137	0.818	0.0207	0.0886
46	0.115	0.282	0.295	0.259	0.119	0.71	0.0603	0.136	0.0678	0.363	0.0156	0.0357
48	0.266	0.688	0.784	0.748	0.376	1.63	0.168	0.356	0.176	0.703	0.03	0.0848
49/69	0.963	2.26	2.28	2.73	1.55	5.37	0.657	1.22	0.743	2.86	0.102	0.321

50/53	0.309	0.703	0.664	0.628	0.273	1.73	0.188	0.339	0.267	1.07	0.0696	0.158
51	0.118	0.254	0.316	0.217	0.129	0.581	0.0695	0.135	0.103	0.465	0.0161	0.0333
52	2.45	5.65	6.01	8.56	5	12.4	1.93	3.12	1.96	5.02	0.249	0.873
54	0.00675	0.0167	0.0106	0.0107	0.00358	0.034	0.00421	0.00548	0.00372	0.0457	0.00653	0.00261
55	0.0149	0.0415	0.0652	0.0521	0.0392	0.109	0.013	0.0326	0.0266	0.000443	0.0182	0.0154
56	0.249	0.65	0.796	0.923	1.16	1.62	0.207	0.406	0.245	0.777	0.0359	0.121
57	0.0081	0.0172	0.0292	0.0237	0.00785	0.0368	0.00515	0.0119	0.000257	0.000316	0.0179	0.00754
58	0.00492	0.0136	0.0297	0.0182	0.015	0.0319	0.0047	0.0128	0.00053	0.00048	0.01	0.00426
59/62/75	0.106	0.265	0.27	0.265	0.142	0.632	0.0621	0.142	0.0872	0.267	0.0476	0.0318
60	0.129	0.347	0.536	0.507	0.638	0.859	0.112	0.239	0.131	0.398	0.0306	0.0537
61/70/74/76	1.47	4.17	4.48	7.03	8.62	8.81	1.39	2.39	1.51	4.22	0.238	0.677
63	0.0411	0.0901	0.121	0.119	0.0916	0.193	0.0298	0.0572	0.0418	0.0894	0.0211	0.0138
64	0.618	1.47	1.12	1.88	0.858	3.63	0.433	0.849	0.509	0.527	0.0571	0.197
66	0.55	1.45	1.72	2.18	2.69	3.57	0.455	0.868	0.542	1.54	0.0639	0.212
67	0.0315	0.0748	0.099	0.0921	0.0654	0.169	0.0213	0.049	0.0316	0.0883	0.0202	0.0114
68	0.0844	0.122	0.122	0.125	0.0672	0.146	0.0651	0.106	0.0813	0.0689	0.0703	0.0381
72	0.0139	0.0206	0.0333	0.0225	0.0111	0.05	0.00788	0.0161	0.0117	0.0143	0.0175	0.0078
73	0.0172	0.0245	0.0157	0.025	0.0166	0.05	0.00989	0.0173	0.0148	0.000412	0.0169	0.0128
77	0.0556	0.186	0.37	0.259	0.626	0.322	0.0364	0.118	0.0569	0.557	0.0163	0.0459
78	0.000118	0.000266	0.000268	0.0333	0.0242	0.0631	0.000285	0.00032	0.00172	0.000451	0.0273	0.00911
79	0.0000315	0.0305	0.000311	0.0434	0.0577	0.078	0.0102	0.000191	0.00134	0.000602	0.0123	0.00454
80	0.000174	0.000236	0.0619	0.0153	0.0243	0.000304	0.0000358	0.0000875	0.0000502	0.103	0.0225	0.0105
81	0.000132	0.000219	0.0000448	0.0131	0.0504	0.0316	0.000169	0.00038	0.00197	0.0506	0.025	0.00842
82	0.0853	0.244	0.373	0.419	0.602	0.417	0.0968	0.157	0.117	0.28	0.0229	0.0759
83	0.0925	0.157	0.243	0.28	0.21	0.257	0.0651	0.12	0.132	0.223	0.0206	0.0294
84	0.422	0.778	1.09	1.68	1.15	1.72	0.4	0.58	0.49	1.08	0.0863	0.283
85/116	0.0935	0.261	0.386	0.549	0.769	0.567	0.142	0.21	0.181	0.396	0.0401	0.0752
86/97/109/119	0.291	0.601	0.808	1.16	1.41	1.27	0.28	0.38	0.355	0.672	0.0672	0.171

88	0.000137	0.000235	0.000311	0.0000906	0.000138	0.000215	0.0000939	0.0000502	0.000792	0.000487	0.0195	0.0715
89	0.0143	0.0401	0.0556	0.0549	0.0343	0.0847	0.0141	0.0251	0.014	0.0372	0.00936	0.00783
90/101/113	1.35	3.46	4.07	7.07	7.74	6.26	1.3	2.06	1.59	3.76	0.271	0.903
91	0.208	0.381	0.482	0.736	0.491	0.853	0.173	0.283	0.216	0.549	0.0267	0.0629
92	0.238	0.51	0.646	1.06	0.905	1	0.203	0.349	0.287	0.607	0.0568	0.165
93/100	0.0149	0.0387	0.0355	6.27	4.37	0.0762	0.0136	0.025	0.0159	4.19	0.0205	0.0151
94	0.0101	0.0173	0.0198	0.0304	0.00648	0.0463	0.00843	0.0142	0.00503	0.012	0.00922	0.00601
95	1.43	3.13	3.55	0.000178	0.0000883	5.97	1.31	1.91	1.55	0.00137	0.24	0.948
96	0.0152	0.0282	0.04	0.0371	0.0173	0.0691	0.0118	0.0184	0.0108	0.0402	0.00671	0.00599
87/125	0.395	1.06	1.61	2.39	3.18	2.13	0.445	0.798	0.561	1.32	0.127	0.358
98	0.0109	0.0117	0.00702	0.22	0.135	0.0144	0.00693	0.00766	0.00381	0.148	0.0121	0.0173
99	0.556	1.45	1.75	2.98	3.21	2.86	0.57	0.872	0.675	1.62	0.0881	0.413
102	0.04	0.096	0.119	0.035	0.0157	0.201	0.0351	0.0688	0.0399	0.0372	0.0138	0.0161
103	0.0132	0.0261	0.0374	0.0375	0.0163	0.0596	0.00922	0.019	0.0121	0.0244	0.00746	0.00645
104	0.00139	0.00365	0.00268	0.00341	0.000824	0.0058	0.000762	0.00156	0.00105	0.00334	0.00472	0.00327
105	0.115	0.453	0.608	0.846	3.33	0.833	0.149	0.289	0.203	0.529	0.0316	0.0693
106	0.000118	0.000107	0.000241	0.0000952	0.0000754	0.000269	0.0000364	0.000073	0.000384	0.0000746	0.00516	0.00276
107	0.0283	0.0643	0.0855	0.119	0.267	0.125	0.0267	0.0528	0.0428	0.0737	0.0163	0.0167
108/124	0.0369	0.0917	0.125	0.165	0.376	0.169	0.0382	0.0649	0.0621	0.0971	0.0106	0.0163
110	0.0000412	0.000209	0.000191	0.00018	0.000169	0.0000639	0.0000543	0.000118	0.00189	0.000417	0.336	0.131
111	0.0000361	0.000105	0.000423	0.000115	0.0000939	0.0000799	0.0000297	0.0000714	0.0000752	0.0000487	0.00797	0.00308
112	0.0000659	0.0000709	0.000479	0.00024	0.000238	0.0000486	0.0000362	0.0000161	0.0000254	0.0000165	0.00985	0.00809
114	0.0229	0.0527	0.0566	0.0717	0.146	0.0861	0.023	0.0406	0.0337	0.0457	0.233	0.0838
115	1.1	2.52	3.77	5.49	8.36	5.07	1.09	1.82	1.39	3.28	0.191	0.671
117	0.317	0.323	0.412	0.383	0.373	0.387	0.263	0.287	0.335	0.305	0.551	0.286
118	0.421	1.38	2.05	3.12	9.17	2.74	0.498	0.894	0.631	1.71	0.0955	0.254
120	0.0000292	0.000124	0.000109	0.000145	0.000149	0.0000728	0.0000361	0.0000562	0.0000507	0.0000328	0.00928	0.00329
121	0.00005	0.000138	0.000156	0.0000781	0.0000266	0.0000158	0.00301	0.0000707	0.0000496	0.000394	0.00807	0.00343

122	0.0129	0.0314	0.0438	0.0292	0.0516	0.0535	0.00974	0.0215	0.000247	0.0188	0.00571	0.00678
123	0.00763	0.0328	0.0589	0.075	0.143	0.0491	0.0124	0.0375	0.000468	0.041	0.00879	0.0141
126	0.282	0.319	0.564	0.365	0.438	0.463	0.267	0.35	0.372	0.382	0.00372	0.141
127	0.000205	0.0000993	0.000313	0.00022	0.000145	0.000191	0.0000406	0.000235	0.0000855	0.0000923	0.00279	0.000996
129/138/163	0.363	0.971	1.52	2.11	6.4	1.82	0.376	0.873	0.413	1.16	0.0839	0.171
130	0.0241	0.0572	0.0978	0.118	0.261	0.103	0.0245	0.0516	0.027	0.0676	0.0062	0.00948
131	0.0078	0.0236	0.0337	0.0508	0.0577	0.0438	0.00847	0.0159	0.00719	0.0268	0.00659	0.00884
132	0.181	0.397	0.591	0.845	1.37	0.744	0.172	0.348	0.184	0.485	0.0403	0.104
133	0.00578	0.0172	0.0311	0.0295	0.0485	0.0286	0.00756	0.0143	0.0049	0.0146	0.00303	0.00175
134	0.0514	0.128	0.142	0.211	0.254	0.196	0.0486	0.0964	0.0382	0.127	0.0129	0.0268
135/151	0.265	0.71	0.776	1.17	1.45	1.12	0.215	0.487	0.244	0.586	0.0613	0.139
136	0.218	0.52	0.534	0.857	0.682	0.806	0.183	0.329	0.177	0.456	0.0358	0.134
137	0.0205	0.0513	0.0693	0.117	0.215	0.0924	0.0289	0.0413	0.0195	0.0663	0.0124	0.0109
139/140	0.0117	0.0293	0.0444	0.0633	0.0607	0.0567	0.0146	0.029	0.0115	0.0331	0.0181	0.014
141	0.077	0.233	0.318	0.416	1.16	0.378	0.0785	0.188	0.0915	0.224	0.0202	0.0403
143	0.00239	0.00356	0.00579	0.0155	0.000479	0.00031	0.000306	0.00531	0.00181	0.00477	0.0076	0.00887
142	0.00038	0.00285	0.000394	0.0032	0.000296	0.00589	0.000706	0.00257	0.000183	0.000155	0.00618	0.00222
144	0.038	0.102	0.118	0.187	0.234	0.159	0.0322	0.0653	0.0339	0.0879	0.01	0.0186
145	0.000502	0.00336	0.00102	0.00406	0.00127	0.00531	0.00104	0.00122	0.00017	0.000963	0.00817	0.00423
146	0.0656	0.163	0.24	0.299	0.626	0.278	0.0594	0.135	0.0675	0.157	0.0168	0.0251
147/149	0.574	1.47	1.85	2.71	3.88	2.49	0.497	1.08	0.55	1.45	0.11	0.282
148	0.0012	0.00315	0.00627	0.00519	0.0014	0.00488	0.00145	0.00278	0.000912	0.00191	0.0079	0.00286
150	0.00177	0.00514	0.0114	0.00829	0.00428	0.0128	0.00195	0.00418	0.00146	0.00299	0.00858	0.00415
152	0.00147	0.00366	0.00344	0.00747	0.00263	0.00732	0.00245	0.00141	0.000312	0.0023	0.007	0.00343
153/168	0.349	1.01	1.48	1.95	5.49	1.77	0.331	0.812	0.364	0.991	0.0781	0.163
154	0.0109	0.0184	0.0455	0.0309	0.0284	0.0373	0.00722	0.0167	0.00909	0.0168	0.00944	0.00475
155	0.000743	0.00419	0.00306	0.00627	0.00153	0.00463	0.00186	0.00168	0.000715	0.000832	0.00628	0.00372
156/157	0.0165	0.0561	0.0679	0.125	0.491	0.0951	0.0216	0.0499	0.0196	0.0591	0.00552	0.00735

158	0.03	0.0926	0.128	0.196	0.582	0.162	0.0366	0.0786	0.0382	0.107	0.0117	0.0184
159	0.0000914	0.000106	0.0197	0.0000725	0.02	0.000108	0.0001	0.0000978	0.00734	0.0314	0.000933	0.00197
160	0.000157	0.000191	0.00011	0.0000428	0.000604	0.00045	0.000168	0.000231	0.000241	0.000287	0.00501	0.00368
161	0.000221	0.00309	0.00041	0.000291	0.0000783	0.000206	0.00022	0.000126	0.000938	0.000139	0.00351	0.00183
162	0.000145	0.000142	0.0165	0.000065	0.0225	0.0000645	0.0000792	0.00015	0.00588	0.0181	0.00173	0.00268
164	0.0208	0.0548	0.0835	0.113	0.294	0.0947	0.0192	0.0513	0.0211	0.0649	0.00871	0.00756
165	0.00111	0.00269	0.00075	0.000358	0.000236	0.00415	0.000107	0.000203	0.000712	0.000124	0.00402	0.00179
167	0.00938	0.0274	0.0454	0.0485	0.189	0.0402	0.0128	0.0257	0.0109	0.0268	0.00199	0.00301
169	0.0000928	0.0000791	0.0134	0.00408	0.0287	0.0154	0.000105	0.000231	0.000144	0.000177	0.00236	0.000977
170	0.0198	0.0781	0.126	0.119	0.325	0.0971	0.0201	0.0829	0.0408	0.0645	0.00506	0.0037
171/173	0.0204	0.0624	0.0695	0.0925	0.216	0.0984	0.0534	0.0495	0.00105	0.043	0.0144	0.021
172	0.0123	0.0291	0.0419	0.0351	0.102	0.041	0.0346	0.157	0.017	0.0205	0.00408	0.0724
174	0.0695	0.205	0.343	0.263	0.782	0.293	0.0642	0.192	0.0692	0.159	0.0157	0.0447
175	0.00256	0.0145	0.0192	0.0181	0.0343	0.0175	0.00643	0.0114	0.00143	0.0088	0.0133	0.00464
176	0.0149	0.0425	0.0587	0.0595	0.0934	0.0707	0.0121	0.0347	0.012	0.0296	0.00744	0.00549
177	0.0349	0.0922	0.15	0.114	0.334	0.145	0.0353	0.0971	0.0512	0.0753	0.0104	0.0406
178	0.0189	0.046	0.0885	0.0695	0.156	0.0836	0.0259	0.0449	0.0183	0.0368	0.00995	0.00587
179	0.0651	0.167	0.239	0.222	0.324	0.278	0.0672	0.137	0.0587	0.121	0.0111	0.0331
180/193	0.0719	0.226	0.487	0.346	1.64	0.396	0.0809	0.262	0.0985	0.206	0.00568	0.0458
181	0.0000934	0.000186	0.000161	0.00024	0.000107	0.000117	0.000132	0.0000836	0.000188	0.0000401	0.0289	0.0197
182	0.00195	0.0056	0.00537	0.00814	0.0128	0.00767	0.00757	0.00391	0.00563	0.00322	0.0449	0.0191
183	0.0437	0.13	0.214	0.183	0.56	0.204	0.0355	0.126	0.0442	0.101	0.0107	0.0262
184	0.003	0.00434	0.00702	0.00861	0.00894	0.00747	0.00626	0.00567	0.00796	0.00255	0.0529	0.0229
185	0.0114	0.0309	0.0516	0.041	0.108	0.0429	0.00925	0.024	0.0175	0.0202	0.0143	0.0119
186	0.000198	0.00111	0.000166	0.00403	0.00182	0.00373	0.00208	0.000156	0.000462	0.0000474	0.0109	0.00471
187	0.102	0.282	0.502	0.394	1.15	0.508	0.0848	0.248	0.106	0.233	0.0173	0.0388
188	0.000583	0.00803	0.00827	0.00935	0.011	0.00851	0.0118	0.00759	0.000457	0.000955	0.0396	0.0219
189	0.000226	0.0922	0.117	0.102	0.233	0.0919	0.218	0.119	0.000514	0.000189	0.0144	0.274

190	0.0161	0.0247	0.0623	0.0383	0.0924	0.0381	0.015	0.026	0.0389	0.028	0.00478	0.042
191	0.00484	0.00611	0.00902	0.0272	0.0212	0.0113	0.0000903	0.0042	0.0000388	0.0000357	0.00427	0.00343
192	0.0000348	0.0000994	0.000135	0.000123	0.000217	0.000159	0.00166	0.0227	0.00003	0.0000547	0.00556	0.00503
194	0.00891	0.0219	0.0468	0.0277	0.127	0.0299	0.0139	0.0262	0.0131	0.0289	0.00465	0.00175
195	0.00661	0.0157	0.0335	0.0231	0.064	0.0213	0.00691	0.0184	0.00674	0.0188	0.00337	0.00307
196	0.00942	0.027	0.0628	0.0378	0.137	0.0416	0.0137	0.0293	0.0159	0.0291	0.00583	0.00309
197	0.0123	0.02	0.0249	0.0215	0.0252	0.0245	0.013	0.0173	0.00153	0.0225	0.0101	0.00451
198/199	0.0269	0.0777	0.164	0.114	0.407	0.148	0.028	0.0833	0.0288	0.0914	0.00843	0.00511
200	0.0132	0.0247	0.0326	0.0267	0.0537	0.0325	0.00975	0.0191	0.000939	0.0174	0.00373	0.00577
201	0.00694	0.0197	0.0363	0.0266	0.0569	0.037	0.0074	0.0184	0.012	0.0171	0.00917	0.0112
202	0.0241	0.0473	0.0983	0.0701	0.109	0.0927	0.0211	0.0442	0.0332	0.0472	0.0319	0.0253
203	0.0143	0.0379	0.0902	0.0604	0.246	0.0775	0.0161	0.0413	0.025	0.0449	0.00756	0.0034
205	0.0000434	0.000104	0.000157	0.000136	0.0000389	0.0000469	0.000388	0.000128	0.000939	0	0.00369	0.00175
206	0.00651	0.0184	0.029	0.0259	0.056	0.0265	0.00901	0.0209	0.000218	0.0216	0.0115	0.00532
207	0.00267	0.00899	0.0113	0.00772	0.0174	0.0147	0.00382	0.0116	0.000769	0.00876	0.0143	0.0118
208	0.00515	0.0111	0.0248	0.0168	0.0297	0.0227	0.00518	0.0129	0.000448	0.0153	0.00639	0.00628
209	0.0392	0.0492	0.0457	0.0599	0.0477	0.0505	0.0398	0.0472	0.102	0.0466	0.0641	0.0897
OH-PCB Congener												
4 OH-PCB2	0.387	1.18	1.29	0.337	0.142	1.87	0.235	0.857	0.306	0.575	0.0927	0.037
6 OH-PCB2	0.127	0.202	0.637	0.264	0.157	0.313	0.163	0.214	0.0601	0.152	0.00433	0.0992
Surrogate recoveries												
PCB 14	82%	90%	84%	100%	87%	84%	90%	84%	19%	82%	49%	
PCB D-65	95%	105%	82%	108%	99%	91%	102%	90%	27%	84%	81%	
PCB 166	120%	112%	109%	116%	119%	106%	120%	107%	46%	102%	111%	
13C 4'OH-PCB12	75%	57%	52%	62%	71%	58%	60%	52%	20%	42%	53%	
13C 4'OH-PCB120	89%	86%	63%	82%	78%	69%	73%	70%	30%	60%	0.76%	
13C 4OH-PCB187	37%	27%	21%	53%	17%	51%	24%	22%	21%	34%	0.02%	

Table A-2 Raw data for sample batch AA010 showing necessary metadata and uncorrected congener masses for PCBs and OH-PCBs (ng)

Batch ID	AA010-01	AA010-02	AA010-03	AA010-04	AA010-05	AA010-06	AA010-07	AA010-08	AA010-09	AA010-10	AA010-11	AA010-12	
Sample ID	AV 0658	AV 0600	AV 0653	AV 0797	AV 0584	AV 0590	AV 0586	AV 0585	AV 0669	AV 0634	AV 0694		
Sampling Location	St. Columbanus	Guadalupe Reyes	Monroe	St. Columbanus	St. Columbanus	Monroe	Zapata	Metcalf	Metcalf	Guadalupe Reyes	Zapata	Batch Blank	
Sampling Date	4/8/2009	2/4/2009	4/16/2009	10/19/2009	1/7/2009	1/8/2009	1/6/2009	1/9/2009	4/23/2009	3/5/2009	5/29/2009		
Sampling Start Time	7:30	8:30	7:00	7:30	7:40	8:30	7:15	7:40	7:30	7:00	7:00		
Sampling Stop Time	15:30	15:30	15:00	15:30	16:00	15:30	13:15	15:00	15:30	15:00	15:00		
Sampling rate (m3/min)	0.4	0.4	0.4	0.4	0.4	0.4	0.4		0.4	0.4	0.4		
Air Volume (m^3	192	168	192	192	200	168	144	176	192	192	192		
Mean Temp (K)	281	264	286	286	270	265	271	269	286	286	294		
PCB Congener													LOQ (ng)
1	0.688	0.386	1.87	0.579	0.594	0.375	2	0.963	0.665	1.01	2.2	0.175	0.0803
2	0.391	0.21	0.333	0.252	0.367	0.291	4.74	2.39	0.307	0.472	0.241	0.0213	0.0169
3	12.2	0.429	6.82	2.99	1.2	0.553	9.41	4.63	12.1	12.5	6.27	0.115	0.0912
4	1.84	0.74	4.78	2.09	1.06	0.793	1.28	1.36	2	3	8.75	0.711	0.309
5	0.118	0.0472	0.19	0.0913	0.0675	0.0339	0.0911	0.065	0.106	0.147	0.266	0.03	0.0139
6	0.707	0.253	1.58	0.738	0.349	0.221	0.65	0.49	0.669	1.13	2.74	0.557	0.22
7	0.198	0.0619	0.352	0.169	0.101	0.0586	0.113	0.112	0.162	0.25	0.517	0.075	0.0353
8	3.44	1.19	7.58	3.57	1.64	1.03	2.09	1.99	3.08	5.33	12.1	1.56	0.691
9	0.242	0.0881	0.534	0.234	0.123	0.0719	0.143	0.133	0.199	0.355	0.897	0.11	0.0501
10	0.0638	0.0294	0.146	0.0671	0.0455	0.0313	0.0496	0.0467	0.0761	0.0995	0.328	0.036	0.0167
11	7.74	1.7	8.2	4.27	1.95	1.21	2.53	3.03	7.22	7.4	6.98	0.524	0.33
12/13	0.286	0.125	0.412	0.239	0.226	0.0895	0.423	0.295	0.255	0.333	0.408	0.117	0.0606
15	1.03	0.248	1.78	1.02	0.412	0.227	0.646	0.711	0.923	1.48	3.1	0.296	0.159
16	1.68	0.416	2.75	1.62	0.639	0.377	0.766	0.833	1.55	2.29	5.33	0.68	0.336
17	1.62	0.428	2.93	1.64	0.656	0.428	0.803	0.889	1.6	2.36	5.55	0.967	0.419

18/30	3.41	0.886	5.8	3.27	1.38	0.827	1.8	1.84	3.21	4.73	11.4	2.17	0.944
19	0.349	0.135	0.616	0.38	0.194	0.124	0.208	0.206	0.496	0.538	1.55	0.233	0.0964
20/28	3.55	0.607	5.1	3.51	1.13	0.667	1.6	2.13	3.32	4.56	10.1	1.33	0.715
21/33	2.21	0.393	3.13	2.28	0.745	0.406	0.953	1.25	1.81	2.82	5.78	0.525	0.356
22	1.19	0.203	1.63	1.22	0.388	0.214	0.511	0.68	1.13	1.58	3.36	0.316	0.21
23	0.149	0	0.0363	0.248	0.0662	0	0.0275	0.0219	0.0497	0	0.0371	0.00231	0.00591
24	0.0643	0.0277	0.0786	0.0674	0.0355	0.0187	0.0387	0.0336	0.0599	0.0708	0.176	0.0198	0.0129
25	0.318	0.065	0.44	0.321	0.147	0.0659	0.166	0.184	0.285	0.386	0.798	0.234	0.0946
26/29	0.631	0.115	0.91	0.612	0.23	0.118	0.288	0.34	0.563	0.756	1.68	0.314	0.135
27	0.19	0.0601	0.339	0.187	0.0844	0.0531	0.0958	0.112	0.229	0.287	0.666	0.109	0.0497
31	3.37	0.578	4.66	3.14	1.11	0.606	1.42	1.86	2.87	4.08	8.64	1.29	0.683
32	0.87	0.222	1.35	0.743	0.348	0.21	0.435	0.491	0.96	1.26	2.94	0.526	0.237
34	0	0	0.0303	0.0729	0	0	0	0	0	0	0.0394	0.00775	0.00711
35	0.143	0.0257	0.139	0.149	0.0561	0.0297	0.0629	0.0588	0.167	0.156	0.174	0.0108	0.0075
36	0.0599	0.0311	0.0518	0.0691	0.051	0.0348	0.0277	0.0389	0.0534	0.0484	0.0449	0.0151	0.00668
37	0.53	0.0814	0.705	0.699	0.207	0.105	0.269	0.383	0.491	0.705	1.32	0.0741	0.0749
38	0.0524	0	0	0	0	0.0108	0.019	0.0141	0	0.0261	0.0225	0.000991	0.00577
39	0.0628	0	0.0272	0.0472	0	0	0.0173	0.017	0.027	0.0222	0.0284	0.00235	0.00753
40/71	0.561	0.0822	0.778	0.608	0.205	0.0944	0.312	0.378	0.595	0.773	1.37	0.163	0.129
41	0.189	0.0353	0.212	0.187	0.0751	0.0333	0.107	0.126	0.156	0.204	0.372	0.0586	0.045
42	0.432	0.0664	0.566	0.442	0.153	0.0681	0.219	0.286	0.413	0.553	0.952	0.133	0.0929
43	0	0.0116	0.109	0.0823	0.0356	0.0136	0.043	0.0504	0.0722	0.0978	0.219	0.0484	0.0272
44/47/65	1.96	0.282	2.48	1.75	0.723	0.374	1.26	1.31	1.81	2.24	4.03	0.549	0.521
45	0.376	0.0696	0.491	0.292	0.121	0.0566	0.176	0.163	0.358	0.473	0.863	0.19	0.0886
46	0.149	0.0227	0.196	0.12	0.0532	0.023	0.0671	0.0684	0.132	0.192	0.37	0.0772	0.0357
48	0.349	0.0543	0.502	0.38	0.153	0.0602	0.181	0.223	0.319	0.465	0.879	0.138	0.0848
49/69	1.11	0.175	1.53	1.03	0.455	0.219	0.663	0.71	1.1	1.37	2.54	0.446	0.321
50/53	0.37	0.107	0.489	0.299	0.2	0.0971	0.2	0.216	0.377	0.451	0.791	0.264	0.158

51	0.175	0.0272	0.202	0.143	0.0667	0.0358	0.0772	0.086	0.179	0.191	0.333	0.0671	0.0333
52	2.93	0.397	3.86	2.24	1.09	0.544	1.81	2.03	2.54	3.02	5.4	0.793	0.873
54	0.00669	0.00288	0.00893	0.0053	0	0	0	0	0	0	0	0.00343	0.00261
55	0.036	0	0.0231	0.0543	0.0329	0.00791	0.0207	0.0275	0.0325	0.0266	0.0423	0.0068	0.0154
56	0.249	0.0482	0.379	0.379	0.156	0.0669	0.206	0.287	0.281	0.394	0.618	0.0503	0.121
57	0.0315	0	0.0119	0	0.0142	0.00434	0.0113	0.0116	0.0132	0.0088	0.0187	0.00283	0.00754
58	0.0232	0	0	0	0.00938	0.0048	0.0101	0.00945	0.0118	0.00995	0.0198	0.00162	0.00426
59/62/75	0.139	0.0269	0.169	0.139	0.0676	0.0291	0.081	0.0941	0.138	0.173	0.29	0.0549	0.0318
60	0.132	0.0322	0.221	0.228	0.115	0.0381	0.133	0.199	0.178	0.227	0.357	0.033	0.0537
61/70/74/76	1.81	0.24	2.38	1.96	0.762	0.367	1.36	1.73	1.53	2.07	3.57	0.267	0.677
63	0.0694	0.0102	0.0675	0.0677	0.0289	0.0103	0.0345	0.0417	0.0496	0.0524	0.0836	0.00656	0.0138
64	0.713	0.0973	0.963	0.721	0.25	0.125	0.396	0.496	0.709	0.89	1.64	0.2	0.197
66	0.6	0.0872	0.868	0.789	0.283	0.132	0.435	0.654	0.61	0.819	1.42	0.114	0.212
67	0.0451	0.00832	0.0557	0.0512	0.0192	0.00999	0.0231	0.0307	0.0486	0.0464	0.0744	0.00773	0.0114
68	0.0874	0.0268	0.0797	0.0699	0.038	0.024	0.0489	0.0413	0.0684	0.0839	0.127	0.0126	0.0381
72	0.0267	0.00758	0.0171	0.0199	0.013	0.00486	0.0111	0.0108	0.0207	0.0153	0.02	0.00353	0.0078
73	0.0507	0.00445	0.00801	0.0157	0	0	0	0	0	0	0	0.0137	0.0128
77	0.0713	0.0256	0.0695	0.122	0.0666	0.0254	0.0849	0.12	0.054	0.0703	0.107	0.00412	0.0459
78	0	0	0	0.0323	0	0	0	0	0.0346	0.0152	0.0219	0.00264	0.00911
79	0	0	0.0255	0	0.0529	0.0112	0.044	0	0.0352	0.0217	0.0233	0.00302	0.00454
80	0	0.0129	0.0128	0	0.0415	0.00775	0.0168	0.0242	0	0.00732	0.00529	0.00274	0.0105
81	0	0	0	0	0	0	0	0	0.0231	0.0162	0.0207	0.00148	0.00842
82	0.138	0.0168	0.14	0.114	0.0444	0.0302	0.0873	0.0805	0.0986	0.116	0.189	0.00575	0.0759
83	0.0794	0.0123	0.0794	0.0916	0.495	0.259	0.884	0.899	0.943	1.07	1.97	0.00853	0.0294
84	0.535	0.0533	0.568	0.412	0.0115	0.00693	0.011	0.0154	0.0225	0.0222	0.0364	0.0444	0.283
85/116	0.139	0.0219	0.143	0.124	0.0567	0.0278	0.0893	0.0959	0.117	0.146	0.205	0.027	0.0752
86/97/109/119	0.364	0.042	0.387	0.264	0	0.0811	0.221	0.214	0.242	0.257	0.474	0.0242	0.171
88	0	0	0	0.0141	0.1	0.0559	0.146	0.158	0.198	0.211	0.379	0.0059	0.0715

89	0.0301	0.00247	0.0221	0.0299	0.00518	0	0.00355	0.00552	0.00603	0.00471	0	0.00268	0.00783
90/101/113	1.68	0.169	1.87	1.28	0.0174	0.00755	0.0305	0.0198	0.0332	0.0268	0.0689	0.0864	0.903
91	0.242	0.0277	0.271	0.196	0.135	0.0787	0.216	0.213	0.274	0.318	0.558	0.0187	0.0629
92	0.283	0.0278	0.312	0.22	0.769	0.372	1.45	1.38	1.46	1.68	3	0.0161	0.165
93/100	0.0227	0.00683	0.0252	0.0269	0.0148	0.00558	0.0112	0.015	0	0.0189	0.13	0.00446	0.0151
94	0.0162	0.00301	0.00997	0.015	0.00407	0.00236	0.00364	0.00455	0.00907	0.00895	0.0141	0.00211	0.00601
95	1.73	0.174	1.98	1.22	0.604	0.325	0.993	0.964	1.24	1.39	2.5	0.123	0.948
96	0.0203	0.00396	0.0224	0.0133	0.0066	0.00291	0.0109	0.0079	0.0167	0.0182	0.0302	0.00444	0.00599
87/125	0.533	0.0675	0.594	0.445	0.225	0.103	0.392	0.379	0.368	0.502	0.865	0.0341	0.358
98	0	0	0	0	0	0	0	0	0	0	0	0.00144	0.0173
99	0.744	0.0706	0.806	0.574	0.163	0	0	0	0	0	0	0.0434	0.413
102	0.0657	0.00797	0.0674	0.0553	0.0215	0.0106	0.0345	0.0303	0.0489	0.0518	0	0.0077	0.0161
103	0.0178	0.00456	0.0152	0.0167	0.00588	0.004	0.0104	0.00896	0.016	0.0127	0.0206	0.00283	0.00645
104	0.00362	0.00213	0	0	0	0.00225	0.00154	0.00258	0.00252	0.00199	0.00184	0.00136	0.00327
105	0.197	0.0249	0.195	0.204	0.0775	0.0436	0.157	0.125	0.131	0.176	0.283	0.00699	0.0693
106	0.009	0.00383	0.0143	0	0	0	0	0	0	0	0	0.000811	0.00276
107/124	0.0461	0.00764	0.0486	0.0466	0.0217	0.0128	0.0282	0.0261	0.0369	0.0304	0.0566	0.00232	0.0167
108	0.05	0.00614	0.0501	0.0452	0.0297	0.0109	0.0342	0.0274	0.0428	0.0383	0.0649	0.0021	0.0163
110	0	0	0	0	0	0	0	0	0	0	0	0.00353	0.131
111	0	0	0	0	0	0	0	0	0	0	0	0.000164	0.00308
112	0	0	0	0	0	0	0	0	0	0	0	0.00117	0.00809
114	0.0372	0.00575	0.0281	0.0367	0.0163	0.00969	0.019	0.0211	0.0288	0.0266	0.0372	0.00255	0.0838
115	1.4	0.139	1.49	1.11	0.455	0.242	0.924	0.857	0.933	1.15	2.08	0.0617	0.671
117	0.121	0.0758	0.108	0.0912	0.0882	0.0809	0.104	0.0931	0.0871	0.0967	0.126	0.0578	0.286
118	0.656	0.0658	0.683	0.596	0.216	0	0	0.427	0.419	0.536	0.937	0.0204	0.254
120	0	0	0	0	0.00979	0	0	0	0	0	0	0.000249	0.00329
121	0.0077	0.00124	0.00287	0.00606	0.0706	0.0379	0.122	0.119	0.136	0.145	0.264	0.00163	0.00343
122	0.0301	0.00371	0.0253	0.0281	0.00856	0.00483	0.00817	0.0123	0.0253	0.02	0.0247	0.00066	0.00678

123	0.0292	0.0082	0.0272	0	0	0.122	0.549	0.0216	0	0.0194	0.0289	0.00107	0.0141
126	0.114	0.0744	0.0975	0.111	0.0836	0.0703	0.0795	0.0929	0.0917	0.0901	0.0993	0.0622	0.141
127	0	0	0	0	0	0	0	0	0	0	0	0.000623	0.000996
129/138/163	0.533	0.0539	0.553	0.537	0.174	0.0836	0.404	0.252	0.347	0.428	0.771	0.0141	0.171
130	0.0399	0	0.0324	0.0275	0.0065	0.00557	0.0238	0.0111	0.0229	0.0227	0.05	0.000926	0.00948
131	0.0157	0.00229	0.0139	0.00222	0	0	0.00873	0.00576	0.00878	0.0102	0.0224	0.000148	0.00884
132	0.241	0.0246	0.00961	0.211	0.0816	0.0412	0.156	0.102	0.159	0.199	0.339	0.00382	0.104
133	0.0112	0	0	0.00807	0	0	0.00459	0.00481	0.00535	0.0061	0.0096	0.000539	0.00175
134	0.0793	0.00805	0.0768	0.0566	0.0188	0.016	0.0408	0.0288	0.0412	0.0601	0.101	0.000629	0.0268
135/151	0.375	0.0339	0.399	0.301	0.121	0.0535	0.197	0.148	0.246	0.268	0.43	0.00913	0.139
136	0.289	0.026	0.324	0.214	0.0984	0.0531	0.228	0.127	0.195	0.22	0.36	0.00899	0.134
137	0.0333	0.00163	0.0289	0.0345	0.0112	0.00431	0.0165	0.0128	0.0203	0.0245	0.047	0.000278	0.0109
139/140	0.0194	0.00273	0.0222	0.0142	0.00924	0.00449	0.0117	0.00812	0.0124	0.0169	0.0252	0.00135	0.014
141	0.129	0.0128	0.129	0.12	0.0427	0.0158	0.0814	0.0518	0.0791	0.101	0.162	0.00337	0.0403
143	0	0	0	0	0	0	0	0	0	0	0	0.000486	0.00887
142	0	0.000569	0.259	0.012	0	0	0	0	0	0	0	0.000573	0.00222
144	0.0563	0.00638	0.0576	0.0436	0.017	0.00809	0.0343	0.0234	0.0351	0.0433	0.0647	0.00162	0.0186
145	0	0	0	0	0	0	0	0	0	0	0	0.000409	0.00423
146	0.0865	0.00819	0.0905	0.0822	0.0265	0.0138	0.0556	0.0397	0.0619	0.0704	0.119	0.00162	0.0251
147/149	0.754	0.0749	0.853	0.66	0.241	0.113	0.457	0.325	0.537	0.605	0.992	0.0216	0.282
148	0	0	0	0	0	0	0	0	0	0	0	0.000471	0.00286
150	0	0	0	0	0	0	0	0	0	0	0	0.000332	0.00415
152	0	0	0	0	0	0	0	0	0	0	0	0.000593	0.00343
153/168	0.529	0.0504	0.544	0.509	0.153	0.0753	0.386	0.24	0.34	0.412	0.676	0.0151	0.163
154	0.0101	0.00179	0.00986	0.0105	0.00601	0.00268	0.00471	0.00701	0.00975	0.009	0.0153	0.000189	0.00475
155	0	0	0	0	0	0	0	0	0	0	0	0.000843	0.00372
156/157	0.036	0.00626	0.0275	0.0346	0.0135	0.00858	0.0262	0.0159	0.0185	0.0214	0.0412	0.000448	0.00735
158	0	0	0	0.056	0.0161	0.00878	0.0397	0.0265	0.0338	0.0421	0.0705	0.0017	0.0184

159	0	0	0	0	0	0	0	0	0	0	0	0.00126	0.00197
160	0	0	0	0	0	0	0	0	0	0	0	0.000938	0.00368
161	0	0	0	0	0	0	0	0	0	0	0	0.000623	0.00183
162	0	0	0	0	0	0	0	0	0	0	0	0.000509	0.00268
164	0.033	0.00299	0.0317	0.0315	0.0113	0.00552	0.0273	0.0137	0.024	0.0248	0.0447	0.00168	0.00756
165	0	0	0	0	0	0	0	0	0	0	0	0.00054	0.00179
167	0.0185	0	0.0126	0.014	0	0	0.0103	0.00651	0	0.00986	0.0182	0.000572	0.00301
169	0	0	0	0	0	0	0	0	0	0	0	0.00236	0.000977
170	0.0481	0.0148	0.0399	0.0602	0	0.0168	0.0339	0.0266	0.0263	0.0292	0.0536	0.00174	0.0037
171/173	0.0391	0.0251	0.0383	0.0521	0	0	0	0.0172	0.0268	0.0366	0.045	0.00192	0.021
172	0.0234	0.0289	0.0253	0.0247	0	0.0262	0.0193	0.0192	0.0219	0.0174	0.022	0.00162	0.0724
174	0.11	0.0243	0.114	0	0	0	0	0.0423	0.0741	0.0846	0.119	0.00256	0.0447
175	0.00618	0	0.00586	0	0	0	0	0	0	0	0	0.00021	0.00464
176	0.0263	0	0.0265	0.0205	0.0104	0.00322	0.0123	0.00717	0.0174	0.02	0.0222	0.00124	0.00549
177	0.053	0.0138	0.0586	0.0676	0.0305	0.0229	0.0347	0.0225	0.0393	0.0467	0.0665	0.00542	0.0406
178	0.028	0	0.0272	0.0278	0	0	0.0165	0.00753	0.0189	0.0194	0.0303	0.000818	0.00587
179	0.0969	0.0134	0.0963	0.0839	0.0349	0.0103	0.0445	0.0303	0.0644	0.0769	0.0968	0.00184	0.0331
180/193	0.136	0.0315	0.15	0.152	0.0732	0.0305	0.0914	0.0537	0.077	0.0917	0.155	0.00852	0.0458
181	0.0101	0	0	0	0.0366	0.0166	0.0223	0	0	0	0	0.000915	0.0197
182	0	0	0	0	0	0	0	0	0.209	0.259	0.34	0.00148	0.0191
183	0.0775	0.00955	0.0734	0.0837	0.0219	0.0161	0.0429	0.025	0.0486	0	0	0.00366	0.0262
184	0	0	0.00403	0.00442	0.00872	0.0035	0.0051	0.00413	0.00382	0.00617	0.00613	0.00306	0.0229
185	0.0226	0	0.016	0.116	0.0412	0.0248	0.0648	0	0.014	0	0	0.00311	0.0119
186	0	0	0	0	0	0	0	0	0	0	0	0.000505	0.00471
187	0.169	0.0174	0.162	0.146	0.053	0.0239	0.0872	0.0509	0.11	0.127	0.183	0.00143	0.0388
188	0	0	0	0.00511	0.00952	0.00174	0.00216	0.00385	0.00463	0.00407	0.00163	0.00218	0.0219
189	0.0325	0.0391	0.0425	0.0705	0.119	0.026	0.0329	0.0713	0.0449	0.0461	0.0143	0.00677	0.274
190	0.0154	0.0166	0.0148	0.0216	0	0.0105	0.0158	0.0165	0.0211	0.0178	0.0176	0.00664	0.042

191	0	0	0	0	0	0	0	0	0	0	0	0.00109	0.00343
192	0.00514	0	0	0	0.0446	0	0	0	0	0	0.0044	0.000923	0.00503
194	0.0235	0.0104	0.0274	0.0236	0.0259	0.0164	0.0241	0.0229	0.0149	0.028	0.0243	0.00133	0.00175
195	0.0183	0	0.0167	0.0154	0	0.0117	0.0154	0.0197	0.0148	0.0142	0.0176	0.0081	0.00307
196	0.0223	0.00889	0.0222	0.0258	0.0179	0.0113	0.021	0.0213	0.0212	0.0203	0.023	0.00619	0.00309
197	0	0	0	0	0	0	0	0	0	0	0	0.000675	0.00451
198/199	0.0582	0.0258	0.0632	0.0655	0.057	0.027	0.047	0.0325	0.0481	0.0564	0.0724	0.00985	0.00511
200	0.0161	0	0.0178	0.0201	0	0.0116	0.024	0	0.0226	0.0179	0.0225	0.000728	0.00577
201	0.0154	0.00639	0.0127	0.0128	0.0106	0.00467	0.0109	0.0114	0.0133	0.0116	0.0161	0.00192	0.0112
202	0.0318	0.0092	0.0291	0.0272	0.0216	0.011	0.02	0.0193	0.0283	0.0281	0.0369	0.00639	0.0253
203	0.0334	0.0089	0.0305	0.0342	0.0251	0.0134	0.0254	0.0167	0.0279	0.0312	0.0379	0.00695	0.0034
205	0.0106	0.00998	0.00557	0.00605	0	0	0	0	0	0.00962	0.00639	0.000744	0.00175
206	0.0171	0	0.0212	0.0205	0	0	0	0	0.0236	0.0442	0.0203	0.000637	0.00532
207	0.00657	0.00591	0.00693	0.00956	0.00953	0.00882	0.00563	0	0.00983	0.00866	0.00975	0.00437	0.0118
208	0.0111	0.00669	0.0106	0.0129	0.00934	0.0068	0.00784	0.00641	0.0115	0.021	0.0141	0.00457	0.00628
209	0.05	0.0474	0.0465	0.0482	0.0934	0.0479	0.0516	0.0438	0.0409	0.0578	0.0404	0.0536	0.0897
OH-PCB Congener													
4 OH-PCB2	0.471	0.0624	0.537	0.462	0.394	0.137	0.258	0.253	0.268	0.482	0.107	0.00203	0.037
6 OH-PCB2	0.168	0.0383	0.0858	0.15	0.0685	0.0211	0.0499	0.0403	0.109	0.074	0.0533	0.00895	0.0992
Surrogate recoveries													
PCB 14	65%	71%	74%	78%	33%	61%	76%	71%	62%	67%	68%	56%	
PCB D-65	78%	74%	88%	96%	35%	73%	75%	70%	72%	74%	81%	60%	
PCB 166	87%	87%	99%	105%	47%	96%	92%	95%	100%	101%	109%	82%	
13C 4'OH-PCB12	69%	85%	71%	86%	32%	73%	64%	72%	69%	67%	72%	66%	
13C 4'OH-PCB120	70%	82%	83%	80%	36%	75%	69%	80%	83%	79%	85%	9.4%	
13C 4OH-PCB187	54%	41%	50%	47%	31%	32%	56%	52%	56%	38%	55%	0.92%	

Table A-3 Raw data for sample batch AA011 showing necessary metadata and uncorrected congener masses for PCBs and OH-PCBs (ng)

Batch ID	AA011-01	AA011-02	AA011-03	AA011-04	AA011-05	AA011-06	AA011-07	AA011-08	AA011-09	AA008-10	
Sample ID	AV 0661	AV 0731	AV 0820	AV 0621	AV 0737	AV 0748	AV 0792	AV 0827	AV 0816		
Sampling Location	Carver	Monroe	Metcalf	Carver	Metcalf	Guad Reyes	Carver	Monroe	Zapata	Batch Blank	
Sampling Date	4/27/2009	7/22/2009	11/12/2009	2/27/2009	8/18/2009	8/10/2009	9/23/2009	10/26/2009	10/22/2009		
Sampling Start Time	7:30	7:00	7:30	7:15	7:00	7:00	7:00	7:00	7:00		
Sampling Stop Time	15:30	13:15	13:30	15:30	14:00	13:00	15:30	15:30	15:40		
Sampling rate (m3/min)	0.4	0.4	0.4	0.4	0.4	0.4	0.4	0.4	0.4		
Air Volume (m^3	192	150	144	198	168	144	204	204	208		
Mean Temp (K)	295	296	282	269	298	299	293	285	284		
PCB Congener											LOQ (ng)
1	0.875	1.97	2.3	0.409	0.336	0.813	1.12	2.52	1.41	0.0202	0.0803
2	0.559	0.299	0.711	0.707	0.102	0.221	1.17	0.582	0.239	0.00354	0.0169
3	11.4	12.7	7.03	51.9	2.1	1.52	2.82	9.62	7.59	0.0381	0.0912
4	2.5	7.53	1.73	0.929	1.38	2.03	3.22	7.71	5.56	0.0538	0.309
5	0.184	0.272	0.108	0.08	0.0748	0.124	0.18	0.295	0.17	0.00376	0.0139
6	1.05	2.58	0.773	0.439	0.548	0.906	1.3	2.64	1.62	0.025	0.22
7	0.337	0.556	0.184	0.114	0.124	0.196	0.305	0.633	0.326	0.00892	0.0353
8	5.39	12.7	3.65	2.02	2.77	4.58	6.21	12.6	7.59	0.118	0.691
9	0.315	0.871	0.231	0.124	0.168	0.273	0.384	0.914	0.541	0.0102	0.0501
10	0.0824	0.266	0.065	0.0375	0.0524	0.0664	0.0979	0.247	0.264	0.00388	0.0167
11	9.31	4.3	3	4.1	3.66	5.05	6.05	5.67	2.49	0.114	0.33
12/13	0.403	0.461	0.575	0.223	0.186	0.243	0.751	0.545	0.247	0.0193	0.0606
15	1.81	2.97	3.44	0.765	1.22	1.56	2.08	2.8	1.59	0.0436	0.159
16	2.58	4.38	3.16	0.882	1.57	2.15	2.87	4.05	2.94	0.0748	0.336
17	2.5	4.77	2.95	0.9	1.63	2.08	2.91	4.39	3.12	0.0666	0.419

18/30	5.12	9.39	5.36	1.86	3.22	4.25	5.82	8.51	6.29	0.151	0.944
19	0.485	1.23	0.321	0.158	0.36	0.415	0.587	1	1.02	0.0138	0.0964
20/28	5.88	8.57	18.3	2.55	4.47	4.88	6.46	7.54	5.4	0.179	0.715
21/33	3.61	5.26	12.5	1.62	2.41	3.1	3.68	4.7	3.16	0.118	0.356
22	2.02	2.89	7.39	0.849	1.58	1.73	2.19	2.49	1.86	0.0681	0.21
23	0.199	0.0342	0.0728	0.0518	0.0936	0.0608	0.316	0.0327	0.0304	0.00141	0.00591
24	0.0778	0.107	0.1	0.0242	0.0522	0.0603	0.0811	0.117	0.104	0.00488	0.0129
25	0.509	0.701	1.46	0.203	0.332	0.409	0.52	0.685	0.457	0.0132	0.0946
26/29	0.999	1.44	2.75	0.424	0.671	0.794	1.06	1.41	0.879	0.024	0.135
27	0.308	0.512	0.383	0.112	0.213	0.259	0.348	0.48	0.393	0.00985	0.0497
31	5.14	7.65	15.5	2.27	3.7	4.42	5.49	6.92	4.67	0.166	0.683
32	1.31	2.42	2.16	0.472	0.97	1.12	1.39	2.13	1.69	0.043	0.237
34	0	0.0406	0.0637	0.0253	0.0497	0.0343	0.12	0.0304	0.0321	0.0022	0.00711
35	0.214	0.136	0.365	0.0736	0.122	0.0761	0.248	0.11	0.0828	0.00083	0.0075
36	0	0	0.0294	0	0	0	0	0	0	0.0000698	0.00668
37	1.09	1.18	7.93	0.483	0.909	0.0515	1.21	0.878	0.674	0.0345	0.0749
38	0	0	0.047	0	0	0	0	0	0	0.000138	0.00577
39	0	0.0227	0.052	0	0	0	0	0	0	0.000386	0.00753
40/71	1.05	1.37	5.8	0.445	0.766	0.765	1.19	1.01	0.897	0.0494	0.129
41	0.269	0.386	1.63	0.151	0.228	0.126	0.346	0.286	0.261	0.0171	0.045
42	0.755	1.01	3.85	0.355	0.555	0.649	0.875	0.747	0.661	0.0326	0.0929
43	0.145	0.163	0.541	0.072	0.0927	0	0.13	0	0	0.00804	0.0272
44/47/65	3.91	4	14.6	2.46	2.3	3	3.63	3.25	2.65	0.212	0.521
45	0.604	0.809	1.58	0.211	0.333	0.479	0.686	0.712	0.612	0.0176	0.0886
46	0.231	0.305	0.667	0.0912	0.149	0.175	0.262	0.271	0.23	0.00774	0.0357
48	0.632	0.914	3.06	0.307	0.449	0.551	0.725	0.732	0.553	0.0265	0.0848
49/69	1.91	2.46	7.33	0.892	1.28	1.64	2.14	2.03	1.64	0.112	0.321
50/53	0.546	0.689	1.26	0.23	0.346	0.439	0.596	0.642	0.526	0.05	0.158

51	0.502	0.23	0.452	0.103	0.175	0.177	0.214	0.176	0.128	0.00838	0.0333
52	4.89	5.42	14	3.17	2.95	4.55	5.23	5.21	3.99	0.359	0.873
54	0.0109	0.0138	0.0195	0.00521	0.00502	0.00699	0.0121	0.0126	0.0113	0.000521	0.00261
55	0.0612	0.0464	0.345	0.0262	0.0448	0.0254	0.0723	0.0314	0.0359	0.00615	0.0154
56	0.57	0.721	6.7	0.347	0.558	0.704	0.77	0.463	0.44	0.0515	0.121
57	0	0.0156	0.0877	0.0102	0	0.013	0.0131	0	0.0104	0.00125	0.00754
58	0	0	0.0522	0.0064	0.0129	0.0235	0.0157	0.0539	0.00765	0.00073	0.00426
59/62/75	0.216	0.282	1.09	0.113	0.171	0.185	0.238	0.221	0.191	0.0112	0.0318
60	0.341	0.402	4.12	0.2	0.326	0.397	0.408	0.246	0.246	0.0244	0.0537
61/70/74/76	3.39	4.09	24.7	2.29	2.78	3.7	4.03	3.13	2.56	0.29	0.677
63	0.0981	0.0848	0.485	0.0453	0.0745	0.064	0.0932	0.0571	0.0534	0.00477	0.0138
64	1.33	1.72	6.64	0.661	0.96	0.774	1.5	1.28	1.15	0.0787	0.197
66	1.21	1.59	12.2	0.765	1.16	1.47	1.61	1.08	0.985	0.0907	0.212
67	0.0788	0.0778	0.448	0.0371	0.0558	0.0854	0.0756	0.056	0.0532	0.00368	0.0114
68	0.229	0.0591	0.0923	0.0434	0.0762	0.06	0.0759	0.0428	0.0352	0.0102	0.0381
72	0.0245	0.0163	0.0746	0.00844	0.0146	0.0158	0.0278	0.0143	0.0127	0.00157	0.0078
73	0.0185	0.0133	0.0398	0.00738	0.0126	0	0.0178	0.0755	0.0598	0.00571	0.0128
77	0.176	0.122	1.54	0.103	0.149	0.651	0.223	0.0778	0.0779	0.0185	0.0459
78	0	0	0.0544	0.00875	0	0.0698	0	0	0	0.000256	0.00911
79	0	0	0.0878	0	0	0.0995	0	0.0238	0.0275	0.00056	0.00454
80	0	0	0.0564	0	0	0.081	0	0	0	0.00209	0.0105
81	0	0	0.103	0.00899	0	0.0412	0	0	0	0.000204	0.00842
82	0.292	0.245	1.31	0.132	0.203	0.295	0.286	0.168	0.162	0.0304	0.0759
83	0.166	0.136	0.455	1.43	1.58	2.53	2.59	0.0889	0.0968	0.0125	0.0294
84	0.957	0.846	2.43	0.572	0.625	0.882	1.01	0.732	0.639	0.116	0.283
85/116	0.343	0.267	1.47	0.169	0.242	0.324	0.377	0.213	0.165	0.0326	0.0752
86/97/109/119	0.688	0.602	2.54	0.301	0.484	0.633	0.714	0.463	0.334	0.0702	0.171
88	0	0	0	0	0	0	0	0	0	0.0286	0.0715

89	0.0448	0.0363	0.17	0.0221	0.0367	0.0369	0.0476	0.0288	0.0239	0.00301	0.00783
90/101/113	3.21	2.83	11.2	2.1	0.0593	0.0635	0.0628	2.54	1.87	0.363	0.903
91	0.41	0.399	1.14	0.248	0.291	0.391	0.434	0.321	0.269	0.0267	0.0629
92	0.535	0.447	1.57	0.298	2.65	4.36	4.21	0.394	0.306	0.0666	0.165
93/100	0.0322	0.0306	0.111	0.0209	0.0248	0.0189	0.0328	0.0247	0.0182	0.0053	0.0151
94	0.0215	0.018	0.0663	0.0108	0.0133	0	0.0264	0.0158	0.0118	0.00198	0.00601
95	3.09	2.75	6.72	1.97	1.95	2.9	3.16	2.54	2.03	0.383	0.948
96	0.0298	0.0311	0.0714	0.015	0.0189	0.0238	0.0305	0.025	0.0206	0.00272	0.00599
87/125	1.22	1.06	4.9	0.71	0.865	1.31	1.38	0.876	0.743	0.144	0.358
98	0	0	0	0	0	0	0	0	0	0.00688	0.0173
99	1.46	1.41	5.71	0	0	0	0	1.17	0.883	0.165	0.413
102	0.107	0.0914	0.312	0.056	0.069	0.0864	0.102	0.08	0.0681	0.00715	0.0161
103	0.0264	0.0216	0.0552	0.0163	0.0164	0.0185	0.0256	0.0165	0.0144	0.00261	0.00645
104	0.00331	0.00285	0.0122	0.00263	0.00258	0.00252	0.00222	0.00227	0.00132	0.00116	0.00327
105	0.485	0.352	3.94	0.15	0.323	0.526	0.512	0.234	0.197	0.0281	0.0693
106	0	0	0.0487	0.00689	0	0	1.44	0	0	0.000715	0.00276
107	0.0745	0.0594	0.388	0.0307	0.0725	0.0734	0.0852	0.0435	0.0392	0.00636	0.0167
108/124	0.104	0.0796	0.568	0.0469	0.068	0.118	0.111	0.0582	0.0444	0.00669	0.0163
110	0	0	0	0	0	0	0	0	0	0.0119	0.131
111	0	0	0.0423	0	0	0	0	0	0	0.000275	0.00308
112	0	0	0	0	0	0	0	0	0	0.00285	0.00809
114	0.0563	0.0413	0.272	0.0236	0.033	0.0483	0	0.0255	0.0228	0.00398	0.0838
115	2.94	2.46	11.5	1.47	1.99	3.14	3.14	1.94	1.57	0.27	0.671
117	0.103	0.104	0.29	0.0836	0.106	0.101	0.128	0.0988	0.082	0.0678	0.286
118	1.5	1.17	10.4	0.599	0.998	1.76	0.0305	0.863	0.648	0.102	0.254
120	0	0	0.0447	0	0	0	0	0	0	0.000149	0.00329
121	0	0	0.0295	0.0035	0.218	0.334	0.338	0	0	0.000621	0.00343
122	0.0373	0.0239	0.161	0.0094	0.0174	0.0295	0.0584	0.0179	0.0168	0.00263	0.00678

123	0.0244	0.0291	0.21	0.0186	0	0.0387	0.05	0.0244	0.0257	0.00562	0.0141
126	0.141	0.0887	0.297	0.086	0.111	0.128	0.14	0.0741	0.0704	0.0558	0.141
127	0	0	0.0464	0	0	0	0	0	0	0.0000983	0.000996
129/138/163	1.38	0.883	6.74	0.368	1.01	1.63	1.33	0.61	0.465	0.0691	0.171
130	0.076	0.056	0.294	0.0231	0.05	0.1	0.0821	0.0396	0.0257	0.0038	0.00948
131	0.0297	0.0282	0.0887	0.0127	0.0175	0.0324	0.0297	0.019	0.0142	0.0034	0.00884
132	0.535	0.395	1.5	0.195	0.395	0.629	0.55	0.287	0.239	0.0415	0.104
133	0.0228	0.014	0.0785	0.0093	0.0172	0.0207	0.0234	0.0104	0.0072	0.000504	0.00175
134	0.141	0.113	0.369	0.0582	0.1	0.161	0.152	0.0864	0.0802	0.0106	0.0268
135/151	0.74	0.508	1.72	0.278	0.502	0.722	0.739	0.476	0.301	0.0558	0.139
136	0.497	0.383	0.754	0.234	0.342	0.484	0.489	0.366	0.269	0.0535	0.134
137	0.066	0.0532	0.269	0.0229	0.0506	0.081	0.0656	0.0329	0.021	0.00377	0.0109
139/140	0.0392	0.0333	0.112	0.019	0.0274	0.0351	0.0411	0.0228	0.0185	0.00466	0.014
141	0.302	0.188	1.3	0.0845	0.212	0.311	0.275	0.133	0.0982	0.0162	0.0403
143	0	0	0	0	0	0	0	0	0	0.0033	0.00887
142	0.00376	0.00262	0.0233	0.00167	0	0	0.00316	0.00146	0.000874	0.000143	0.00222
144	0.109	0.0783	0.294	0.048	0.0842	0.106	0.109	0.0724	0.0462	0.00752	0.0186
145	0.00187	0.00201	0.0176	0.000988	0.0012	0.00134	0.0024	0.000779	0.0012	0.000945	0.00423
146	0.197	0.13	0.725	0.0596	0.153	0.202	0.191	0.0976	0.0728	0.00995	0.0251
147/149	1.69	1.18	4.4	0.591	1.16	1.74	1.7	0.992	0.684	0.114	0.282
148	0.00361	0.00335	0.0222	0.00255	0.00286	0.00271	0.00336	0.00114	0.00136	0.000189	0.00286
150	0.00604	0.0035	0.019	0.00241	0.00361	0.0039	0.00505	0.00369	0.00266	0.000812	0.00415
152	0.00302	0.00255	0.0153	0.00317	0.00295	0.0042	0.0044	0.00185	0.00129	0.000723	0.00343
153/168	1.25	0.812	6	0.346	0.94	1.34	1.21	0	0	0.0661	0.163
154	0.0279	0.0153	0.0558	0.0137	0.0151	0.02	0.022	0.0124	0.00808	0.000977	0.00475
155	0.00387	0.00235	0.0173	0.00384	0.00288	0.0024	0.00261	0.00482	0.0017	0.00106	0.00372
156/157	0.0711	0.0429	0.495	0.019	0.0547	0.107	0.0654	0.028	0.0224	0.00287	0.00735
158	0.125	0.0827	0.644	0.0347	0.0988	0.152	0.118	0.0585	0.0448	0.00737	0.0184

159	0	0	0.032	0	0	0.0281	0	0	0	0.000883	0.00197
160	0	0	0.0362	0	0	0	0	0	0	0.00128	0.00368
161	0	0	0.0289	0	0	0	0	0.555	0.384	0.000465	0.00183
162	0	0	0.0376	0.0102	0	0.014	0	0	0	0.00111	0.00268
164	0.0701	0.0452	0.335	0.0195	0.0545	0.0831	0.0668	0.0334	0.0305	0.00282	0.00756
165	0	0	0.0244	0	0	0	0	0	0	0.00033	0.00179
167	0.0325	0.018	0.199	0	0.0319	0.042	0.0326	0.0117	0.0114	0.00124	0.00301
169	0	0	0.0712	0	0	0	0	0	0	0.000147	0.000977
170	0.128	0.0559	0.434	0.0276	0.132	0.139	0.0948	0.034	0.028	0.00139	0.0037
171/173	0	0.0547	0.277	0	0.0901	0.0674	0.0705	0.0337	0.0283	0.00835	0.021
172	0.0513	0.0237	0.143	0.0296	0	0.0385	0.0294	0.0244	0.0515	0.0279	0.0724
174	0.308	0.171	1.05	0.0532	0.265	0.271	0.262	0.099	0.0929	0.0179	0.0447
175	0.0132	0.00637	0.0627	0	0.0108	0.0106	0.0137	0	0	0.000141	0.00464
176	0.0531	0.0309	0.134	0.0113	0.0415	0.0477	0.0527	0.0248	0.0167	0.00188	0.00549
177	0.157	0.0748	0.459	0.03	0.142	0.141	0.141	0.0472	0.047	0.0164	0.0406
178	0.0719	0.0389	0.208	0.0138	0.0436	0.0626	0.0581	0.0254	0.0224	0.0016	0.00587
179	0.191	0.117	0.372	0.0376	0.13	0.168	0.17	0.0894	0.0648	0.0132	0.0331
180/193	0.429	0.189	2.12	0.0543	0.36	0.396	0.348	0.113	0.076	0.0183	0.0458
181	0.074	0	0.0351	0	0	0	0	0	0	0.00591	0.0197
182	0.00549	0.00415	0.036	0	0	0	0	0	0	0.00268	0.0191
183	0.206	0.113	0.804	0.0323	0.153	0.181	0.166	0.0648	0.0509	0.0107	0.0262
184	0.00498	0.0049	0.023	0.00312	0.00415	0.0048	0.00363	0.00518	0.00454	0.00356	0.0229
185	0.0389	0.0207	0.171	0.0105	0.0332	0.0281	0.0374	0.0194	0.0195	0.00443	0.0119
186	0.00161	0.0014	0.0197	0.00118	0.00233	0	0	0.00136	0	0.000703	0.00471
187	0.405	0.231	1.57	0.0627	0.311	0.396	0.352	0.145	0.096	0.0154	0.0388
188	0.00196	0.00501	0.0234	0.00257	0.00481	0	0.00351	0.00432	0.0112	0.00539	0.0219
189	0	0.0255	0.037	0.0446	0.043	0	0	0.0507	0.104	0.106	0.274
190	0.0689	0.0304	0.133	0.0355	0.0609	0.0535	0.0461	0.0382	0.034	0.0167	0.042

191	0	0	0.0487	0	0	0	0	0	0	0.00128	0.00343
192	0	0	0.0244	0	0	0	0	0	0	0.00188	0.00503
194	0.0298	0.0223	0.214	0	0.0414	0.0486	0.0366	0.0129	0.00774	0.000242	0.00175
195	0.0238	0.0153	0.113	0.0095	0.0265	0.0314	0.026	0.0121	0.0134	0.000501	0.00307
196	0.0456	0.0279	0.248	0.0146	0.0493	0.0538	0.0489	0.0188	0.0179	0.000839	0.00309
197	0	0.021	0.0563	0.0153	0.0405	0.0217	0.0173	0.0209	0	0.000762	0.00451
198/199	0.121	0.0835	0.7	0.0253	0.104	0.143	0.117	0.0461	0.0332	0.00156	0.00511
200	0.0305	0.0251	0.113	0.0112	0.0375	0.0354	0.0288	0.0173	0	0.00234	0.00577
201	0.0319	0.0205	0.118	0.00587	0.0247	0.0315	0.0269	0.0122	0.00859	0.0045	0.0112
202	0.0612	0.0504	0.184	0.0186	0.0516	0.0758	0.0585	0.0322	0.024	0.00913	0.0253
203	0.0641	0.0488	0.429	0.0144	0.069	0.0776	0.0691	0.0269	0.0243	0.000751	0.0034
205	0	0	0.0441	0	0	0	0	0	0.00628	0.000393	0.00175
206	0.0268	0.0201	0.144	0	0.0271	0.038	0.0282	0.0112	0	0.000976	0.00532
207	0.0106	0.00996	0.047	0.00514	0.013	0.0129	0.0109	0.00739	0	0.00454	0.0118
208	0.0174	0.0189	0.0724	0.00629	0.0185	0.0239	0.0189	0.0104	0	0.00293	0.00628
209	0.058	0.041	0.0561	0.0388	0.0694	0.0656	0.0449	0.0477	0.0487	0.0414	0.0897
OH-PCB Congener											
4 OH-PCB2	0.373	0.129	0.181	0.228	0.131	0.147	0.26	0.147	0.0906	0.0135	0.037
6 OH-PCB2	0.188	0.0846	0.0437	0.0623	0.155	0.143	0.136	0.108	0.0679	0.0309	0.0992
Surrogate recoveries											
PCB 14	63%	83%	93%	99%	41%	79%	90%	86%	77%	65%	
PCB D-65	73%	93%	89%	103%	49%	88%	104%	101%	88%	90%	
PCB 166	79%	117%	144%	108%	64%	106%	116%	108%	103%	106%	
13C 4'OH-PCB12	60%	56%	49%	71%	22%	62%	61%	43%	54%	44%	
13C 4'OH-PCB120	61%	79%	63%	77%	42%	82%	78%	57%	66%	0.88%	
13C 4OH-PCB187	39%	55%	30%	50%	43%	37%	47%	18%	9.4%	0.90%	

Table A-4 Raw data for sample batch AA009 showing necessary metadata and uncorrected congener masses for PCBs and OH-PCBs (ng)

Batch ID	AA009-01	AA009-02	AA009-03	AA009-04	AA009-05	AA009-06	AA009-07	AA009-08	AA009-09	AA009-10	AA009-11	AA009-12	
Sample ID	FV05315	FV 5322	FV 5395	FV 5398	FV 5316	FV 5328	FV 5313	F 5349	FV 5324	FV 5312	FV 5350		
Sampling Location	Marquette	Washington Park Academy	Guadalupe Reyes	Zapata	Monroe	St. Columbanus	Carver	Owens	Metcalf	St. Columbanus	Adams	Batch Blank	
Sampling Date	7/23/2009	6/10/2009	7/31/2009	7/30/2009	7/28/2009	7/22/2009	7/13/2009	6/15/2009	6/9/2009	6/3/2009	6/2/2009		
Sampling Start Time	7:30	7:30	6:30	6:30	7:00	7:30	7:30	7:30	7:30	7:30	7:30		
Sampling Stop Time	13:45	15:30	12:30	12:30	12:30	13:30	14:30	14:30	15:30	15:30	15:30		
Sampling rate (m3/min)	0.4	0.4	0.4	0.4	0.4	0.4	0.4	0.4	0.4	0.4	0.4		
Air Volume (m^3	150	192	144	144	132	144	168	168	192	192	192		
Mean Temp (K)	296	289	296	295	298	296	297	297	289	287	286		
PCB Congener													LOQ (ng)
1	0.035	0.0309	0.0319	n/a	n/a	0.211	0.333	0.0199	0.22	0.0401	0.0606	0.036	0.0954
2	0.03	0.0279	0.022	n/a	n/a	0.222	0.12	0.0118	0.223	0.0253	0.0206	0.0107	0.0304
3	0.0786	0.0714	0.066	n/a	n/a	0.496	0.417	0.0343	0.499	0.0701	0.118	0.0675	0.126
4	0.139	0.107	0.116	n/a	n/a	0.149	0.159	0.868	0.833	0.0974	0.195	0.0458	0.161
5	0.00985	0.00456	0.00722	n/a	n/a	0.00987	0.0113	0.033	0.0337	0.00457	0.00664	0.00414	0.00847
6	0.0772	0.0353	0.0521	n/a	n/a	0.0646	0.0822	0.3	0.286	0.037	0.0514	0.0238	0.0601
7	0.0174	0.00876	0.0128	n/a	n/a	0.0176	0.0207	0.063	0.0641	0.00997	0.0146	0.0091	0.0198
8	0.397	0.16	0.266	n/a	n/a	0.32	0.407	1.37	1.33	0.177	0.254	0.112	0.272
9	0.0198	0.00915	0.013	n/a	n/a	0.0174	0.0214	0.0729	0.0712	0.00934	0.0137	0.00816	0.0175
10	0.0051	0.00453	0.00481	n/a	n/a	0.0057	0.00682	0.0275	0.0281	0.00362	0.00688	0.00231	0.00692
11	0.456	0.295	0.322	n/a	n/a	0.439	0.872	0.968	0.948	0.387	0.46	0.303	0.678
12/13	0.0339	0.0187	0.0245	n/a	n/a	0.0348	0.05	0.0745	0.0721	0.02	0.0236	0.0162	0.0398
15	0.159	0.0483	0.133	n/a	n/a	0.153	0.194	0.346	0.324	0.0641	0.0728	0.039	0.116
16	0.307	0.0861	0.0144	n/a	n/a	0.243	0.29	0.717	0.702	0.0955	0.135	0.0536	0.128

17	0.269	0.0778	0.582	n/a	n/a	0.21	0.257	0.661	0.659	0.0862	0.131	0.0515	0.121
18/30	0.577	0.163	0.00631	n/a	n/a	0.434	0.507	1.44	1.43	0.18	0.271	0.0958	0.241
19	0.0477	0.0212	0.038	n/a	n/a	0.0422	0.0477	0.177	0.183	0.0221	0.0358	0.0119	0.0297
20/28	0.651	0.162	0.667	n/a	n/a	0.643	0.777	1.2	1.18	0.229	0.292	0.133	0.359
21/33	0.432	0.106	0.674	n/a	n/a	0.396	0.495	0.752	0.732	0.146	0.188	0.0828	0.208
22	0.236	0.0582	0.422	n/a	n/a	0.24	0.301	0.41	0.412	0.0864	0.108	0.0476	0.139
23	0.0051	0.0000745	0.00525	n/a	n/a	0.00518	0.0000955	0.00721	0.000105	0.0000159	0.00448	0.00266	0.00576
24	0.00984	0.00343	0.0303	n/a	n/a	0.00754	0.00854	0.0214	0.0242	0.003	0.0049	0.00305	0.00669
25	0.0529	0.0175	0.113	n/a	n/a	0.0488	0.0671	0.0928	0.0942	0.0207	0.0259	0.0147	0.0412
26/29	0.106	0.0296	0.00528	n/a	n/a	0.095	0.123	0.2	0.192	0.0369	0.0483	0.0248	0.0622
27	0.0337	0.0119	0.141	n/a	n/a	0.026	0.0365	0.0755	0.0812	0.0118	0.0182	0.00824	0.0179
31	0.65	0.156	0.0451	n/a	n/a	0.582	0.735	1.15	1.12	0.215	0.276	0.119	0.328
32	0.178	0.047	0.133	n/a	n/a	0.138	0.171	0.379	0.386	0.0548	0.0771	0.0306	0.0758
34	0.0047	0.0000517	0.156	n/a	n/a	0.00325	0.000158	0.00681	0.0000951	0.0000168	0.00372	0.00262	0.00487
35	0.0117	0.00616	0.00918	n/a	n/a	0.0145	0.0265	0.0208	0.0229	0.00487	0.0124	0.00824	0.021
36	0.0000251	0.00312	0.209	n/a	n/a	0.0000147	0.0000351	0.0000405	0.000077	0.00356	0.0000354	0.00396	0.00608
37	0.076	0.0299	0.0847	n/a	n/a	0.137	0.157	0.152	0.141	0.0523	0.0543	0.0285	0.11
38	0.00588	0.00302	0.0000546	n/a	n/a	0.00578	0.0000255	0.0000314	0.0000559	0.00709	0.0000314	0.00524	0.00649
39	0.00508	0.00217	0.0000245	n/a	n/a	0.00393	0.00771	0.0000234	0.0000696	0.00395	0.0000352	0.00482	0.00527
40/71	0.12	0.0495	0.131	n/a	n/a	0.136	0.205	0.178	0.176	0.0573	0.0959	0.0501	0.101
41	0.0313	0.0119	0.0365	n/a	n/a	0.0349	0.0532	0.0568	0.0498	0.0123	0.0209	0.0104	0.0262
42	0.085	0.0344	0.0983	n/a	n/a	0.0984	0.147	0.139	0.129	0.0387	0.0697	0.0312	0.0728
43	0.0125	0.00552	0.0152	n/a	n/a	0.0144	0.0208	0.0227	0.0266	0.00591	0.0121	0.0091	0.0158
44/47/65	0.456	0.233	0.441	n/a	n/a	0.459	0.748	0.609	0.586	0.281	0.424	0.245	0.423
45	0.0751	0.0214	0.0759	n/a	n/a	0.0669	0.0998	0.138	0.144	0.023	0.0418	0.0183	0.0335
46	0.032	0.00884	0.0309	n/a	n/a	0.0293	0.042	0.053	0.057	0.0104	0.0178	0.00951	0.0175
48	0.0699	0.0229	0.0742	n/a	n/a	0.068	0.0997	0.107	0.106	0.0269	0.0475	0.0211	0.043
49/69	0.265	0.132	0.264	n/a	n/a	0.268	0.454	0.37	0.339	0.157	0.24	0.141	0.235

50/53	0.11	0.0711	0.113	n/a	n/a	0.105	0.219	0.199	0.16	0.0811	0.115	0.0795	0.147
51	0.0231	0.00767	0.0216	n/a	n/a	0.0196	0.0241	0.0435	0.0377	0.00896	0.0167	0.00768	0.0149
52	0.857	0.533	0.771	n/a	n/a	0.778	1.56	0.975	0.907	0.584	0.904	0.566	0.881
54	0.00207	0.00104	0.00157	n/a	n/a	0.00111	0.00134	0.00242	0.00342	0.000544	0.00187	0.0023	0.00275
55	0.00633	0.00294	0.0089	n/a	n/a	0.00692	0.0143	0.0116	0.0144	0.00613	0.0175	0.00726	0.0143
56	0.0662	0.0356	0.0715	n/a	n/a	0.124	0.151	0.103	0.104	0.0484	0.0729	0.0366	0.0995
57	0.00357	0.00191	0.00292	n/a	n/a	0.00298	0.00551	0.00365	0.00425	0.00182	0.00629	0.00556	0.00682
58	0.00315	0.00205	0.0047	n/a	n/a	0.002	0.00568	0.00384	0.00629	0.00145	0.00573	0.00606	0.00769
59/62/75	0.0294	0.0145	0.0302	n/a	n/a	0.0311	0.0485	0.0443	0.0437	0.015	0.0282	0.0221	0.0364
60	0.0366	0.0192	0.0412	n/a	n/a	0.0621	0.0777	0.0565	0.0587	0.0261	0.0411	0.0224	0.0547
61/70/74/76	0.508	0.334	0.476	n/a	n/a	0.667	1.04	0.583	0.536	0.4	0.558	0.365	0.674
63	0.0101	0.00584	0.0131	n/a	n/a	0.0134	0.0198	0.0152	0.0173	0.00723	0.0151	0.00945	0.0172
64	0.151	0.0743	0.155	n/a	n/a	0.172	0.272	0.213	0.207	0.0876	0.14	0.0733	0.14
66	0.146	0.0794	0.149	n/a	n/a	0.252	0.323	0.219	0.202	0.107	0.156	0.0816	0.205
67	0.00655	0.00374	0.00939	n/a	n/a	0.00962	0.0142	0.0114	0.0125	0.0045	0.0108	0.00702	0.0101
68	0.0178	0.0159	0.0187	n/a	n/a	0.0166	0.0228	0.0214	0.0235	0.0162	0.0228	0.0194	0.0377
72	0.00315	0.0018	0.00259	n/a	n/a	0.00268	0.00555	0.00413	0.00673	0.00192	0.00599	0.00543	0.00707
73	0.00485	0.00424	0.00383	n/a	n/a	0.00416	0.00883	0.00361	0.00596	0.00352	0.00697	0.00737	0.0121
77	0.0214	0.0143	0.0242	n/a	n/a	0.0412	0.0493	0.04	0.0456	0.0213	0.0215	0.017	0.0423
78	0.00402	0.00385	0.0000253	n/a	n/a	0.00000835	0.000116	0.0000286	0.0000517	0.00195	0.00556	0.00735	0.0078
79	0.006	0.00403	0.0000248	n/a	n/a	0.00419	0.0000311	0.0000125	0.0000291	0.0023	0.00513	0.00723	0.00754
80	0.00355	0.00177	0.0000258	n/a	n/a	0.0000202	0.0000192	0.0000116	0.0000201	0.00175	0.006	0.00663	0.00695
81	0.00436	0.00366	0.00671	n/a	n/a	0.00536	0.0000645	0.00893	0.0129	0.00331	0.00676	0.00736	0.00823
82	0.0472	0.0341	0.0431	n/a	n/a	0.0527	0.0965	0.056	0.0628	0.0374	0.0545	0.038	0.114
83	0.0427	0.0272	0.0281	n/a	n/a	0.0383	0.0684	0.0274	0.0425	0.036	0.0332	0.0283	0.0598
84	0.22	0.158	0.174	n/a	n/a	0.183	0.378	0.179	0.17	0.159	0.212	0.164	0.374
85/116	0.0489	0.0431	0.0448	n/a	n/a	0.0563	0.126	0.0537	0.0612	0.047	0.0603	0.0467	0.125
86/97/109/119	0.139	0.104	0.114	n/a	n/a	0.128	0.285	0.128	0.132	0.115	0.146	0.114	0.261

88	0.000037	0.0000296	0.0000383	n/a	n/a	0.0000751	0.0000853	0.00003	0.0000199	0.0000056	5.07E-06	6.29E-06	0.000104
89	0.00725	0.00497	0.00736	n/a	n/a	0.00774	0.013	0.0104	0.0101	0.00531	0.00926	0.00815	0.0173
90/101/113	0.733	0.538	0.552	n/a	n/a	0.634	1.31	0.557	0.538	0.548	0.673	0.572	1.24
91	0.095	0.0678	0.0748	n/a	n/a	0.0799	0.173	0.0775	0.0787	0.0667	0.0889	0.0696	0.153
92	0.12	0.0923	0.0974	n/a	n/a	0.107	0.231	0.0963	0.1	0.0907	0.115	0.0999	0.196
93/100	0.00843	0.00677	0.00792	n/a	n/a	0.00733	0.0163	0.00686	0.0132	0.00569	0.0105	0.0125	0.0173
94	0.00429	0.00325	0.00379	n/a	n/a	0.00395	0.0106	0.00554	0.00724	0.0025	0.00635	0.00682	0.0099
95	0.74	0.538	0.577	n/a	n/a	0.609	1.31	0.555	0.532	0.535	0.704	0.562	1.22
96	0.00723	0.00459	0.00498	n/a	n/a	0.00576	0.0108	0.00498	0.00687	0.00352	0.00727	0.0071	0.013
87/125	0.292	0.204	0.216	n/a	n/a	0.27	0.464	0.241	0.235	0.219	0.244	0.227	0.519
98	0.00293	0.00124	0.00213	n/a	n/a	0.00143	0.00903	0.00426	0.00463	0.00258	0.00572	0.00667	0.0069
99	0.233	0.176	0.191	n/a	n/a	0.229	0.446	0.211	0.209	0.181	0.227	0.19	0.398
102	0.0217	0.0145	0.0175	n/a	n/a	0.0189	0.0334	0.0183	0.0226	0.0129	0.0187	0.0178	0.0388
103	0.00638	0.00445	0.00617	n/a	n/a	0.007	0.0118	0.00714	0.00895	0.00474	0.00782	0.00862	0.0128
104	0.00251	0.0022	0.00219	n/a	n/a	0.00174	0.00426	0.00252	0.00313	0.00186	0.0037	0.00486	0.00565
105	0.083	0.0457	0.0585	n/a	n/a	0.125	0.161	0.139	0.129	0.0799	0.0692	0.0499	0.244
106	0.00376	0.00252	0.0000328	n/a	n/a	0.00401	0.0000199	0.000066	0.0000977	0.00194	0.0000284	0.00596	0.00595
107	0.0211	0.0142	0.0142	n/a	n/a	0.0247	0.0369	0.0271	0.0262	0.0171	0.0195	0.0196	0.0487
108/124	0.0183	0.0111	0.0128	n/a	n/a	0.0193	0.0335	0.0236	0.0218	0.0135	0.0205	0.021	0.0387
110	0.0000508	0.000031	6.68E-06	n/a	n/a	0.0000206	0.0000558	0.000202	0.000109	0.0000425	0.0000437	0.000336	0.000409
111	0.00331	0.00196	0.00002	n/a	n/a	0.0000277	0.0000286	0.0000172	0.0000401	0.00196	0.0047	0.00698	0.00709
112	0.0043	0.00303	0.0000553	n/a	n/a	0.0000154	0.0000388	0.0000263	0.0000272	0.0000127	0.00546	0.00637	0.00648
114	0.0122	0.00748	0.0121	n/a	n/a	0.014	0.0214	0.015	0.0194	0.00793	0.0113	0.0127	0.0264
115	0.566	0.404	0.43	n/a	n/a	0.556	1.04	0.543	0.498	0.441	0.511	0.421	1.18
117	0.105	0.0922	0.0993	n/a	n/a	0.103	0.102	0.108	0.0925	0.099	0.0861	0.112	0.252
118	0.256	0.168	0.189	n/a	n/a	0.345	0.484	0.346	0.328	0.241	0.23	0.179	0.646
120	0.00314	0.00174	0.0000227	n/a	n/a	0.00002	0.0000285	0.0000143	0.0000731	0.00206	0.00523	0.00589	0.00608

121	0.00223	0.00146	0.00231	n/a	n/a	0.00215	0.00226	0.00335	0.0000256	0.00123	0.00321	0.00518	0.00526
122	0.00695	0.00497	0.00928	n/a	n/a	0.00838	0.0161	0.0106	0.0163	0.00427	0.00859	0.0093	0.0135
123	0.00852	0.00593	0.00489	n/a	n/a	0.00959	0.000116	0.0144	0.0136	0.00711	0.0000413	0.0121	0.0182
126	0.0788	0.0751	0.0823	n/a	n/a	0.0805	0.0905	0.0895	0.0829	0.0857	0.0716	0.0959	0.0953
127	0.00484	0.00227	0.000031	n/a	n/a	0.00000912	0.000046	0.0000277	0.0000484	0.00265	0.00635	0.00864	0.00905
129/138/163	0.258	0.148	0.179	n/a	n/a	0.379	0.492	0.415	0.403	0.243	0.249	0.131	0.439
130	0.0163	0.0112	0.0129	n/a	n/a	0.0226	0.0318	0.0257	0.0268	0.014	0.0181	0.0128	0.0287
131	0.0086	0.00625	0.00532	n/a	n/a	0.00874	0.0151	0.00769	0.0118	0.0058	0.0127	0.00994	0.0137
132	0.0998	0.0697	0.071	n/a	n/a	0.109	0.193	0.118	0.125	0.0815	0.106	0.0607	0.143
133	0.00587	0.00284	0.00481	n/a	n/a	0.00604	0.0106	0.00636	0.0108	0.00438	0.00898	0.00829	0.0109
134	0.0223	0.0162	0.0194	n/a	n/a	0.0256	0.0536	0.0264	0.0211	0.0199	0.035	0.0228	0.0415
135/151	0.134	0.0982	0.0947	n/a	n/a	0.125	0.238	0.122	0.128	0.0948	0.144	0.0895	0.15
136	0.113	0.0813	0.0796	n/a	n/a	0.0938	0.189	0.0865	0.0909	0.0732	0.12	0.071	0.101
137	0.0155	0.0091	0.0103	n/a	n/a	0.0191	0.034	0.0192	0.0258	0.0128	0.0205	0.0131	0.0241
139/140	0.011	0.00757	0.0091	n/a	n/a	0.0106	0.0157	0.0115	0.0111	0.00805	0.0166	0.0155	0.02
141	0.0506	0.031	0.0361	n/a	n/a	0.0615	0.0993	0.0661	0.068	0.0414	0.0525	0.0291	0.0744
143	0.00696	0.00458	0.00337	n/a	n/a	0.00309	0.000166	0.00404	0.00699	0.0025	0.00403	0.00557	0.00665
142	0.00172	0.00161	0.00156	n/a	n/a	0.00208	0.0000743	0.00205	0.00478	0.00189	0.00526	0.0048	0.00547
144	0.0205	0.0163	0.0163	n/a	n/a	0.0192	0.0416	0.0193	0.0245	0.0159	0.0255	0.0186	0.0278
145	0.00237	0.00194	0.00147	n/a	n/a	0.00204	0.00302	0.00157	0.00279	0.00167	0.00525	0.00603	0.00614
146	0.0359	0.022	0.0256	n/a	n/a	0.0467	0.067	0.0435	0.0479	0.0296	0.0406	0.0229	0.052
147/149	0.305	0.216	0.213	n/a	n/a	0.308	0.549	0.292	0.298	0.226	0.317	0.185	0.352
148	0.00165	0.00188	0.00114	n/a	n/a	0.00172	0.00207	0.00154	0.00322	0.00141	0.00388	0.00549	0.00565
150	0.00247	0.00206	0.00178	n/a	n/a	0.00195	0.00282	0.00188	0.00236	0.0015	0.00395	0.00543	0.00567
152	0.00283	0.00148	0.00125	n/a	n/a	0.00245	0.00351	0.00187	0.00382	0.00144	0.00385	0.00496	0.00514
153/168	0.191	0.126	0.146	n/a	n/a	0.275	0.385	0.261	0.254	0.173	0.206	0.111	0.312
154	0.0058	0.00377	0.00425	n/a	n/a	0.00495	0.00871	0.0043	0.00592	0.00353	0.00863	0.00751	0.00902
155	0.00224	0.00195	0.0017	n/a	n/a	0.00213	0.00416	0.00277	0.00537	0.0018	0.00494	0.00462	0.00483

156/157	0.0222	0.00937	0.0166	n/a	n/a	0.04	0.0418	0.0537	0.0601	0.0236	0.0252	0.0179	0.046
158	0.0251	0.0148	0.0194	n/a	n/a	0.0354	0.0532	0.0409	0.0442	0.024	0.029	0.0179	0.0452
159	0.00602	0.00368	0.000025	n/a	n/a	0.0000101	0.0000376	0.0000401	0.0000095	0.00302	0.0113	0.0107	0.0157
160	0.00305	0.00357	0.00247	n/a	n/a	0.0000126	0.0000584	0.0000187	0.0000354	0.00121	0.00526	0.00715	0.00753
161	0.00303	0.0022	0.00187	n/a	n/a	0.00187	0.0025	0.00239	0.0046	0.00147	0.00564	0.00624	0.00622
162	0.0037	0.0000313	7.38E-06	n/a	n/a	0.000014	0.0000259	0.00634	0.0000196	0.00375	0.0104	0.00908	0.00939
164	0.018	0.01	0.0132	n/a	n/a	0.0236	0.0309	0.0273	0.0253	0.015	0.02	0.0129	0.027
165	0.00209	0.00142	0.00186	n/a	n/a	0.00000954	0.00325	0.00177	0.00393	0.00151	0.00546	0.00604	0.00603
167	0.0106	0.00568	0.0103	n/a	n/a	0.0139	0.0173	0.0178	0.0223	0.0099	0.0135	0.00923	0.0188
169	0.00906	0.00354	0.0000383	n/a	n/a	0.0000161	0.0000149	0.0164	0.0292	0.00701	0.0137	0.00829	0.00845
170	0.047	0.0194	0.0359	n/a	n/a	0.095	0.116	0.105	0.108	0.0459	0.0356	0.0128	0.0767
171/173	0.0191	0.0116	0.0177	n/a	n/a	0.0261	0.0624	0.0335	0.0361	0.0151	0.0271	0.0203	0.0354
172	0.0147	0.0095	0.0132	n/a	n/a	0.0225	0.0341	0.0265	0.0354	0.0111	0.0189	0.0106	0.0233
174	0.0469	0.0243	0.0406	n/a	n/a	0.0751	0.119	0.0894	0.101	0.0456	0.0486	0.0227	0.131
175	0.00376	0.00201	0.0036	n/a	n/a	0.00538	0.0087	0.00533	0.012	0.00325	0.0104	0.00792	0.0101
176	0.0098	0.0054	0.0077	n/a	n/a	0.0102	0.0171	0.0105	0.0142	0.00732	0.0133	0.0105	0.0152
177	0.0248	0.014	0.0272	n/a	n/a	0.0525	0.077	0.0543	0.0708	0.0258	0.0271	0.0165	0.0561
178	0.0106	0.00591	0.00768	n/a	n/a	0.0179	0.0287	0.0163	0.0305	0.00927	0.0144	0.011	0.0201
179	0.0315	0.0187	0.0231	n/a	n/a	0.0323	0.0577	0.0301	0.0334	0.0219	0.0319	0.0206	0.0373
180/193	0.0889	0.0359	0.084	n/a	n/a	0.198	0.264	0.207	0.208	0.102	0.082	0.0317	0.192
181	0.00487	0.00457	0.00666	n/a	n/a	0.0000197	0.0000243	0.0000233	0.0000276	0.00353	0.00946	0.00915	0.00961
182	0.00561	0.00522	0.00555	n/a	n/a	0.00854	0.0149	0.0101	0.016	0.00642	0.0145	0.0111	0.0133
183	0.0281	0.0182	0.0244	n/a	n/a	0.0491	0.0739	0.0489	0.0679	0.0306	0.0355	0.0191	0.0576
184	0.0046	0.00496	0.00469	n/a	n/a	0.00531	0.0127	0.00577	0.0102	0.00444	0.0121	0.0092	0.0139
185	0.00953	0.00766	0.00856	n/a	n/a	0.0000175	0.000052	0.0115	0.0000591	0.00678	0.0157	0.0102	0.0142
186	0.00228	0.00196	0.00156	n/a	n/a	0.00272	0.00539	0.00282	0.00727	0.00204	0.00688	0.00775	0.00798
187	0.0611	0.0339	0.0544	n/a	n/a	0.0934	0.13	0.0903	0.0966	0.0558	0.0655	0.0336	0.103
188	0.00265	0.00221	0.00209	n/a	n/a	0.00293	0.00452	0.00281	0.00481	0.00249	0.00819	0.00638	0.00703

189	0.00896	0.0057	0.0111	n/a	n/a	0.000025	0.00231	0.0227	0.0000843	0.00682	0.0124	0.00859	0.00941
190	0.0192	0.0108	0.0198	n/a	n/a	0.0273	0.0437	0.0298	0.031	0.0173	0.0235	0.0148	0.029
191	0.00977	0.00614	0.00553	n/a	n/a	0.061	0.0143	0.00806	0.00024	0.00805	0.0108	0.00999	0.0127
192	0.00675	0.00428	0.00574	n/a	n/a	0.0000544	0.0142	0.00634	0.0000166	0.00247	0.00719	0.009	0.00918
194	0.036	0.015	0.0326	n/a	n/a	0.0654	0.0954	0.0748	0.0945	0.0323	0.0289	0.0181	0.0437
195	0.0149	0.00708	0.0126	n/a	n/a	0.0236	0.0488	0.0292	0.0546	0.0147	0.0276	0.0178	0.026
196	0.021	0.00857	0.0192	n/a	n/a	0.0298	0.0663	0.041	0	0.0195	0.0312	0.0187	0.0351
197	0.033	0.0138	0.022	n/a	n/a	0.0327	0.0594	0.0445	0.0526	0.0232	0.0307	0.0194	0.0217
198/199	0	0	0	n/a	n/a	0	0	0	0	0	0	0	0.0553
200	0	0	0	n/a	n/a	0	0	0	0	0	0	0	0.0104
201	0.00956	0.00733	0.00881	n/a	n/a	0.0102	0.0244	0.0119	0.0197	0.00746	0.0173	0.0153	0.0195
202	0.0225	0.0157	0.0185	n/a	n/a	0.0231	0.045	0.0233	0.0327	0.017	0.0262	0.0229	0.0358
203	0.0336	0.0141	0.0239	n/a	n/a	0.0403	0.0792	0.0563	0.106	0.0294	0.0364	0.0212	0.044
205	0.0087	0.00531	0.00804	n/a	n/a	0.0132	0	0.0149	0.0242	0.00588	0.0157	0.0164	0.0185
206	0.0897	0.0133	0.0242	n/a	n/a	0.049	0.0482	0.0792	0.0915	0.0396	0.0411	0.0213	0.0464
207	0.0143	0.00554	0.00596	n/a	n/a	0.00734	0.0118	0.00951	0.0228	0.00682	0.0172	0.0153	0.0181
208	0.031	0.00718	0.0074	n/a	n/a	0.0151	0.019	0.015	0.0299	0.0109	0.0165	0.0151	0.0207
209	0.0734	0.0719	0.0727	n/a	n/a	0.0978	0.192	0.148	0.121	0.0921	0.14	0.0793	0.137
OH-PCB Congener													
6 OH-PCB2	0.081	0.0338	0.0789	0.377	0.0295	0.0959	0.0264	0.108	0.0298	0.0359	0.0293	0.0385	0.0447
3' OH-PCB65	0.0206	0	0.0145	0.0276	0	0.0259	0.0407	0.0432	0.0176	0	0.0196	0.00418	0.000504
Surrogate recoveries													
PCB 14	53%	45%	44%	n/a	n/a	44%	17%	31%	55%	36%	34%	34%	
PCB D-65	67%	55%	54%	n/a	n/a	53%	20%	36%	65%	47%	37%	47%	
PCB 166	78%	65%	66%	n/a	n/a	65%	26%	43%	74%	60%	37%	69%	
13C 4'OH-PCB12	88%	32%	42%	28%	44%	41%	3%	47%	44%	27%	38%	41%	
13C 4'OH-PCB120	79%	63%	73%	66%	114%	68%	23%	61%	80%	35%	65%	73.16%	
13C 4OH-PCB187	83%	55%	81%	83%	127%	69%	24%	56%	71%	30%	38%	83.02%	

Table A-5 Raw data for sample batch AA013 showing necessary metadata and uncorrected congener masses for PCBs and OH-PCBs (ng)

Batch ID	AA013-01	AA013-02	AA013-03	AA013-04	AA013-05	AA013-06	AA013-07	AA013-08	AA013-09	AA013-10	
Sample ID	FV 5550	FV 5212	FV 5097	FV 5172	FV 5174	FV 5213	FV 5209	FV 5217	FV 5072		
Sampling Location	Carver	Metcalf	Monroe	Zappata	St. Columbanus	Metcalf	Monroe	Guadalupe Reyes	Guadalupe Reyes	Batch Blank	
Sampling Date	12/1/2009	3/17/2009	5/14/2009	1/6/2009	1/7/2009	1/9/2009	1/8/2009	2/4/2009	3/5/2009		
Sampling Start Time	7:30	7:30	7:30	7:15	7:40	7:40	8:30	8:30	7:00		
Sampling Stop Time	14:30	15:30	15:30	13:15	16:00	15:00	15:30	15:30	15:00		
Sampling rate (m3/min)	0.4	0.4	0.4	0.4	0.4	0.4	0.4	0.4	0.4		
Air Volume (m^3	168	192	192	144	200	176	168	168	192		
Mean Temp (K)	281	290	291	271	270	269	265	264	286		
PCB Congener											LOQ (ng)
1	0.0133	0.0489	0.0453	0.0495	0.0416	0.0197	0.0203	0.0342	0.0378	0.0295	0.0954
2	0.00638	0.0107	0.0142	0.0467	0.0426	0.0058	0.0152	0.0182	0.0331	0.021	0.0304
3	0.0224	0.0483	0.0389	0.128	0.0971	0.0168	0.0347	0.049	0.0714	0.0718	0.126
4	0.0413	0.123	0.12	0.211	0.128	0.034	0.0582	0.0739	0.0813	0.11	0.161
5	0.00362	0.00574	0.00442	0.00596	0.00603	0.00334	0.0033	0.00681	0.00454	0.00435	0.00847
6	0.0229	0.042	0.0409	0.0521	0.0441	0.018	0.0219	0.0423	0.0334	0.0348	0.0601
7	0.0071	0.0116	0.0106	0.013	0.0117	0.00674	0.00699	0.0125	0.0088	0.00842	0.0198
8	0.106	0.2	0.188	0.225	0.177	0.0851	0.0965	0.178	0.138	0.158	0.272
9	0.00686	0.0124	0.0106	0.012	0.0113	0.00642	0.00615	0.0117	0.00942	0.00884	0.0175
10	0.00214	0.00447	0.00555	0.0068	0.00437	0.00299	0.00243	0.00309	0.0032	0.00366	0.00692
11	0.465	0.391	0.346	0.468	0.45	0.326	0.301	0.88	0.423	0.42	0.678
12/13	0.0191	0.0227	0.0252	0.0207	0.0208	0.0178	0.0112	0.0369	0.02	0.0242	0.0398
15	0.0534	0.0628	0.0507	0.0641	0.0627	0.0371	0.0419	0.0934	0.0462	0.0771	0.116
16	0.064	0.0829	0.0951	0.0921	0.0831	0.0364	0.0494	0.102	0.0514	0.0742	0.128
17	0.0596	0.0804	0.0877	0.0895	0.078	0.0366	0.0451	0.102	0.0531	0.07	0.121

18/30	0.114	0.174	0.179	0.185	0.162	0.0764	0.0872	0.187	0.104	0.146	0.241
19	0.0134	0.0214	0.0239	0.025	0.0197	0.00913	0.0103	0.0225	0.0118	0.0188	0.0297
20/28	0.174	0.191	0.183	0.192	0.19	0.106	0.112	0.336	0.136	0.234	0.359
21/33	0.104	0.117	0.123	0.12	0.117	0.0645	0.0713	0.186	0.0835	0.127	0.208
22	0.0658	0.0755	0.0745	0.0755	0.075	0.0403	0.0465	0.127	0.0492	0.0918	0.139
23	0	0	0	0	0	0	0	0	0	0.00411	0.00576
24	0	0	0	0	0.00522	0.0034	0.00407	0	0	0.00385	0.00669
25	0.0188	0.0229	0.0207	0.0204	0.0223	0.0132	0.0135	0.0482	0.0151	0.0276	0.0412
26/29	0.0314	0.035	0.0366	0.0337	0.0356	0.0184	0.0218	0.0633	0.0238	0.0394	0.0622
27	0.0102	0.0117	0.0116	0.0125	0.0105	0.00531	0.00731	0.0171	0.00748	0.0102	0.0179
31	0.172	0.193	0.175	0.186	0.185	0.103	0.109	0.314	0.131	0.212	0.328
32	0.0411	0.0511	0.0564	0.0523	0.0467	0.0231	0.0281	0.0691	0.0302	0.0465	0.0758
34	0	0	0	0	0	0	0	0	0	0.00257	0.00487
35	0.0152	0.0122	0	0.00785	0.0108	0.00613	0.00866	0.0309	0.00828	0.0148	0.021
36	0	0	0	0	0	0	0	0	0	0.00336	0.00608
37	0.0456	0.0458	0.035	0.0426	0.0504	0.0257	0.0321	0.112	0.0305	0.0859	0.11
38	0	0	0	0	0	0	0	0	0	0.002	0.00649
39	0	0	0	0	0	0	0.00342	0.00811	0	0.000796	0.00527
40/71	0.037	0.0443	0.0478	0.0485	0.0478	0.0281	0.0348	0.0783	0.0396	0.0568	0.101
41	0.00974	0.0127	0.0125	0.0143	0.00972	0.00462	0.0087	0.0178	0.00744	0.0148	0.0262
42	0.0273	0.0352	0.0329	0.038	0.0342	0.0196	0.0251	0.0551	0.0287	0.0442	0.0728
43	0	0.00677	0	0.00703	0.00545	0	0.00549	0.00947	0.00648	0.00638	0.0158
44/47/65	0.191	0.18	0.219	0.207	0.211	0.142	0.149	0.289	0.183	0.197	0.423
45	0.0131	0.0187	0.0201	0.0199	0.0149	0.00764	0.0138	0.0206	0.0103	0.0169	0.0335
46	0.00611	0.00654	0.00895	0.00855	0.00683	0.00374	0.0062	0.0103	0.0062	0.00786	0.0175
48	0.0183	0.024	0.0199	0.0213	0.0203	0.012	0.014	0.0309	0.0168	0.0223	0.043
49/69	0.0965	0.0961	0.11	0.104	0.109	0.0808	0.0739	0.152	0.0948	0.102	0.235
50/53	0.0425	0.0505	0.0539	0.0477	0.0543	0.0486	0.0459	0.0587	0.0451	0.0489	0.147

51	0.00649	0.00481	0.00587	0.0072	0.00724	0.00444	0.00479	0.0114	0.00599	0.00669	0.0149
52	0.4	0.361	0.441	0.421	0.463	0.351	0.271	0.531	0.435	0.343	0.881
54	0.000799	0.000684	0.00159	0.000606	0.00064	0.000824	0.000748	0.00105	0.000465	0.000676	0.00275
55	0.00688	0.00737	0	0.0077	0.00783	0.00333	0.00518	0.0113	0.00414	0.00855	0.0143
56	0.0396	0.0431	0.0367	0.0414	0.0428	0.0249	0.0293	0.0697	0.0329	0.0654	0.0995
57	0	0	0	0	0	0	0	0	0	0.00231	0.00682
58	0	0	0.000107	0	0	0	0	0	0	0.00281	0.00769
59/62/75	0.0129	0.0147	0.0151	0.0119	0.0121	0.00898	0.00973	0.019	0.0104	0.0155	0.0364
60	0.0216	0.0257	0.0196	0.0229	0.0239	0.0132	0.0171	0.0377	0.0187	0.0337	0.0547
61/70/74/76	0.302	0.284	0.273	0.303	0.349	0.223	0.214	0.466	0.298	0.356	0.674
63	0.00785	0.00652	0	0.0093	0.00978	0.00416	0.00708	0.0121	0.00582	0.00989	0.0172
64	0.0591	0.063	0.0744	0.0692	0.0685	0.0498	0.0442	0.101	0.0615	0.0753	0.14
66	0.0847	0.0911	0.0827	0.0916	0.0959	0.0615	0.0623	0.151	0.0794	0.132	0.205
67	0.00473	0.00431	0	0.00553	0.00604	0	0.00382	0.00893	0	0.00509	0.0101
68	0.0142	0.0148	0.0125	0.0146	0.0165	0.0106	0.014	0.0186	0.0134	0.0146	0.0377
72	0.00262	0.00249	0.00214	0.0021	0.00271	0.00153	0.00237	0.004	0.00126	0.00273	0.00707
73	0	0.00484	0	0.00354	0.00334	0	0.00289	0.00364	0	0.00291	0.0121
77	0.0182	0.0192	0	0.0193	0.016	0.00777	0.0177	0.0259	0.0134	0.0289	0.0423
78	0	0	0	0	0	0	0	0	0	0.000434	0.0078
79	0	0	0	0	0	0	0	0	0	0.000553	0.00754
80	0	0	0	0	0	0	0	0	0	0.000495	0.00695
81	0	0	0	0	0	0	0	0	0	0.00092	0.00823
82	0.0401	0.0263	0.0302	0.0318	0.0381	0.0263	0.0237	0.0515	0.03	0.0398	0.114
83	0.0176	0.019	0.0247	0.0162	0.0227	0.0175	0.0165	0.0307	0.0146	0.0232	0.0598
84	0.121	0.102	0.126	0.116	0.132	0.0921	0.0816	0.164	0.127	0.11	0.374
85/116	0.0369	0.0317	0.0406	0.0288	0.0338	0.0237	0.0247	0.0431	0.0301	0.0405	0.125
86/97/109/119	0.0744	0.0672	0.0635	0.0633	0.0826	0.0454	0.0585	0.104	0.0652	0.0741	0.261
88	0	0	0	0	0	0	0	0	0	0.0000252	0.000104

89	0.00572	0	0	0.00435	0.00394	0.00258	0.00294	0.00514	0.00348	0.00403	0.0173
90/101/113	0.417	0.359	0.417	0.401	0.493	0.318	0.29	0.592	0.44	0.384	1.24
91	0.043	0.0393	0.0489	0.0416	0.0474	0.0361	0.03	0.0604	0.0453	0.0381	0.153
92	0.0671	0.0625	0.0729	0.0628	0.0779	0.0505	0.0471	0.0937	0.0704	0.0604	0.196
93/100	0	0.00427	0	0.00249	0.0036	0.00351	0.0033	0.00549	0.00442	0.00354	0.0173
94	0.00306	0.00153	0.00226	0.00184	0.00249	0.00183	0.00137	0.00308	0.00172	0.00163	0.0099
95	0.365	0.326	0.418	0.369	0.436	0.312	0.25	0.504	0.422	0.313	1.22
96	0.0023	0.00202	0.00219	0.00248	0.00259	0.00175	0.00196	0.00331	0.00244	0.00217	0.013
87/125	0.189	0.147	0.188	0.168	0.196	0.129	0.127	0.25	0.178	0.192	0.519
98	0	0	0	0	0	0	0	0	0	0.000607	0.0069
99	0.124	0.109	0.127	0.121	0.147	0.0903	0.0882	0.173	0.126	0.122	0.398
102	0.0108	0.0104	0.0107	0.0102	0.0127	0.00884	0.00687	0.0135	0.0111	0.00897	0.0388
103	0.00388	0.00333	0.00251	0.00302	0.00345	0.0033	0.00289	0.00487	0.00329	0.00259	0.0128
104	0.0014	0.00127	0	0.000978	0.00107	0.000969	0.00143	0.00122	0.000847	0.000914	0.00565
105	0.0782	0.0525	0.0462	0.0586	0.0676	0.0298	0.0495	0.0938	0.0429	0.121	0.244
106	0.0000351	0	0	0	0	0.0000429	0	0	0	0.0000748	0.00595
107	0.0159	0.012	0	0.0125	0.0153	0.00781	0.0112	0.0214	0.0116	0.0194	0.0487
108/124	0.0124	0.0101	0.00866	0.00988	0.0121	0.00649	0.00833	0.0158	0.00928	0.013	0.0387
110	0	0	0.000273	0	0	0	0	0.00012	0	0.0000868	0.000409
111	0	0	0	0	0	0	0	0	0	0.000343	0.00709
112	0	0	0	0	0	0	0	0	0	0.000349	0.00648
114	0.01	0.0079	0	0.00697	0.00949	0.00464	0.00762	0.0118	0.00662	0.0102	0.0264
115	0.367	0.297	0.318	0.337	0.407	0.233	0.27	0.515	0.325	0.416	1.18
117	0.0728	0.079	0.0714	0.075	0.0889	0.0684	0.0743	0.096	0.0802	0.0821	0.252
118	0.232	0.168	0.15	0.187	0.238	0.104	0.156	0.296	0.159	0.3	0.646
120	0	0	0	0	0	0	0	0	0	0.000473	0.00608
121	0	0	0.0000888	0	0	0	0	0	0	0.000272	0.00526
122	0.00887	0	0	0	0	0	0	0	0	0.00689	0.0135

123	0.00692	0	0	0	0	0	0	0.00716	0.0048	0.00446	0.0182
126	0	0	0	0	0	0	0	0	0	0.000633	0.0953
127	0	0	0	0	0	0	0	0	0	0.000691	0.00905
129/138/163	0.226	0.138	0.131	0.165	0.177	0.0804	0.139	0.272	0.11	0.345	0.439
130	0.0123	0.00795	0.0065	0.00977	0.01	0.00504	0.00769	0.0147	0.0069	0.0194	0.0287
131	0.00412	0.00333	0.00349	0.00345	0.00476	0.00228	0.0032	0.00559	0.00384	0.00548	0.0137
132	0.0762	0.0568	0.0647	0.0694	0.0679	0.0424	0.0555	0.0951	0.0527	0.0975	0.143
133	0	0.00312	0	0.00177	0.00232	0.00165	0.0025	0.00374	0	0.00464	0.0109
134	0.0133	0.00832	0.013	0.0171	0.0167	0.00432	0.0146	0.0197	0.0133	0.0235	0.0415
135/151	0.0747	0.0587	0.0729	0.0718	0.0737	0.0504	0.051	0.111	0.0661	0.0782	0.15
136	0.0392	0.0332	0.0467	0.0376	0.0403	0.0309	0.0251	0.0519	0.0409	0.0366	0.101
137	0.00985	0.00714	0.00769	0.00926	0.0102	0.00434	0.0069	0.0117	0.00637	0.0148	0.0241
139/140	0.0045	0.00385	0.00395	0.00461	0.00502	0.0031	0.00471	0.00586	0.00453	0.00571	0.02
141	0.0427	0.028	0.03	0.0347	0.0365	0.0197	0.028	0.0602	0.0269	0.0531	0.0744
143	0.00304	0.00355	0	0	0	0.00373	0	0.0025	0	0.0015	0.00665
142	0	0	0	0	0	0	0	0	0	0.00094	0.00547
144	0.0118	0.00983	0.00979	0.0114	0.0118	0.00859	0.00836	0.018	0.0114	0.0116	0.0278
145	0.000465	0	0	0.000265	0.00031	0.000237	0.000543	0.000444	0.000444	0.000265	0.00614
146	0.0258	0.0195	0.0194	0.0215	0.0261	0.0139	0.0188	0.0373	0.017	0.0347	0.052
147/149	0.182	0.139	0.161	0.173	0.179	0.108	0.133	0.262	0.147	0.211	0.352
148	0.000673	0	0	0	0.00059	0.000285	0	0	0	0.000455	0.00565
150	0.000695	0	0	0.000573	0.000536	0.000413	0.000697	0.00062	0.000444	0.000614	0.00567
152	0.000472	0	0	0.000505	0.000577	0.000194	0.000429	0.000527	0.000469	0.000464	0.00514
153/168	0.178	0.114	0.118	0.145	0.156	0.0753	0.11	0.242	0.107	0.23	0.312
154	0.0023	0.00156	0.00187	0.00188	0.00211	0.00202	0.00216	0.00348	0.00207	0.00232	0.00902
155	0.000656	0.000639	0	0.000885	0.000569	0.000531	0.000538	0.00114	0.000839	0.000542	0.00483
156/157	0.0226	0.0121	0	0.0138	0.0122	0.00553	0.0117	0.0191	0.00712	0.0363	0.046
158	0.0222	0.0134	0.0134	0.016	0.0176	0.00914	0.014	0.0257	0.0115	0.0329	0.0452

159	0	0	0	0	0	0	0	0	0	0.00035	0.0157
160	0	0	0	0	0	0.00068	0	0	0	0.000909	0.00753
161	0	0.00069	0	0	0	0	0	0	0	0.0000894	0.00622
162	0	0	0	0	0	0	0	0	0	0.000544	0.00939
164	0.0137	0.00726	0.00806	0.00828	0.00893	0.00449	0.00838	0.0155	0.0068	0.0177	0.027
165	0	0	0	0	0	0	0	0	0	0.000112	0.00603
167	0.00816	0.0056	0	0.00691	0.00708	0.0000985	0.00579	0.00958	0.00413	0.0135	0.0188
169	0	0	0	0	0	0	0	0	0	0.000166	0.00845
170	0.0428	0.0248	0	0.0282	0.021	0.00734	0.0179	0.074	0.00888	0.0707	0.0767
171/173	0.0148	0.012	0.0128	0.0112	0.0101	0.00615	0.00875	0.0244	0.00611	0.0226	0.0354
172	0.0104	0.00779	0	0.00593	0.00629	0	0	0.0157	0	0.0173	0.0233
174	0.051	0.032	0.0254	0.0382	0.0321	0.0136	0.0252	0.0926	0.0183	0.0749	0.131
175	0	0	0	0.00166	0.00177	0	0.00128	0.00317	0	0.00332	0.0101
176	0.00482	0.00413	0	0.00472	0.00525	0.00239	0.0034	0.0098	0.00402	0.00634	0.0152
177	0.0265	0.0206	0.0249	0.0199	0.0173	0.00966	0.0143	0.0475	0.00997	0.0413	0.0561
178	0.00912	0.00731	0	0.00698	0.00823	0.00425	0.00515	0.017	0.00441	0.0132	0.0201
179	0.0163	0.0127	0.014	0.0175	0.0163	0.00892	0.0113	0.0348	0.0123	0.0211	0.0373
180/193	0.11	0.0578	0.0445	0.065	0.0568	0.016	0.041	0.181	0.0233	0.17	0.192
181	0	0	0	0	0	0	0.00164	0	0	0.000471	0.00961
182	0	0	0	0	0.00342	0.00371	0.00284	0.00232	0.00292	0.00314	0.0133
183	0.0318	0.0205	0.0146	0.0228	0.0222	0.0126	0.0154	0.0526	0.015	0.0429	0.0576
184	0.00241	0.003	0	0.00285	0.00284	0.00417	0.00308	0.00331	0.00319	0.00333	0.0139
185	0.00664	0.00414	0.00588	0.00537	0.0045	0.0046	0.00439	0.00978	0.0026	0.00596	0.0142
186	0	0	0	0	0	0	0	0	0	0.000274	0.00798
187	0.0609	0.0356	0.0319	0.0426	0.0456	0.0182	0.0306	0.1	0.0266	0.0779	0.103
188	0	0.001	0	0	0	0	0.000868	0	0	0.000809	0.00703
189	0	0	0	0	0	0	0	0	0	0.00112	0.00941
190	0.0113	0.00854	0	0.00843	0.0115	0.00695	0.00718	0.0187	0.0064	0.0166	0.029

191	0	0	0	0	0	0	0.00381	0	0	0.00484	0.0127
192	0	0	0	0.0000282	0	0	0	0	0	0.000314	0.00918
194	0.0245	0.0148	0	0.0175	0.0123	0	0.0124	0.0408	0.00996	0.0336	0.0437
195	0.00998	0.00939	0	0.00762	0.00599	0	0.00687	0.0194	0	0.0133	0.026
196	0.0205	0.0159	0	0.0108	0.00956	0	0.00924	0.0289	0.00797	0.0231	0.0351
197	0	0	0	0	0	0	0	0	0	0.00232	0.0217
198/199	0.0524	0.0246	0.0256	0.0244	0.0198	0	0.0191	0.055	0.0118	0.0551	0.0553
200	0.00692	0	0	0	0	0	0	0.0118	0	0.0103	0.0104
201	0.00581	0.00444	0	0.00476	0.00514	0	0.00435	0.00887	0	0.00744	0.0195
202	0.0145	0.0114	0.0149	0.0121	0.0131	0.00876	0.00998	0.0185	0.00848	0.016	0.0358
203	0.0321	0.0171	0	0.0164	0.0134	0	0.0139	0.0353	0.00808	0.0316	0.044
205	0	0	0	0	0	0	0.00361	0	0	0.00368	0.0185
206	0.0212	0.0195	0	0.0143	0.00892	0	0.0104	0.023	0	0.0281	0.0464
207	0.0046	0.00429	0	0.0029	0.00244	0	0.00369	0.00419	0	0.00464	0.0181
208	0.00839	0.00634	0	0.00465	0.00396	0	0.00473	0.00794	0	0.00935	0.0207
209	0.0373	0.046	0.0451	0.0405	0.0414	0.045	0.045	0.0417	0.036	0.0552	0.137
OH-PCB Congener											
6 OH-PCB2	0.00972	0.00676	0.00459	0.028	0.00826	0.0244	0.0334	0.038	0.0147	0.00101	0.0447
3' OH-PCB65	0.00417	0.00271	0.00338	0.00491	0.00146	0.00945	0	0.0048	0.00332	0.000453	0.000504
Surrogate recoveries											
PCB 14	50%	43%	46%	62%	41%	40%	52%	29%	55%	43%	
PCB D-65	88%	66%	67%	77%	62%	64%	67%	61%	76%	68%	
PCB 166	130%	134%	108%	115%	112%	100%	110%	126%	126%	124%	
13C 4'OH-PCB12	40%	33%	59%	47%	85%	16%	38%	38%	55%	63%	
13C 4'OH-PCB120	46%	37%	47%	32%	84%	32%	16%	32%	61%	44%	
13C 4OH-PCB187	70%	41%	49%	26%	88%	29%	57%	52%	51%	53%	

Table A-6 Raw data for sample batch AA014 showing necessary metadata and uncorrected congener masses for PCBs and OH-PCBs (ng)

Batch ID	AA014-01	AA014-02	AA014-03	AA014-04	AA014-05	AA014-06	AA014-07	AA014-08	AA014-09	AA014-10	AA014-11	
Sample ID	FV 5167	FV 5354	FV 5492	FV 5334	FV 5364	FV 5370	FV 5358	FV 5461	FV 5460	FV 5397		
Sampling Location	St. Columbanus	Guadalupe Reyes	Guadalupe Reyes	Zapata	Zapata	Monroe	Monroe	St. Columbanus	Metcalf	Metcalf	Batch Blank	
Sampling Date	4/8/2009	8/10/2009	11/6/2009	5/29/2009	10/22/2009	10/26/2009	7/22/2009	10/19/2009	11/12/2009	8/18/2009		
Sampling Start Time	7:30	7:00	6:00	7:00	7:00	7:00	7:00	7:30	7:30	7:00		
Sampling Stop Time	15:30	13:00	14:45	15:00	15:40	15:30	13:15	15:30	13:30	14:00		
Sampling rate (m3/min)	0.4	0.4	0.4	0.4	0.4	0.4	0.4	0.4	0.4	0.4		
Air Volume (m^3	192	144	210	192	208	204	150	192	144	168		
Mean Temp (K)	281	299	285	294	284	285	296	286	282	298		
PCB Congener												LOQ (ng)
1	0.0545	0.0676	0.124	0.0288	0.108	0.0467	0.283	0.0401	0.0506	0.133	0.0642	0.0954
2	0.017	0.0154	0.0152	0.00904	0.0194	0.0192	0.101	0.0178	0.0152	0.0522	0.00902	0.0304
3	0.0652	0.0553	0.0953	0.0327	0.0922	0.0977	0.343	0.0539	0.055	0.168	0.0357	0.126
4	0.191	0.174	0.208	0.0453	0.169	0.0936	0.458	0.105	0.095	0.327	0.0615	0.161
5	0.00733	0.00795	0.00962	0.00348	0.00957	0.00564	0.0198	0.00646	0.00627	0.0197	0.00436	0.00847
6	0.0525	0.0587	0.0745	0.0235	0.0561	0.0421	0.183	0.0449	0.0432	0.158	0.0284	0.0601
7	0.0157	0.0163	0.0169	0.00883	0.017	0.013	0.0439	0.013	0.0132	0.038	0.0114	0.0198
8	0.244	0.276	0.363	0.11	0.285	0.205	0.866	0.215	0.22	0.797	0.126	0.272
9	0.0148	0.0181	0.0193	0.00711	0.0182	0.0126	0.051	0.0133	0.0118	0.0404	0.00928	0.0175
10	0.00725	0.00802	0.00738	0.00284	0.00819	0.00422	0.0166	0.00433	0.00411	0.0115	0.00387	0.00692
11	0.292	0.253	0.284	0.206	0.244	0.274	0.609	0.276	0.305	0.523	0.232	0.678
12/13	0.0191	0.0233	0.0355	0.0166	0.0187	0.0185	0.0519	0.0198	0.0225	0.0537	0.0166	0.0398
15	0.0705	0.0716	0.274	0.0408	0.0834	0.0644	0.248	0.0677	0.0774	0.299	0.043	0.116
16	0.0948	0.111	0.236	0.0466	0.129	0.108	0.383	0.125	0.146	0.571	0.059	0.128
17	0.091	0.0974	0.205	0.0439	0.115	0.0951	0.346	0.104	0.123	0.489	0.0546	0.121

18/30	0.177	0.187	0.421	0.0837	0.231	0.191	0.745	0.212	0.262	1.03	0.104	0.241
19	0.0261	0.0274	0.0525	0.00838	0.0268	0.022	0.0894	0.0229	0.0275	0.085	0.011	0.0297
20/28	0.198	0.19	0.809	0.127	0.251	0.218	0.805	0.258	0.32	1.28	0.13	0.359
21/33	0.127	0.127	0.45	0.0795	0.167	0.146	0.504	0.181	0.213	0.881	0.0875	0.208
22	0.073	0.0715	0.317	0.0499	0.0931	0.086	0.284	0.104	0.122	0.507	0.0519	0.139
23	0.00957	0.0000498	0.00643	0.00000395	0.0000097	0.0000171	0.00379	0.00468	0.00416	0.00279	0.000386	0.00576
24	0.00515	0.00333	0.00944	0.00163	0.0037	0.00334	0.00883	0.00429	0.00589	0.0115	0.00287	0.00669
25	0.0255	0.0228	0.0632	0.0145	0.0237	0.0215	0.0658	0.0243	0.0295	0.0938	0.0139	0.0412
26/29	0.0358	0.034	0.112	0.0215	0.0447	0.0396	0.123	0.0482	0.0521	0.197	0.0229	0.0622
27	0.0133	0.0144	0.0322	0.00646	0.0162	0.0147	0.0438	0.0149	0.0187	0.0595	0.00795	0.0179
31	0.181	0.169	0.649	0.115	0.247	0.203	0.76	0.249	0.307	1.26	0.124	0.328
32	0.0531	0.0558	0.148	0.0275	0.0675	0.0609	0.204	0.0642	0.0772	0.308	0.0309	0.0758
34	0.0000349	0.0000242	0.00492	0.0000116	0.00000945	0.0000208	0.00387	0.00282	0.0000112	0.00492	0.00191	0.00487
35	0.00805	0.00624	0.0186	0.00507	0.00491	0.00766	0.0188	0.00818	0.0119	0.0143	0.00442	0.021
36	0.0000849	0.0000151	0.0000296	0.0000144	0.000031	0.0000273	0.0000193	0.00000588	0.0000175	0.0000247	0.000205	0.00608
37	0.0461	0.0501	0.328	0.0343	0.0491	0.0453	0.167	0.0598	0.0714	0.18	0.0232	0.11
38	0.0000475	0.0000147	0.0028	0.00153	0.0000129	0.0000227	0.0000188	0.0000342	0.0000169	0.0000526	0.00058	0.00649
39	0.00013	0.0000204	0.0000319	0.00000389	0.0000191	0.0000252	0.0000375	0.0000158	0.000015	0.0000425	0.00026	0.00527
40/71	0.0458	0.05	0.307	0.0344	0.0569	0.0529	0.133	0.0612	0.081	0.25	0.0393	0.101
41	0.0116	0.0118	0.082	0.00745	0.0185	0.0171	0.0372	0.0166	0.0229	0.0751	0.0129	0.0262
42	0.0333	0.0362	0.206	0.0248	0.0402	0.0396	0.093	0.0416	0.058	0.187	0.0285	0.0728
43	0.00503	0.00661	0.0295	0.00614	0.00741	0.00647	0.0129	0.00819	0.00782	0.0318	0.0075	0.0158
44/47/65	0.186	0.191	0.758	0.148	0.219	0.213	0.433	0.239	0.266	0.735	0.174	0.423
45	0.0147	0.0186	0.102	0.0112	0.0249	0.0216	0.0617	0.0267	0.0355	0.143	0.0141	0.0335
46	0.00581	0.00937	0.0465	0.0049	0.0117	0.00969	0.0248	0.0115	0.0159	0.0586	0.00872	0.0175
48	0.0216	0.0233	0.124	0.0151	0.0293	0.026	0.0663	0.0296	0.0391	0.137	0.0218	0.043
49/69	0.102	0.113	0.416	0.0834	0.127	0.119	0.234	0.133	0.152	0.422	0.0962	0.235
50/53	0.0582	0.0755	0.144	0.0541	0.0746	0.0668	0.0975	0.0716	0.0833	0.155	0.0801	0.147

51	0.00825	0.0096	0.0363	0.00486	0.0103	0.00937	0.0171	0.00963	0.0142	0.0394	0.00792	0.0149
52	0.336	0.367	0.981	0.292	0.397	0.391	0.661	0.438	0.43	1.02	0.319	0.881
54	0.000487	0.000733	0.00209	0.000633	0.000934	0.000502	0.00141	0.000516	0.000502	0.00152	0.000285	0.00275
55	0.0102	0.00561	0.0347	0.00293	0.00497	0.00495	0.00697	0.00607	0.011	0.00904	0.00398	0.0143
56	0.0436	0.0463	0.281	0.0334	0.0471	0.0518	0.131	0.0571	0.0712	0.141	0.0353	0.0995
57	0.00443	0.00149	0.00646	0.0000164	0.00102	0.000931	0.00129	0.000832	0.0000465	0.00444	0.000169	0.00682
58	0.00687	0.0011	0.00641	0.0000305	0.00115	0.00196	0.00142	0.0013	0.00249	0.00321	0.000394	0.00769
59/62/75	0.0122	0.0139	0.0631	0.0101	0.0146	0.012	0.027	0.0149	0.0189	0.0488	0.0145	0.0364
60	0.0322	0.0248	0.138	0.018	0.0246	0.0259	0.0698	0.0308	0.0414	0.0729	0.0217	0.0547
61/70/74/76	0.305	0.292	1.17	0.244	0.326	0.317	0.656	0.36	0.39	0.711	0.259	0.674
63	0.0151	0.00679	0.0337	0.0046	0.00729	0.00559	0.0109	0.00772	0.014	0.0141	0.00418	0.0172
64	0.0655	0.0655	0.35	0.0515	0.0748	0.0731	0.165	0.0821	0.106	0.279	0.057	0.14
66	0.0843	0.0845	0.483	0.0666	0.0958	0.0978	0.239	0.109	0.128	0.273	0.0703	0.205
67	0.00919	0.00413	0.027	0.00241	0.00446	0.00371	0.00809	0.00586	0.00714	0.0116	0.000393	0.0101
68	0.0203	0.0167	0.0287	0.0168	0.0166	0.016	0.0193	0.018	0.02	0.0198	0.0208	0.0377
72	0.0037	0.00143	0.00524	0.00112	0.00176	0.000752	0.00218	0.00136	0.00328	0.00237	0.000457	0.00707
73	0.00466	0.00608	0.0062	0.00597	0.00469	0.00355	0.00586	0.00556	0.00595	0.00516	0.00621	0.0121
77	0.0259	0.0225	0.106	0.0149	0.0203	0.0228	0.0445	0.0225	0.0239	0.0278	0.0107	0.0423
78	0.000108	0.0000564	0.0000564	0.0000268	0.0000184	0	0.00003	0.00012	0.000027	0.0000509	0.000691	0.0078
79	0.0000614	0.0000509	0.000119	0.000015	0.000018	0.00000456	0.000026	0.0000318	0.0000491	0.0000221	0.000287	0.00754
80	0.000115	0.0000309	0.000085	0.000017	0.0000736	0.000104	0.0000267	0.0000174	0	0	0.000332	0.00695
81	0.000144	8.93E-06	0.0000536	0.0000236	0.0000425	0	0	0.0000569	0.0000238	0.00531	0.00106	0.00823
82	0.0445	0.0368	0.113	0.0289	0.033	0.039	0.0698	0.0346	0.0405	0.0521	0.0772	0.114
83	0.0413	0.035	0.0728	0.0219	0.0307	0.0335	0.0489	0.0341	0.0269	0.0235	0.0348	0.0598
84	0.105	0.0988	0.253	0.0865	0.103	0.101	0.163	0.118	0.108	0.163	0.241	0.374
85/116	0.041	0.049	0.116	0.0292	0.0487	0.0393	0.672	0.0307	0.0499	0.0564	0.0835	0.125
86/97/109/119	0.0996	0.0788	0.231	0.0647	0.0862	0.0962	0.22	0.095	0.0847	0.114	0.169	0.261
88	0.00169	0.0000309	6.18E-06	0.0000163	0.0000392	0.00000664	0	0.0000324	0.000022	0.0000604	0.0000895	0.000104

89	0.00451	0.00475	0.0123	0.00335	0.00494	0.00321	0.00504	0.003	0.00482	0.00749	0.0111	0.0173
90/101/113	0.406	0.379	0.899	0.312	0.377	0.393	0.604	0.442	0.4	0.522	0.773	1.24
91	0.0438	0.0435	0.103	0.0344	0.044	0.042	0.0667	0.0478	0.0448	0.0668	0.099	0.153
92	0.0637	0.0628	0.142	0.0494	0.0659	0.0625	0.0889	0.0676	0.0666	0.0774	0.115	0.196
93/100	0.00299	0.00141	0.00646	0.00225	0.00305	0.00216	0.00447	0.00347	0.00303	0.00424	0.00629	0.0173
94	0.00281	0.0018	0.00516	0.000919	0.00169	0.00134	0.00249	0.00344	0.00207	0.00298	0.00441	0.0099
95	0.324	0.328	0.715	0.27	0.334	0.332	0.496	0.38	0.348	0.527	0.78	1.22
96	0.00139	0.00191	0.00676	0.00195	0.00239	0.00237	0.00366	0.0025	0.00283	0.00535	0.00792	0.013
87/125	0.169	0.146	0.412	0.125	0.136	0.153	0.16	0.17	0.175	0.215	0.318	0.519
98	0.0000309	0.0000704	0.0000704	0.0000113	0.0000474	0.0000275	0.0000246	0.0000144	0.0000569	0.0000334	0.0000494	0.0069
99	0.129	0.122	0.308	0.0999	0.125	0.129	0.204	0.132	0.129	0.164	0.243	0.398
102	0.0117	0.0102	0.0279	0.0082	0.0106	0.0108	0.0186	0.0117	0.0131	0.0171	0.0253	0.0388
103	0.00393	0.00415	0.00634	0.00338	0.00394	0.00279	0.00412	0.00413	0.00324	0.00382	0.00565	0.0128
104	0.000915	0.00109	0.002	0.00129	0.000903	0.000486	0.000898	0.00127	0.000974	0.000571	0.000846	0.00565
105	0.117	0.0688	0.393	0.0568	0.0733	0.0903	0.181	0.0869	0.105	0.105	0.156	0.244
106	0.000149	0.0000281	0.000157	0.00141	0.00141	0.0000734	0.000074	0.0000151	0.0000465	0.0000419	0.000062	0.00595
107	0.0206	0.0149	0.0476	0.0116	0.0162	0.0144	0.0264	0.0187	0.0197	0.0203	0.0301	0.0487
108/124	0.0152	0.012	0.0367	0.00946	0.0119	0.0115	0.0182	0.0112	0.0122	0.0143	0.0212	0.0387
110	0.0000579	0.0000675	0.000117	0.000262	0.0002	0.000087	0.0000552	0.0000506	0.000164	0.0000498	0.0000738	0.000409
111	0.00000317	7.89E-06	0.0000671	0.0000244	0	0.000017	0.0000364	0.0000888	0.0000246	0.0000592	0.0000876	0.00709
112	0.000158	0.0000784	0.0000157	0.0000795	0.0000208	0.0000337	0.123	0.0000235	0.0000454	0.0000434	0.0000643	0.00648
114	0.012	0.00759	0.027	0.00724	0.00751	0.0107	0.0142	0.00831	0.0103	0.0103	0.0153	0.0264
115	0.457	0.355	1.17	0.304	0.35	0.4	0.000223	0.418	0.443	0.526	0.78	1.18
117	0.117	0.0893	0.157	0.109	0.094	0.0997	0.0651	0.116	0.101	0.107	0.158	0.252
118	0.289	0.198	0.857	0.164	0.193	0.227	0.423	0.245	0.258	0.276	0.408	0.646
120	0.00000632	0.0000236	0.0000511	0.0000104	0.0000333	0.0000507	0.00000905	0.0000502	0.000014	0.0000538	0.0000797	0.00608
121	0.0000556	7.27E-06	0.00372	0.00000641	0.00107	0	0.0000223	0.0000491	0.00000971	0.000019	0.0000281	0.00526
122	0.00729	0.0000714	0.013	0.00299	0.00367	0.00297	0.00995	0.0000694	0.00526	0.000252	0.000373	0.0135

123	0.0000772	0.00549	0.0142	0.00411	0.00546	0.00598	0.0102	0.0000828	0.0000384	0.00532	0.00789	0.0182
126	0	0	0	0	0	0	0	0	0	0	0.000767	0.0953
127	0	0	0	0	0	0	0	0	0	0	0.000386	0.00905
129/138/163	0.345	0.186	0.861	0.131	0.171	0.252	0.403	0.266	0.371	0.426	0.0686	0.439
130	0.0207	0.0125	0.0437	0.0094	0.0106	0.0126	0.0208	0.0128	0.0188	0.019	0.00561	0.0287
131	0.00499	0.00344	0.00976	0.000537	0.00363	0.00493	0.00562	0.00599	0.00605	0.00813	0.00212	0.0137
132	0.0888	0.0593	0.207	0.00224	0.0566	0.0808	0.114	0.0799	0.0998	0.112	0.031	0.143
133	0.00346	0.000102	0.0092	0.000612	0.00313	0.00234	0.00346	0.0024	0.00421	0.00317	0.000056	0.0109
134	0.0219	0.0185	0.0435	0.00204	0.0185	0.0211	0.0284	0.0217	0.0000431	0.0245	0.0112	0.0415
135/151	0.0792	0.0647	0.167	0.0469	0.06	0.081	0.104	0.0851	0.00412	0.114	0.0374	0.15
136	0.0411	0.0378	0.0845	0.0291	0.0386	0.0443	0.0596	0.0477	0.0000486	0.0673	0.027	0.101
137	0.0155	0.0111	0.0354	0.00723	0.00948	0.00986	0.0151	0.0107	0.0134	0.0146	0.00389	0.0241
139/140	0.0047	0.00471	0.0107	0.0025	0.00351	0.0045	0.00636	0.00526	0.00521	0.00753	0.0039	0.02
141	0.057	0.0355	0.127	0.0255	0.0293	0.0459	0.0647	0.0536	0.0633	0.0743	0.0143	0.0744
143	0.0000301	0.0000117	0.00116	0.00315	0.00000603	0.0000966	0.000792	0.000052	0.0000417	0.0000902	0.00085	0.00665
142	0.0000749	0.0000944	0.0000371	0.0468	0.0000225	0.000075	0.000341	0.000883	0.000013	0.0000663	0.000564	0.00547
144	0.0121	0.0102	0.0259	0.00826	0.0104	0.012	0.0156	0.0133	0.237	0.0178	0.0074	0.0278
145	0.00000322	8.75E-06	0.00105	0.000613	0.0000136	0.000511	0.000465	0.000354	0.000086	0.000347	0.00013	0.00614
146	0.0338	0.0239	0.0000468	0.0161	0.0000661	0.0283	0.0397	0.0296	0.0385	0.0415	0.0121	0.052
147/149	0.211	0.156	0.439	0.119	0.141	0.198	0.267	0.209	0.0128	0.277	0.0837	0.352
148	0.00029	0.00051	0.00107	0.0000366	0.000313	0.000387	0.000021	0.0000144	0.0884	0.0000272	0.000025	0.00565
150	0.00037	0.000667	0.000674	0.000597	0.000574	0.000306	0.000346	0.000589	0.038	0.000503	0.0000293	0.00567
152	0.000464	0.000307	0.000906	0.000103	0.000465	0.000182	0.000419	0.000309	0.0000183	0.000431	0.0000397	0.00514
153/168	0.227	0.139	0.504	0.0976	0.121	0.185	0.261	0.202	0.255	0.297	0.0588	0.312
154	0.00213	0.00152	0.00367	0.00214	0.00202	0.00199	0.00266	0.00182	0.0128	0.00283	0.000914	0.00902
155	0.000522	0.000827	0.000736	0.0000428	0.000641	0.000696	0.000436	0.00092	0.0000511	0.000909	0	0.00483
156/157	0.0364	0.0186	0.112	0.0119	0.0245	0.0215	0.0367	0.0237	0.0405	0.0409	0.00029	0.046
158	0.0337	0.021	0.0782	0.0149	0.0191	0.0254	0.0372	0.0259	0.0327	0.0375	0.00684	0.0452

159	0.0000106	0.0000192	7.02E-06	0.00000778	0.0000199	0.00000497	0.0000219	0.0000356	0.0000386	0.000105	0.00814	0.0157
160	0.000037	0.00153	0.00012	0.0000296	0.000108	0.0000849	0.0000446	0.0000542	0.0000449	0.000109	0.0000384	0.00753
161	0.0000158	0.0000257	0.0554	0.0000938	0.0156	0.0000355	0.0000168	0.0000414	0.0000192	0.0000241	0.0000361	0.00622
162	0.0000184	0.000005	0.0000256	0.0000162	0.0000207	0.0000155	0.00000653	0.0000223	0.0000536	0.0000879	0.000327	0.00939
164	0.0231	0.0133	0.0482	0.00855	0.0116	0.0164	0.0245	0.0164	0.0226	0.0263	0.00528	0.027
165	0.0000539	0.0000137	0.0000669	0.0000111	0.000104	0.0000189	0.0000358	0.0000407	0.0000204	0.0000129	0.0000207	0.00603
167	0.0124	0.0105	0.0347	0.00442	0.00799	0.00957	0.0143	0.00877	0.0148	0.016	0.000123	0.0188
169	0	0	0	0	0	0	0	0	0	0	0.000391	0.00845
170	0.0822	0.0552	0.253	0.0208	0.0344	0.0548	0.105	0.0859	0.13	0.249	0.00109	0.0767
171/173	0.0272	0.0133	0.0634	0.00693	0.0103	0.0228	0.0314	0.0261	0.036	0.0505	0.000559	0.0354
172	0.0143	0.0135	0.0428	0.0000811	0.00817	0.0169	0.0185	0.0176	0.0276	0.0397	0.000333	0.0233
174	0.0854	0.045	0.214	0.023	0.0276	0.0698	0.1	0.0944	0.126	0.164	0.0756	0.131
175	0.00333	0.00418	0.01	0.00313	0.00119	0.00304	0.00388	0.00507	0.00581	0.0063	0.0011	0.0101
176	0.00681	0.00483	0.0186	0.00501	0.00373	0.00679	0.01	0.0102	0.0104	0.0113	0.00322	0.0152
177	0.0486	0.0262	0.118	0.0141	0.0187	0.038	0.0536	0.049	0.068	0.0875	0.015	0.0561
178	0.013	0.00858	0.0325	0.00631	0.00413	0.0127	0.0163	0.0157	0.0215	0.0226	0.000854	0.0201
179	0.0237	0.016	0.0548	0.0113	0.0137	0.0255	0.0307	0.0278	0.034	0.0347	0.00984	0.0373
180/193	0.217	0.112	0.571	0.0522	0.0668	0.154	0.246	0.232	0.347	0.514	0.0172	0.192
181	0.00012	0.0000788	0.00485	0.0000832	0.0000543	0.0000939	0.0000405	0.000023	0.0000363	0.000175	0.000734	0.00961
182	0.00351	0.00577	0.00962	0.00425	0.00346	0.00352	0.0042	0.00395	0.00609	0.00752	0.00173	0.0133
183	0.0453	0.0272	0.112	0.0126	0.016	0.0383	0.0514	0.0496	0.0696	0.0838	0.0118	0.0576
184	0.00375	0.00494	0.00454	0.00498	0.00377	0.00358	0.00357	0.00523	0.0057	0.0036	0.00617	0.0139
185	0.0086	0.00718	0.0229	0.00323	0.00445	0.00801	0.00965	0.0109	0.0107	0.0151	0.00188	0.0142
186	0.00000489	0.00116	0.0000631	0.00173	0.000762	0.0000824	0.000026	0.0000246	0.000101	0.0000607	0.000404	0.00798
187	0.0903	0.0505	0.205	0.0315	0.0364	0.0845	0.109	0.095	0.122	0.148	0.0186	0.103
188	0.000781	0.00115	0.00161	0.00159	0.000505	0.0007	0.0011	0.00142	0.00181	0.00116	0.000697	0.00703
189	0	0	0.0305	0.00802	0	0	0	0	0.0163	0	0.000783	0.00941
190	0.0225	0.0219	0.0529	0.00974	0.0134	0.0164	0.0258	0.0254	0.0345	0.0564	0.00984	0.029

191	0.00579	0	0.0139	0.000028	0.000025	0.0000535	0.00518	0	0.00665	0.0109	0.000337	0.0127
192	0.0000577	0	0	0.0000189	0.0000155	0.0000379	0.0000424	0	0	0	0.000302	0.00918
194	0.0459	0.0312	0.173	0.0157	0.0209	0.0495	0.0695	0.0639	0.191	0.151	0.000565	0.0437
195	0.0213	0.0152	0.0575	0.00777	0.00918	0.0202	0.0245	0.0288	0.0402	0.054	0.0008	0.026
196	0.0303	0.0185	0.0795	0.0109	0.0152	0.0258	0.0412	0.0407	0.0764	0.0714	0.00211	0.0351
197	0	0	0	0	0	0	0	0	0	0	0.00284	0.0217
198/199	0.0726	0.0514	0.236	0.0275	0.0312	0.0674	0.123	0.0828	0.196	0.14	0.00197	0.0553
200	0.0102	0.0103	0.0277	0	0	0.00926	0.0113	0.0113	0.0155	0.0164	0.000545	0.0104
201	0.00759	0.00915	0.0192	0	0.00481	0.0084	0.0114	0.0116	0.0134	0.0123	0.000724	0.0195
202	0.016	0.0136	0.0425	0.0125	0.0106	0.0183	0.0265	0.0187	0.0247	0.023	0.0102	0.0358
203	0.0444	0.0268	0.129	0.016	0.022	0.0389	0.0679	0.0494	0.118	0.0813	0.000652	0.044
205	0.00623	0	0.0118	0	0	0	0	0	0	0.0112	0.000766	0.0185
206	0.032	0.0422	0.186	0.014	0.0345	0.0345	0.159	0.0567	0.287	0.066	0.0165	0.0464
207	0.00606	0.00726	0.0192	0	0.00809	0.00584	0.0141	0.00669	0.0227	0.00766	0.00116	0.0181
208	0.0105	0.0127	0.0503	0.00646	0.0137	0.00969	0.0487	0.0133	0.0315	0.0143	0.000827	0.0207
209	0.0848	0.0877	0.138	0.0532	0.0799	0.0657	0.107	0.0965	0.101	0.0603	0.0647	0.137
OH-PCB Congener												
6 OH-PCB2	0.0231	0.0108	0.0115	0.0145	0.0113	0.0424	0.0313	0.0237	0.0283	0.055	0.0115	0.0447
3' OH-PCB65	0.00882	0	0.0179	0.00754	0.0127	0.0135	0.0341	0	0.0181	0.0255	0.000826	0.000504
Surrogate recoveries												
PCB 14	49%	40%	53%	49%	41%	54%	38%	43%	41%	58%	26%	
PCB D-65	65%	50%	48%	67%	56%	65%	63%	56%	53%	72%	40%	
PCB 166	79%	58%	80%	89%	67%	77%	88%	67%	62%	88%	74%	
13C 4'OH-PCB12	246%	191%	130%	118%	71%	79%	97%	30%	68%	127%	186%	
13C 4'OH-PCB120	146%	106%	96%	111%	66%	100%	93%	23%	87%	91%	79%	
13C 4OH-PCB187	143%	120%	110%	128%	69%	108%	104%	25%	101%	93%	124%	